NOS2 Induction and HO-1-Mediated Transcriptional Control in Gram-Negative Peritonitis

by

Crystal Michele Withers

Department of Pathology
Duke University

Date:_____

Approved:

_____
Claude A. Piantadosi, Supervisor

_____
Salvatore V. Pizzo

_____
Herman F. Staats

_____
Joe Brice Weinberg

_____
Harvey E. Marshall

Dissertation submitted in partial fulfillment of
the requirements for the degree of Doctor of Philosophy in the Department of Pathology in the Graduate School
of Duke University

2013

ABSTRACT

NOS2 Induction and HO-1-Mediated Transcriptional Control in Gram-Negative Peritonitis

by

Crystal Michele Withers

Department of Pathology
Duke University

Date:_____

Approved:

_____
Claude A. Piantadosi, Supervisor

_____
Salvatore V. Pizzo

_____
Herman F. Staats

_____
Joe Brice Weinberg

_____
Harvey E. Marshall

An abstract of a dissertation submitted in partial fulfillment of the requirements for the degree of Doctor of Philosophy in the Department of Pathology in the Graduate School of Duke University

2013

Abstract

Nitric oxide (NO) is an endogenous gaseous signaling molecule produced by three NO synthase isoforms (NOS1, 2, 3) and important in host defense. The induction of NOS2 during bacterial sepsis is critical for pathogen clearance but its sustained activation has long been associated with increased mortality secondary to multiple organ dysfunction syndrome (MODS). High levels of NO produced by NOS2 incite intrinsic cellular dysfunction, in part by damaging macromolecules through nitration and/or nitrosylation. These include mitochondrial DNA (mtDNA) and enzymes of key mitochondrial pathways required for maintenance of normal O_2 utilization and energy homeostasis. However, animal studies and clinical trials inhibiting NOS2 have demonstrated pronounced organ dysfunction and increased mortality in response to live bacterial infections, confirming that NOS2 confers pro-survival benefits. Of particular interest here, the constitutive NOS1 and NOS3 have been linked to the up-regulation of nuclear genes involved in mitochondrial biogenesis but no comparable role has been described for NOS2. ***Therefore, I hypothesized that NOS2 is indispensible for host protection but must be tightly regulated to ensure NO levels are high enough to activate mitochondrial and other pro-survival genes, but below the threshold for cellular damage***.

This hypothesis was explored with two major Aims. The ***first Aim*** was to define the role of NOS2 in the activation of mitochondrial biogenesis in the heart of *E. coli*-

treated mice. The ***second*** was to investigate the ability of NOS2 to be transcriptionally regulated by an enzyme previously shown to induce mitochondrial biogenesis, heme oxygenase-1 (HO-1). This hypothesis was tested using an i*n vivo* model of sublethal heat-killed *E. coli* (*HkEC*) peritonitis in C57B/L6 (Wt), NOS2$^{-/-}$, and TLR4$^{-/-}$ mice. Additionally, *in vitro* systems of mouse AML-12 or Hepa 1-6 cells pretreated with HO-1 activators or *Hmox1* shRNA prior to inflammatory challenge with lipopolysaccharide (LPS) +/- tumor necrosis factor-α (TNF-α). For the first Aim, Wt, NOS2$^{-/-}$, and TLR4$^{-/-}$ mice were treated with *HkEC* and cardiac tissue analyzed for mitochondrial function, expression of nuclear and mitochondrial proteins needed for mitochondrial biogenesis, and histological expression of NOS2 and TLR4 relative to changes in mitochondrial mass. For the second Aim, Wt mice were pretreated with hemin or carbon monoxide (CO) to activate HO-1 prior to *HkEC*-peritonitis. Liver tissue in these animals was evaluated at four hours for HO-1 induction, *Nos2* mRNA expression, cytokine profiles, and NF-κB activation. Liver cell lines were pretreated with hemin, CO-releasing molecule (CORM), or bilirubin one hour before LPS exposure and the *Nos2* transcriptional response evaluated at two and 24 hours. The MTT assay was used to confirm that *in vitro* treatments were not lethal.

These studies demonstrated that *HkEC* induced mtDNA damage in the heart that was repaired in Wt mice but not in NOS2-deficient mice. In KO mice, sustained mtDNA damage was associated with the reduced expression of nuclear (NRF-1, PGC-1α) and mitochondrial (Tfam, Pol-γ) proteins needed for mitochondrial biogenesis. The findings

thus supported that NOS2 is required for mitochondrial biogenesis in the heart during Gram-negative challenge. Evaluation of the relationship between HO-1 and NOS2 in murine liver was more complex; HO-1 activation in *HkEC*-treated Wt mice attenuated 4-hour *Nos2* gene transcription. In liver cell lines, hemin, CORM, and bilirubin were unable to suppress *Nos2* expression at the time of maximal induction (2 hours). *Nos2* was, however, suppressed by 24 hours, suggesting that the regulatory impact of HO-1 induction was not engaged early enough to reduce *Nos2* transcription at 2 hours. It is concluded that NOS2 induction in bacterial sepsis optimizes the expression of the mitochondrial biogenesis transcriptional program, which subsequently can also be regulated by HO-1/CO in murine liver. This provides a potential new mechanism by which immune suppression and mitochondrial repair can occur in tandem during the acute inflammatory response.

Dedication

It was when I accepted my own fallibility that I saw God waiting with outstretched arms to carry me through this doctoral program. Therefore, I first give all credit and honor to God who created the very subject of my studies and chose to give me a glimpse into the intricacies of His miraculous mind. After all, science is simply trying to figure out what God Himself did in six days. Lord, thank you for reminding me of my mortality so that I might exercise great faith! ☺

I am humbled and grateful for the opportunity to work with my research advisor, Dr. Claude Piantadosi. He not only demonstrated commitment to science but consistency in balancing research, clinical practice, and teaching. Thank you for opening up your lab and resources to me for without them, I would not be where I am today.

I wish to thank Dr. Hagir Suliman for supporting me and for believing in my future. You helped me establish my footing in the lab and confidence in my work.

I am grateful for the support and feedback from my committee members – Dr. Salvatore Pizzo, Dr. Herman Staats, Dr. Brice Weinberg, and Dr. Harvey Marshall. Thank each of you for your time, commitment, and belief in my potential.

I came to the lab with two left feet and at each turn, there were technicians…no, friends…who were there to help me. Craig Marshall, thanks for teaching me that we are bigger than the mice, even when they bite. Ping Fu, thank you for teaching me how to do all the major experiments the right way – you have saved me from myself and

confirmed that God provides. Allie Ulrich, thank you for your smile, your optimism, and your enthusiasm. You inspire me to be more patient, kind, and helpful. And most dearly, Martha Salinas…you have become my best friend and with you, I've made it through the hardest and the happiest times of my life. Thank you for teaching me how to be the opposite of my first reaction – to be patient, forgiving, peaceful, and not give up. I owe you so much…

I thank Charles Albert Withers, II for being my husband, best friend, and biggest fan. I thank him and love him for supporting me through the best and worst with his love and devotion.

My daughter, Layla Josephine Withers, has had the best temperament, smiles, and cuddle times a stressed grad student could ever ask for. Out of my love for her, I pursue my career goals so that she may know first-hand that the sky is the limit. For next baby Withers scheduled to arrive in August 2013, I hope she too will see that sacrifices were made and love poured out so that she can claim no limits.

There are so many others who have journeyed with me so I thank them all, some by name and others by heart. My Mom & Dad, sisters, brothers, nieces, nephews, parents-in-love, aunts, uncles, friends, administrators from the medical school and graduate school, ONEL1FE and WOCC family…there are just so many people who have been there at just the right times so I pray you will be rewarded for the love you've poured out on me. Thanks for walking with me through this part of my life!!

Table of Contents

List of Figures

List of Abbreviations

CLP	cecal ligation and puncture
CO	carbon monoxide
CORM	carbon monoxide releasing molecule
CREB	cAMP responsive element binding protein
E. coli	*Escherichia coli*
ETC	electron transport chain
GFP	green fluorescent protein
H_2O_2	hydrogen peroxide
HkEC	heat-killed *Escherichia coli*
Hmox1/HO-1	heme oxygenase-1 (gene/protein)
IL	interleukin
IMM	inner mitochondrial membrane
LPS	lipopolysaccharide
MODS	multiple organ dysfunction syndrome
mtDNA	mitochondrial DNA
MyD88	myeloid differentiation factor 88
NF-κB	nuclear factor-κB
NO	nitric oxide
Nos2/NOS2	inducible nitric oxide synthase (gene/protein)
NRF	nuclear respiratory factor
Nrf2	nuclear factor (erythroid-derived 2)-like 2
OMM	outer mitochondrial membrane
oxphos	oxidative phosphorylation
PGC	proliferator-activated receptor gamma co-activator
pol-γ	DNA polymerase-γ
qRT-PCR	real-time reverse transcriptase polymerase chain reaction
ROS	reactive oxygen species
RNS	reactive nitrogen species
SIRS	systemic inflammatory response syndrome
STAT	signal transducer and activator of transcription
Tfam	mitochondrial transcription factor A
TIR	toll-interleukin 1 receptor
TLR	toll-like receptor
TNF-α	tumor necrosis factor-α
TRIF	TIR domain-containing adapter inducing interferon-β

Acknowledgements

Graduate support came from the Duke Endowment Fellowship (2008-2011), the James B. Duke Fellowship (2008-2011), and the UNCF/Merck Graduate Dissertation Fellowship (2012-2013).

1. Introduction and Background

1.1 Sepsis: The Clinical Problem

Sepsis is defined by the systemic inflammation that occurs when viral, bacterial, or fungal pathogens overwhelm the normal host barrier defenses, spread systemically, and trigger a robust pro-inflammatory immune response. This innate immune response is necessary for the host to clear the pathogen, but when sustained and dysregulated, may lead to cellular damage and organ dysfunction. Each year, an estimated 750,000 Americans develop severe bacterial sepsis. Of these patients, some 200,000 die from multiple organ dysfunction syndrome (MODS), making sepsis the leading cause of death in non-cardiac intensive care units (ICUs) and 10th among all-cause mortality in the United States [1, 2].

Sepsis can quickly progress to more severe stages so early identification and treatment of systemic infections is critical for patient survival. The diagnosis of sepsis requires that certain clinical criteria be met. These include the identification of a source of infection in connection with criteria for systemic inflammatory response syndrome (SIRS). SIRS is defined by the presence of two or more of the following manifestations: 1) temperature >38°C or <36°C; 2) heart rate >90 beats per minute; 3) respiratory rate >20 breaths per minute or $PaCO_2$ of <32 mmHg; and 4) WBC <4,000/mm^2, >12,000/mm^2, or >10% immature neutrophils [3]. Sepsis complicated by organ dysfunction, hypotension, or hypoperfusion is called *severe sepsis*. Furthermore, when hypotension persists despite aggressive fluid resuscitation and patients require hemodynamic support such as

vasopressors or inotropic agents, this is defined as *septic shock* [3]. Severe sepsis and septic shock are associated with higher mortality due to MODS and have therefore been the focus of most studies investigating the pathogenesis of sepsis.

The pathophysiology of sepsis is quite complex and often involves several organ systems (reviewed in [4]). Patients may present with disseminated intravascular coagulation (DIC) characterized by increased clotting times, low platelet counts, and compromised organ blood flow. Endocrine abnormalities include insulin resistance leading to hyperglycemia and adrenal insufficiency, sometimes requiring glucocorticoid administration. Cardiovascular (CV) dysfunction is common; often beginning with a capillary fluid leak, and after adequate fluid resuscitation, manifesting as a hyperdynamic response where cardiac output is high and systemic vascular resistance is low. This progresses to a hypodynamic state typical of septic shock [5]. Acute renal failure, hepatic encephalopathy, adrenal insufficiency, and bacterial translocation across compromised gut epithelium are also complications of severe sepsis. Therefore, current clinical management of sepsis provides some basic supportive care while incorporating therapies specific to the affected organ systems.

The current standards of care for treatment of patients with severe sepsis are detailed by the 2012 Surviving Sepsis Campaign [6] and summarized here. Immediately after diagnosing severe sepsis or septic shock, appropriate antimicrobial coverage, blood cultures, and early goal-directed volume resuscitation are initiated. If hypotension persists, further hemodynamic support is provided using vasopressors, inotropic agents,

and corticosteroids. Additional therapeutic objectives may include restoring hemoglobin and platelet counts, providing tight glucose control, mechanically ventilating patients with acute lung injury and acute respiratory distress syndrome (ARDS), and prophylactically protecting against deep vein thrombosis and stress ulcers. Despite this bundled care approach for support of systemic organ function, sepsis is still associated with high mortality.

The exact cause of mortality in severe sepsis is often not apparent. Of special note, autopsies of patients who have died from sepsis have not revealed significant histologic evidence of cell death that would correlate with the degree of organ dysfunction [7]. This implies that the cause of death in septic patients is much more complex than simple ischemia with cellular necrosis or apoptosis. Therefore, modern research has turned more attention to understanding broad molecular derangements, such as aberrant control of inflammation and mitochondrial dysfunction, which will be described further in this dissertation.

1.2 TLR4-mediated immune response to bacterial sepsis

The range of physiologic disturbances seen in sepsis has long been associated with the specific underlying problem of an exaggerated and dysregulated host inflammatory response. Initiation of the innate immune response occurs when immune cells, such as macrophages and dendritic cells, detect invading pathogens via Toll-like receptors (TLRs). To date, 10 TLRs have been identified in humans and 12 in mice, each

with extracellular leucine-rich domains that recognize different lipid, protein, and nucleic acid pathogen-associated molecular patterns (PAMPs) [8]. The majority of TLRs are found on the cell surface, with the exceptions being TLR3, TLR7, TLR8, and TLR9, which localize to intracellular endosomes and lysosomes and detect nucleic acids [9]. TLR4 is critical for the recognition of various lipopolysaccharides (LPS) found in Gram-negative bacteria, the pathogen identified in 60% of culture-positive sepsis cases [10-12]. LPS is comprised of three subunits; Lipid A, core polysaccharide, and O antigen [13]. Lipid A is a highly conserved disaccharide and is responsible for most of the toxicity associated with LPS while the polysaccharides of the core and O antigen confer immunogenicity and are specific to the bacterial subtype. The core polysaccharide consists of an inner core that attaches to Lipid A, and an outer core, which is comprised of common sugars such as hexose. Attached to the outer core is the most variable component of LPS, the O antigen, comprised of hydrophobic glycan chains. These lipid chains enable LPS to complex with MD-2, LPS binding protein (LBP) and CD14, thus activating the TLR4 pathway [8, 14, 15]. As summarized in ***Figure 1***, oligomerization of TLR4 enables the intracellular activation of the myeloid differentiation factor 88 (MyD88)- and TIR domain-containing adapter inducing interferon-β (TRIF)-dependent pathways [16-18]. This results in the activation of the nuclear factor-κB (NF-κB) transcription factor [19].

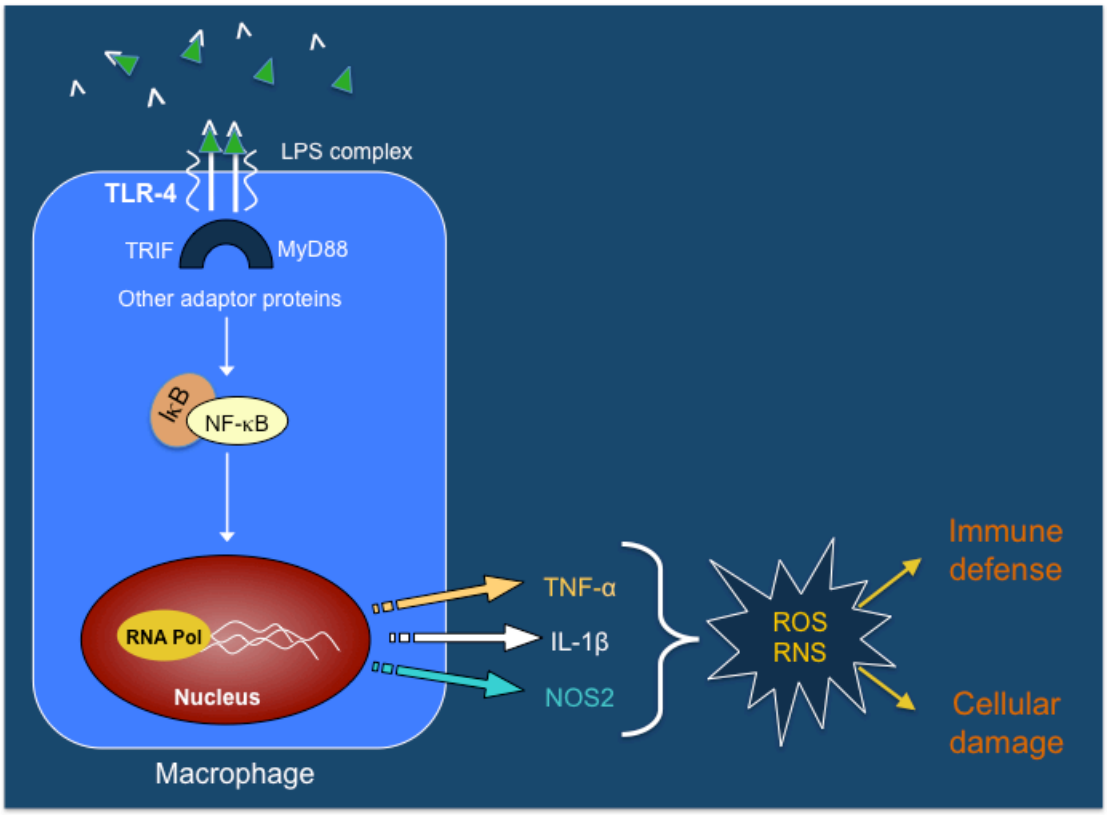

Figure 1: Early host immune response to sepsis. LPS activation of TLR4 signals through MyD88 and TRIF to promote NF-κB nuclear translocation and thus facilitate cytokine and NOS2 expression. These responses lead to an increase in ROS/RNS, which protect the host system against pathogens but also damage cellular components.

The NF-κB family of transcription factors includes 5 members categorized into 2 subfamilies [20]. The NF-κB subfamily includes p105 and p100, which are the precursors to the active p50 and p52, respectively. These proteins do not activate transcription unless they form a heterodimer with a member of the Rel subfamily, p65 (Rel-A), Rel-B, or c-Rel [21]. Although all NF-κB proteins contain the Rel homology domain (RHD) for dimerization and DNA binding, only Rel proteins contain a transactivation domain (THD), enabling transcription. With the exception of Rel-B, which only forms

heterodimers *in vivo*, all other subunits can form homo- and heterodimers, allowing for wide diversity in DNA binding specificity, protein recruitment at target promoters, and degree of transcriptional activity [22]. In order to prevent unwanted NF-κB activity, this transcription factor is sequestered in the cytoplasm by the inhibitor of kappa B (IκB) family of proteins. Notably, p50:p65 (Rel-A) is the major heterodimer formed in most cells and is preferentially retained in the cytoplasm by IκBα [23]. Activation of the TLR pathway leads to phosphorylation and degradation of IκB, enabling NF-κB to translocate into the nucleus where it enables transcription of cytokines such as tumor necrosis factor-α (TNF-α), interleukin-6 (IL-6), and IL-1β [24, 25]. Additionally, NF-κB promotes transcription of the inducible nitric oxide synthase (NOS2), which enzymatically converts L-arginine into the gaseous free radical, nitric oxide (NO). Three isoforms of NOS exist; neuronal NOS1, inducible NOS2, and endothelial NOS3 [26]. NOS1 and NOS3 are constitutively expressed and depend greatly on calcium concentrations in the cell. Conversely, the calcium-independent NOS2 is induced by inflammatory stimuli, largely via NF-κB-mediated transcription, and generates much greater quantities of NO. Therefore, greater fluxes of NO are observed during infection, allowing for more effective pathogen clearance but also more concurrent cellular damage.

In addition to direct toxicity from NO, cytokines and NO also promote the production of reactive oxygen and nitrogen species (ROS/RNS) [27]. These free radicals are derived from O_2 and/or NO in reactions that will be detailed later in the chapter.

Under normal situations, ROS/RNS are limited by cellular antioxidant defenses but when these enzymes are overwhelmed, cell death and organ dysfunction ensue.

A great deal of research has been undertaken in the last 30 years to understand the effect of the immune response on the outcome of sepsis in animals and humans (reviewed in [28, 29]). Experimentally, suppression of the cytokine response has been evaluated in a wide range of mouse models of endotoxemia and sepsis. TNF-α and IL-1β blockade improves survival in murine endotoxemia [30, 31]. Additionally, mice deficient in the anti-inflammatory cytokine, IL-10, died earlier in a model of sepsis produced by cecal ligation and puncture (CLP) [32]. The time before which these animals could be rescued by surgically removing the necrotic bowel was significantly reduced, suggesting that inflammation accelerates the progression of disease and hastens the onset of irreversible sepsis. Conversely, delayed neutralization of IL-10 just 12 hours after CLP sepsis improved survival [33]. Valuable information has also been obtained from knockout and transgenic mice. For example, $TLR4^{-/-}$ and C3H/HeJ mice with defective TLR4 signaling are resistant to lethal LPS and protected from mitochondrial dysfunction, cardiomyocyte impairment, and LPS-induced shock [34-36]. However, these mice are more susceptible to live Gram-negative infection due to their inability to clear the invading pathogens [37]. This suggests that the exaggerated immune response in sepsis does contribute significantly to cellular damage, but is needed for bacterial clearance and host protection, especially in early stages of the infection.

In a similar manner, clinical trials attempting to suppress the immune response in severely septic patients have also been unsuccessful [38, 39]. Studies have employed anti-endotoxin antibodies [40], TNF-α inhibitors [41, 42], and IL-1 receptor antagonists [43] to block host inflammatory responses but these treatments were ineffective or more detrimental than standard supportive care. Efforts to enhance the immune response did not improve overall survival either, although length of hospital stay was shorter in one small trial [44, 45]. The monocyte activator, interferon-γ did promote the recovery of macrophage function and improve survival in a pilot trial of nine patients [46], but not in a larger trial with burn and trauma patients [47, 48]. Collectively, these trials highlight the complexity of the immune phenotypes in sepsis; the balance between host pro- and anti-inflammatory responses is most important for determining outcome. Patient responses are heterogeneous, beginning with a hyperimmune response and shifting to a state of "immunoparalysis" [49, 50], which may demand a more stratified approach to immunotherapy. Alternatively, the sequelae of exaggerated immune responses may be better targeted for therapeutic intervention. Mitochondria are one such target of immune activation in sepsis and their damage, functional recovery, and regulatory pathways will be explored further in this dissertation.

1.3 Mitochondrial response to sepsis

Mitochondria are membrane-bound organelles present in eukaryotic cells that produce 90-95% of the cell's adenosine triphosphate (ATP) through the process of

oxidative phosphorylation (oxphos). This bioenergetic pathway depends heavily on mitochondrial subcellular organization. The outer mitochondrial membrane (OMM) is freely permeable to small molecules but regulates transport of larger molecules with the use of porins and translocase proteins embedded in the membrane. The inner mitochondrial membrane (IMM) is home to the respiratory complexes of the mitochondrial electron transport chain (ETC). As electrons are generated by the citric acid (TCA) cycle in the matrix, an electrochemical proton gradient is established across the IMM. These protons accumulate in the intermembrane space between the OMM and the IMM and ultimately power the mechanical rotation of the ATP synthase (complex V) enzyme, producing ATP.

During oxphos, electrons are removed from O_2 as it is completely reduced to H_2O. However, incomplete reduction of O_2 also occurs, thus generating superoxide (O_2^-), hydrogen peroxide (H_2O_2), hydroxyl ion (OH^-), and hydroxyl radical (•OH). Under normal circumstances, these reactive species are neutralized by antioxidant enzymes like superoxide dismutase (SOD) and glutathione peroxidase. However, the inflammatory milieu in sepsis functionally impairs ETC complexes and exacerbates reactive species production, which overwhelms the detoxification capacity and further compromises mitochondrial function.

1.3.1 Sepsis-induced mitochondrial dysfunction

The concept of bioenergetic failure from mitochondrial dysfunction in sepsis was introduced 40 years ago and has been used by some investigators to explain certain aspects of septic shock symptomatology [51, 52]. Originally, MODS was thought to occur secondary to tissue hypoxia but with the introduction of better pO_2 sensors, it became evident that tissue perfusion and oxygenation are adequate and often supranormal during sepsis [53]. Although tissues are able to extract sufficient oxygen, the ability of cells, and specifically mitochondria, to adequately utilize this oxygen is impaired [54]. This phenomenon, eventually termed 'cytopathic hypoxia', may result from direct inhibition of mitochondrial complexes, increased pyruvate accumulation & lactic acidosis, mitochondrial uncoupling, and/or depletion of factors needed for oxidative phosphorylation (i.e. NAD+/NADH) [54, 55]. This mitochondrial dysfunction results in a decrease in state 3 respiration and an increase in state 4 respiration, which subsequently increases O_2^- and H_2O_2 production [51]. The increase in free radical production further impairs mitochondrial function by decreasing mitochondrial DNA (mtDNA) content, promoting a 3.8 kb mtDNA deletion, and attenuating mitochondrial gene expression [56].

1.3.2 Mitochondrial biogenesis

As mitochondria age, are damaged, or respond to an increased energy demand, the cell will attempt to enhance is respiratory function by promoting mitochondrial quality control (QC). This includes mitochondrial autophagy (mitophagy) and

mitochondrial biogenesis. Mitophagy involves the sequestration and degradation of damaged mitochondria and mitochondrial biogenesis is the process by which new mitochondria are formed. Nisoli further defined mitochondrial biogenesis as the ability to increase oxidative phosphorylation and ATP production to meet energy demands, increase synthesis of new organelle components which are integrated into the existing mitochondria, and import nuclear transcribed proteins into the mitochondria that are needed for appropriate metabolic function [57]. Mitochondrial biogenesis is activated by cellular stress or damage and requires the interplay of both mitochondrial and nuclear genes. The mitochondrial genome encodes 37 genes: 13 genes for ETC subunits, 22 tRNA genes, and 2 rRNA genes. Therefore, most of the hundreds to thousands of proteins that are required for mitochondrial function are encoded by nuclear DNA and must be imported into the mitochondria.

In sepsis, the goal of mitochondrial biogenesis is to restore mitochondrial mass and repair mtDNA damaged by inflammation. Damaged mitochondria send retrograde signals to the nucleus, increasing the expression of nuclear factors involved in mitochondrial biogenesis [58-60] (***Figure 2***). The family of peroxisome proliferator-activated receptor gamma co-activator (PGC) proteins is a group of three co-activators that regulate genes involved in fatty acid oxidation, oxidative phosphorylation, and mitochondrial biogenesis [61, 62]. This family consists of PGC-1α, PGC-1β, and PGC-1 related coactivator (PRC) [61, 63, 64]. They all lack known intrinsic enzymatic activity, but instead function as a scaffold for other proteins that remodel chromatin for

transcription factor binding [62]. Nuclear respiratory factors-1 and 2 (NRF-1 and NRF-2) are transcription factors that drive expression of genes involved in mitochondrial respiration, mtDNA transcription and replication, heme biosynthesis, and protein importation [65]. Collectively, PGC coactivators and NRF transcription factors coordinate the bigenomic activation of mitochondrial biogenesis by promoting nuclear transcription of mitochondrial transcription factors A and B (Tfam and TFB, respectively) and DNA polymerase-γ (pol-γ) [58]. While TFB is important for mitochondrial promoter recognition, Tfam is crucial in mitochondrial biogenesis as it facilitates replication and transcription of mtDNA in mammals [66]. Binding of Tfam, TFB, and pol-γ to mtDNA appropriately activates mtDNA replication [67].

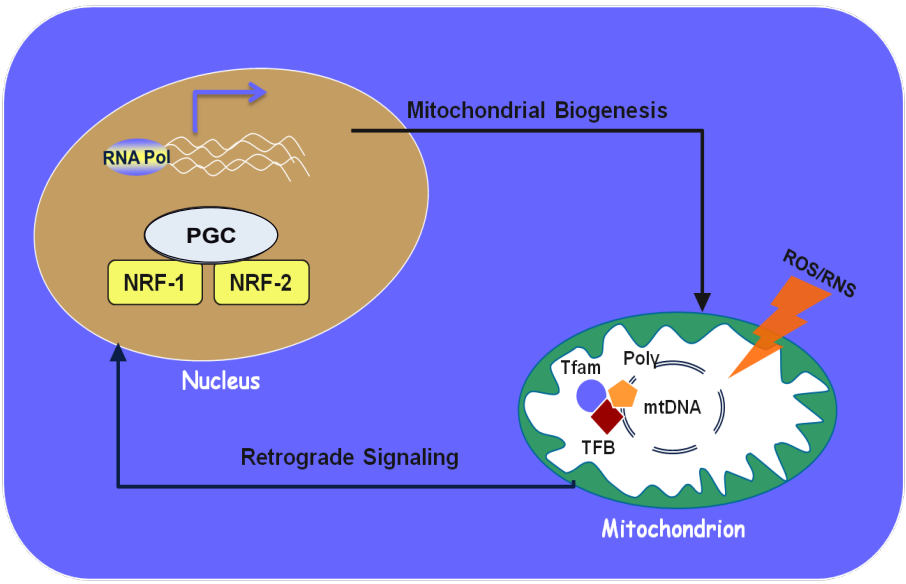

Figure 2: Key nuclear and mitochondrial factors involved in mitochondrial biogenesis. ROS/RNS-induced mitochondrial damage signal to nucleus to increase production of PPAR-γ coactivators (PGC) and DNA-binding transcription factors, nuclear respiratory factors-1 and -2 (NRF-1, NRF-2). These proteins facilitate the transcription of nuclear genes that encode for proteins that promote mitochondrial transcription and replication, e.g. mitochondrial transcription factors A and B (Tfam, TFB) and DNA polymerase-γ.

Extensive work has demonstrated that mitochondrial biogenesis is required for restoration of organ function and host survival. PGC-1, NRF-1, NRF-2, and Tfam have all been shown to be important in mitochondrial recovery and when these key players are reduced or absent, necrosis and organ dysfunction prevail [68, 69]. Importantly, Tfam helps regulate mammalian mtDNA copy number, and in mice, Tfam disruption causes cytopathy, embryonic lethality, and diabetes secondary to mtDNA depletion and loss of oxidative phosphorylation [70]. Mice deficient in PGC-1α were not protected from acute renal damage in response to endotoxemia [71]. Our lab has further demonstrated that the induction of mitochondrial biogenic factors is required for protection against live *S. aureus* sepsis [72], *S. aureus* pneumonia [73], and *E. coli* sepsis [74]. Subsequently, greater emphasis has been placed on understanding how mitochondrial biogenesis is activated and regulated so that this protective process can potentially be exploited for therapeutic benefit in clinical sepsis.

1.3.3 Heme oxygenase-1 and mitochondrial biogenesis

Heme oxygenases (HO) are the rate-limiting enzymes in heme catabolism. They metabolize heme to biliverdin with the production of carbon monoxide (CO) and iron. Similar to NOS, constitutive and inducible isoforms of HO have been described; HO-1 is induced during inflammation and oxidative stress while HO-2 is constitutively active. HO-1 has been known to confer protection through anti-apoptotic, anti-inflammatory,

and anti-tumorigenic mechanisms, many of which are thought to be mediated by CO [75]. More recently, HO-1 and CO have been linked to mitochondrial biogenesis. In a study that subjected mice to CLP sepsis, HO-1/CO promoted PGC-1α expression and reduced mortality [76]. Furthermore, our lab has demonstrated that HO-1/CO activates mitochondrial biogenesis in the heart through the H_2O_2-dependent activation of PI3K/Akt [77]. Moreover, we have confirmed that CO activates the mitochondrial biogenic pathway in human skeletal muscle [78] and, in mice, protects against doxorubicin cardiotoxicity [68] and live *S. aureus* sepsis [72]. Subsequently, our lab continues to study the mechanism for CO protection as a potentially translatable therapeutic option in human sepsis.

1.4 The role of nitric oxide in sepsis

1.4.1 NO and sepsis pathogenesis

Large amounts of NO are produced by NOS2 during sepsis at levels that damage host cells and organ function. Within the cardiovascular system, NO overproduction is associated with hypotension and shock via cGMP-mediated vascular smooth muscle cell relaxation. NO may also compromise myocardial contractility and impair cardiomyocyte survival, thus promoting heart failure and poor clinical outcomes [79-81]. NO impairs mitochondrial activity by inhibiting cytochrome oxidase and ubiqinone, causing an increase in O_2^- and H_2O_2 [82]. When energy supplies are low, the reduction in oxidative metabolism may be beneficial; mitochondrial QC mechanisms have more time

to repair mtDNA damage and restore mitochondrial function. However, when NO combines with excess O_2^- or H_2O_2, peroxynitrite (ONOO-) is formed, which in an acid milieu, decomposes to NO_2 and hydroxyl radicals that damage DNA and protein through nitration and/or oxidation. This especially occurs within the mitochondria where mtDNA is in closest proximity to ROS/RNS generation and associated with very few protective DNA binding proteins [56, 83].

Although NO is clearly involved in the pathogenesis of cellular dysfunction in sepsis, attempts to inhibit NO production have not proven therapeutically beneficial in humans. For example, studies using non-specific NOS inhibitors were terminated during Phase II and Phase III clinical trials because of increased mortality[84-86]. Therefore, the protection afforded by NOS2 likely reflects balanced NO production that activates pro-survival responses with minimal overt NO toxicity, inflammation, and cell damage.

1.4.2 NO and cellular protection

Based on the failed attempts to inhibit NOS2 in sepsis patients, greater emphasis has been placed on studies exploring the protective effects of NO. Physiologically, NO is necessary for vascular patency and indispensible for vascular responsiveness to vasoactive drugs. Although some post-translational S-nitrosylation of nucleic acids, lipids, and proteins may be undesirable, many modifications are necessary for normal or enhanced protein function. For example, S-nitrosylation of caspase-8 in rat hepatocytes protects against TNF-α-mediated apoptosis [87] and deletion of NOS2 exacerbates

apoptosis of cardiomyocytes and hepatocytes [88, 89]. NO has also been shown to protect mitochondria by both maintaining membrane potential and promoting biogenesis [90, 91]. Specifically NOS1 and NOS3 activate guanylate cyclase in neurons and adipocytes, respectively, thereby facilitating cGMP-dependent PGC-1α expression [57, 92-94]. No comparable role for NOS2 had been identified prior to the work presented in this dissertation, but here I hypothesized that NOS2 is necessary for cell survival, in part, by optimizing mitochondrial biogenesis.

1.4.3 Transcriptional regulators of NOS2 expression

Despite confirmed NO-mediated pathology in sepsis, NOS2 is necessary for survival in animal and human studies. This confirms that balanced production of NO is required for optimal host survival (***Figure 3***). Insufficient NO production compromises pathogen clearance, vascular hemodynamics, and mitochondrial regulation while excess NO causes cellular dysfunction and shock. The most regulated step in inducible NO production occurs at the mRNA level so transcriptional control has been a major research interest for diseases characterized by high NOS2 expression.

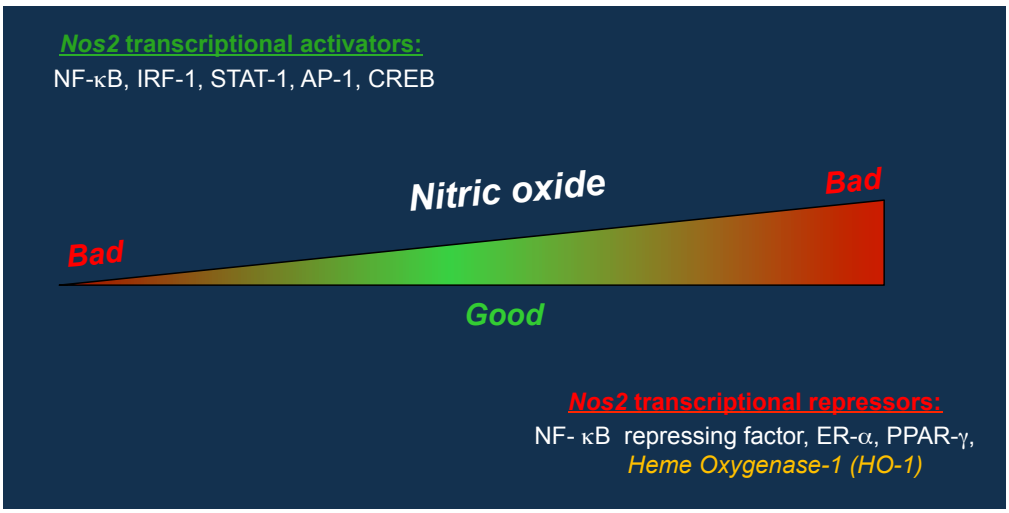

Figure 3: The balance between *Nos2* transcriptional activation and repression. The transcriptional regulation of *Nos2* is important because balanced production of NO is critical for preventing detrimental effects on normal circulatory and cellular physiology.

The *Nos2* gene is transcriptionally silent in unstimulated cells, but during Gram-negative infections, cytokines and LPS synergistically optimize transcription of the gene. While LPS activation of the TLR4 pathway increases nuclear NF-κB, cytokines such as TNF-α, IFN-γ, and IL-1β are needed for the recruitment of additional transcription factors to the *Nos2* gene promoter [95]. IFN-γ is the most potent co-activator of *Nos2* in LPS-treated murine macrophages [96], perhaps because of the ability of IFNs to upregulate IFN-regulatory factor 1 (IRF-1) [97, 98] and signal transducer and activator of transcription-1 (STAT-1) [99]. Activator protein-1 (AP-1) and cAMP responsive element binding protein (CREB) also participate in the transcriptional expression of *Nos2* [100]. These transcription factors collaboratively promote mRNA synthesis, which is quickly translated into proteins that dimerize and associate with cofactors, such as heme and calmodulin, to generate the functional NOS2 enzyme.

Nos2 transcriptional repression is a much more limited area of research. Since NF-kB is well recognized as a necessary component for NOS2 expression, the majority of studies showing reductions in *Nos2* transcription have involved interference in NF-kB promoter binding, whether by preventing heterodimer formation, blocking DNA binding, or increasing cytosolic IκB [100-102]. Other potential repressors of *Nos2* include NF-κB repressing factor, estrogen receptor (ER)-α, and peroxisome proliferator-activated receptor (PPAR)-γ but these have not been well characterized [100]. Of specific interest here, reports have also shown that HO-1 negatively regulates NOS2. Proposed mechanisms include direct inhibition of the NOS2 enzyme by CO [103] and activation of pathways that would ultimately block transcription [104]. Unfortunately, the specific changes in transcription factor recruitment and binding at the *Nos2* promoter that are mediated by HO-1/CO activity have not been thoroughly investigated.

1.4.4 Cross talk between HO-1 and NOS2 pathways

NO and CO are gaseous modulators that are made endogenously and mediate intracellular signaling through their interaction with specific targets [105]. These gases share several common characteristics. Both gases act as second messengers in cellular processes such as smooth muscle relaxation, vascular responsiveness, and anti-inflammation [106]. However, when levels are too high, both contribute to disease pathology. NO and CO have been shown to competitively inhibit O_2 binding to cytochrome oxidase, thus increasing ROS production within the mitochondria [107, 108]. In response to Gram-negative challenge, HO-1 and NOS2 are highly inducible and yield

high levels of their respective gases. Subsequently, these similarities have prompted investigations focused on characterizing the interaction between the HO-1/CO and NOS2/NO pathways.

In several inflammatory models, NO/NOS2 has been shown to further enhance HO-1 activity and CO production. This relationship has been confirmed in cardiomyocytes, adrenal gland, vascular smooth muscle cells (SMC), hepatocytes, and Kupffer cells [109-113]. Various mechanisms have been described and include induction of HO-1 by cGMP signaling and recruitment of transcription factors to the *Hmox1* promoter (i.e. NF-κB p50/p65 and nuclear Nrf2) [109, 111, 112]. As a result, some of the protective effects of NOS2 may result from HO-1 downstream signaling.

Conversely, several studies suggest that HO-1 inhibits NOS2 expression and/or activity. Experimental designs have included rats subject to ischemia/reperfusion injury or endotoxemia [114, 115], LPS treated macrophages [103, 116, 117], and IL-1β-treated astrocytes [104]. Several mechanisms for NOS2 suppression have been suggested. HO-1 can inhibit NOS2 activity by reducing the availability of heme, a cofactor that is required for the dimerization and activity of NOS2, or the direct binding of CO to the enzyme [103, 118]. CO can also repress NOS2 at the transcriptional level, as seen in reports linking HO-1/CO to reduced p38 MAPK signaling, deactivation of STAT-1 or STAT-3 [114], or enhanced IL-10 production [114, 119-121]. Otterbein, et al. demonstrated that CO increased IL-10 levels, thereby reducing serum TNF-α levels in LPS-treated mice and RAW264.7 macrophages [119]. Most recently, our lab demonstrated that HO-1/CO has

this same effect in a model of murine *E. coli* sepsis [120] but no direct relationship between HO-1, IL-10, and NOS2 has been confirmed. Much less is known about the ability of other HO-1 metabolites to reduce NOS2 expression or activity but a few studies have associated hyperbilirubinemia with NOS2 inhibition in rat models [122-124].

Unfortunately, most studies showing NOS2 inhibition by HO-1 are inadequate because they often report associated changes in transcriptional pathways that were never proven to directly reduce *Nos2* activation. This lack of a definite link between the transcriptional network and NOS2 promoter activity must be addressed before we can expect to develop meaningful clinical applications. Therefore, the Aim of the second part of this thesis was to 1) demonstrate that HO-1 suppresses *Nos2* gene induction during Gram-negative challenge and 2) better characterize the mechanism for this relationship in liver cells. Due to significant limitations of the model chosen for this study, actual transcriptional regulatory mechanisms were not assessed. However, this work suggests that future evaluation of NOS2 transcriptional control should focus more on the recruitment of specific transcription factors, such as NF-κB, STAT-1, STAT-3, and CREB, to the *Nos2* promoter. Ideally, this knowledge would enhance our ability to therapeutically target the HO-1/CO pathway in inflammatory conditions and thus simultaneously attenuate inflammation and recruit mitochondrial repair mechanisms.

1.5 Mouse models of sepsis

Animal models have been used for decades to recapitulate the systemic findings

in sepsis. Due to the complex nature of human sepsis, finding an appropriate *in vivo* model has been challenging. Most studies have been conducted in mice and rats because of their small size, low cost, and availability of genetic variants. However, these models of sepsis are limited by the difficulties in monitoring cardiopulmonary parameters and recapitulating the dynamic immunologic and physiologic responses that occur in septic patients. Furthermore, new data shows that although the genetic signatures seen in burn, endotoxic, and trauma patients are very similar, they correlate poorly with the genetic profile of their relevant mouse models [125]. Animal models of clinical sepsis must therefore be interpreted cautiously. Meaningful information has been obtained from animal studies, but data over-interpretation may account for the failure of novel clinical approaches that showed promise in preclinical studies [126, 127]. Several commonly used mouse models are reviewed below.

"Endotoxemia" Injection Models: Large doses of LPS injected in the peritoneum or tail vein of mice were used in original models of sepsis. To produce cytokine responses similar to humans, mice must be given 250 times higher doses of LPS [128]. Challenged animals respond by inducing a massive, transient production of cytokines peaking between 1.5-4.5 hours [129]. LPS has also been administered to healthy patients who mount a systemic response that is similar to that of patients with bacterial sepsis. However, translation of therapies derived from animal endotoxemia models to clinical trials for human sepsis has been unsuccessful. This is largely due to significant differences in the physiological response in mice versus humans. For instance, the

cytokine response in endotoxic mice peaks earlier and to a greater degree than in patients with sepsis [130]. Furthermore, endotoxic mice elicit a hypodynamic, low cardiac output CV response without the initial hyperdynamic state observed in human sepsis. This high output CV state may be observed if animals are given LPS infusions and fluid resuscitation but generally, endotoxic models are characterized by a much faster disease progression than what is typically observed in human patients. Comparatively, inoculations of heat-killed and live bacteria enable a response that is directed at the whole microbe but, when given in a single, high-dose, have physiologic responses that mirror that of LPS injections.

"Sepsis" Surgical Models: Animal models that require a surgical intervention are currently considered the closest correlate to human sepsis. Implantation of bacterial fibrin clots into the peritoneum of larger animals creates a sepsis phenotype with a more gradual disease progression, hyper- and hypodynamic CV states, and delayed mortality [131, 132]. Our lab subsequently developed a mouse model of fibrin clot implantation that demonstrates dose-dependent mortality, progressive weight loss, decreased metabolic activity, and gradual cytokine induction [69]. This model correlates well to single-microbe infections implicated in human sepsis, such as *E. coli* urosepsis and *S. aureus* pneumonia. Alternatively, cecal ligation and puncture (CLP) can be used to simulate sepsis from intestinal perforation or mixed-microbe infections. In this instance, the cecum is tied off and pierced with a needle to allow GI flora to leak into the peritoneal cavity [133, 134]. Cytokine levels in this surgical model are significantly lower

and more sustained than the endotoxin model. However, significant variability can occur in mice due to different genetic backgrounds, sex, technical approach, and supportive care given post-operatively [130]. This model is limited by the occurrence of necrotic bowel and abscess formation, and standardization of technique used by various labs.

When evaluating the host response to *E. coli*, our lab most frequently uses surgical fibrin clot implantation and heat-killed bacteria injected IP. Both models are used in this dissertation with the bulk of data generated in the heat-killed *E. coli* (*HkEC*) peritonitis model. Initial survival studies were conducted in the setting of live *E. coli* fibrin clot peritonitis, but *HkEC* was used for mechanistic studies to avoid differences in bacterial load in control versus NOS2 and TLR4-deficient mice. Furthermore, experiments evaluating mitochondrial biogenesis in this dissertation were performed in the heart, but later confirmed by my lab in the liver. *Nos2* transcriptional regulation was subsequently evaluated in the liver since both heme oxygenase-1 and NOS2 show strong induction in this organ.

2. NOS2 promotes mitochondrial biogenesis during *E. coli* peritonitis

The first Aim of this thesis project was to define the protective role of NOS2 in a model of Gram-negative infection as it pertains specifically to mitochondrial biogenesis and cell respiration. Both NOS1 and NOS3 isoforms have been shown to induce mitochondrial biogenesis in neurons and adipocytes, respectively. Therefore, this Aim was based on the hypothesis that NOS2 is indispensible for cell survival and organ function in sepsis through mitochondrial biogenesis. To test this hypothesis, several endpoints were evaluated in C56BL/6 wild type (Wt), $NOS2^{-/-}$, and TLR4-/- mice infected with *E. coli*. These endpoints included survival, mitochondrial function, nuclear transcription factors/co-activators, and mitochondrial effectors that are critical for mitochondrial biogenesis in cardiac tissue. The survival study was originally published by HB Suliman, A Babiker, CM Withers, et al. in 2010 [135]. All mitochondrial biogenesis data using Wt, $NOS2^{-/-}$, and $TLR4^{-/-}$ mice was published by CM Reynolds, HB Suliman, JW Hollingsworth, et al. in 2009 [136].

2.1. NOS2 protection during E. coli fibrin clot peritonitis

To determine whether NOS2 is necessary for survival in *E. coli* sepsis, fibrin clots containing 10^7 live *E. coli* were implanted surgically into the peritoneal cavities of Wt and $NOS2^{-/-}$ mice. Animals were monitored for one week after which any surviving mice were euthanized. As shown in ***Figure 4***, survival differences were observed as early

as two days with NOS2$^{-/-}$ mice being more sensitive to live bacterial sepsis (83% vs 41% survival in Wt vs NOS$^{-/-}$ mice, $p<0.05$). Only 17% of NOS2-deficient mice survived longer than 4 days. This supports prior studies depicting increased susceptibility of NOS2$^{-/-}$ mice to live bacteria [137].

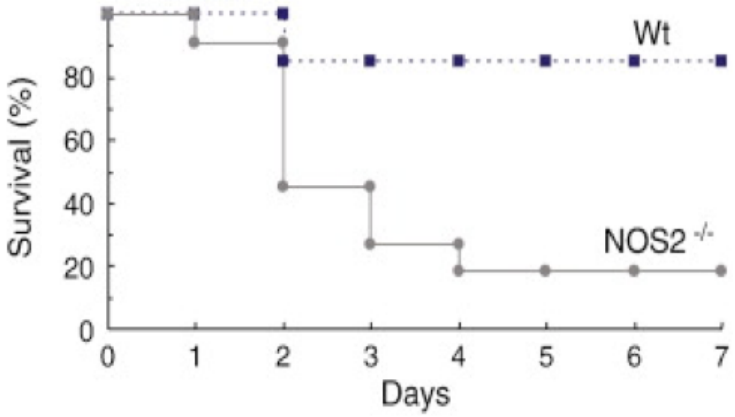

Figure 4: Survival curve for *E. coli* fibrin clot peritonitis. Clots containing 1x10^7 Alive bacteria were surgically implanted into the peritoneum of Wt and NOS2$^{-/-}$ mice. Survival reflected higher mortality in NOS2-deficient animals. ($p<0.05$, n=12 per group).

Bacteremia was assessed in both mouse strains by culturing blood taken from the hearts of mice 24 hours after surgery. Blood cultures showed that while Wt mice were effectively able to control the bacterial inoculum, NOS2$^{-/-}$ mice developed significant bacteremia (***Figure 5***), likely contributing to the lethality in knockout (KO) mice. Since the differences in bacterial burden can significantly alter physiologic responses in NOS2-deficient mice, further mechanistic studies were performed using the sublethal *HkEC* model of peritonitis. Increasing doses of *HkEC* were administered to Wt and NOS2$^{-/-}$

mice (data not shown) and a dose of 10^8 CFU *HkEC* was the highest amount that could be administered without lethality in KO mice.

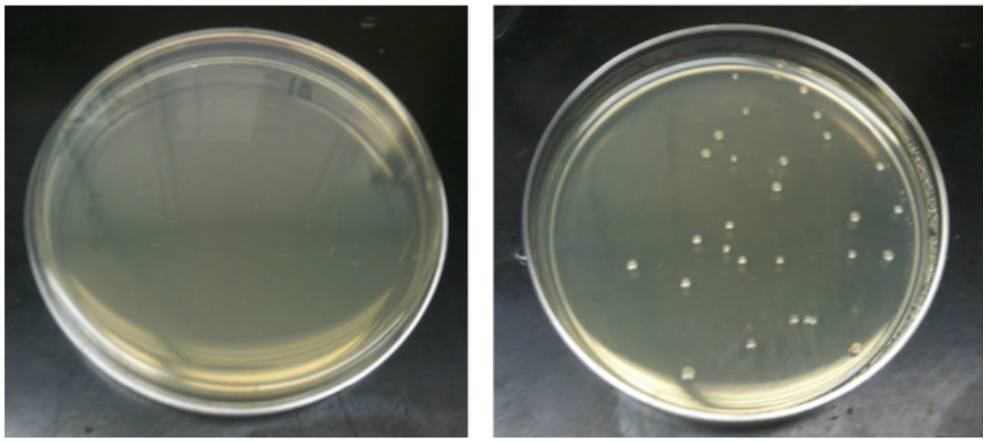

Figure 5: Bacterial burden in Wt and NOS2$^{-/-}$ mice with 10^7 CFU *E. coli* fibrin clot sepsis. Blood from intracardiac aspiration 24 hours after surgery was inoculated on LB agar plates and observed for colony growth 18-24 hours later. NOS2-deficent mice become bacteremic while Wt mice mostly contained their infections. Picture is representative of triplicate experiments.

2.2. *Effect of NOS2 on mitochondrial damage and dysfunction during HkEC peritonitis*

Since mitochondria are damaged by cytokines and NO produced during sepsis, the pro-inflammatory response to sub-lethal *HkEC* IP was evaluated in NOS2$^{-/-}$ and TLR4$^{-/-}$ mice using quantitative real-time RT-PCR (qRT-PCR). The production of pro-inflammatory IL-1β, IL-6, TNF-α, and leukocyte adhesion molecule ICAM-1 increased rapidly in the hearts of Wt mice, dissipating by 72 hours (***Figure 6***). In contrast, NOS2-deficiency attenuated and delayed cytokine expression, indicating that knockout mice are less responsive to Gram-negative challenge. As expected, TLR4$^{-/-}$ mice mounted no

early pro-inflammatory response to *HkEC* but did generate a late TNF-α response, suggesting delayed activation of an alternative inflammatory pathway.

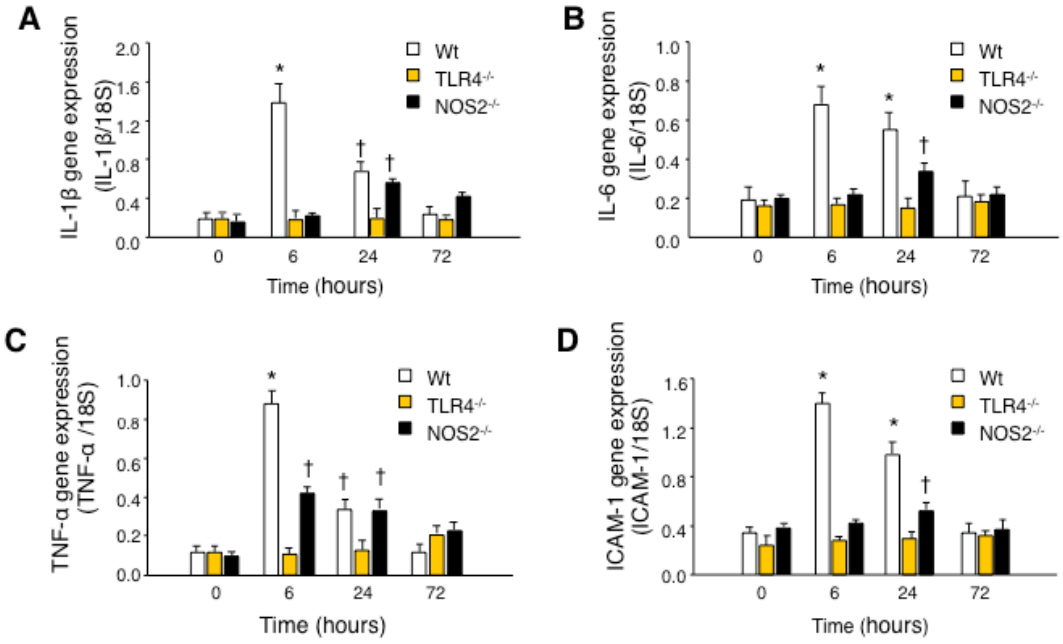

Figure 6: Selected blunting of cytokine responses after *HkEC* in TLR4$^{-/-}$ and NOS2$^{-/-}$ relative to Wt mice. Hearts of Wt, TLR4$^{-/-}$, and NOS2$^{-/-}$ mice collected after *HkEC*. Quantification of A*: IL-1β*, ***B:*** *IL-6*, ***C:*** *ICAM-1*, and ***D:*** *TNF-α* mRNA expression in all three strains by qRT-PCR. †p<0.05 versus 0h Wt. *p<0.05 vs 0h Wt and other strains at same time. (n=3-5 mice per point)

To quantify mitochondrial damage, cytochrome *b* was amplified from isolated mitochondria as an approximation of mtDNA copy number. Copy number fell significantly in both Wt and NOS2-deficient mice 24 hours after *HkEC* peritonitis but only Wt animals were able to fully recover by 72 hours (***Figure 7A***). Consistent with their limited cytokine response, TLR4-deficient mice demonstrated no significant mitochondrial damage until 72 hours, suggesting that late stage mtDNA damage is TLR4-independent. The mtDNA damage observed in Wt and NOS2$^{-/-}$ mice did not,

however, completely correlate with mitochondrial function. After a significant decline in State 3 respiration, both Wt and NOS2-deficient mice regained full mitochondrial function (***Figure 7B***). NOS2$^{-/-}$ mice most likely recovered 72h respiratory capacity in spite of unresolved mtDNA damage because of a compensatory increase in metabolic activity of intact mitochondria. However, it is expected that a second insult would be overwhelming for these KO animals and result in persistent mitochondrial dysfunction and increased mortality.

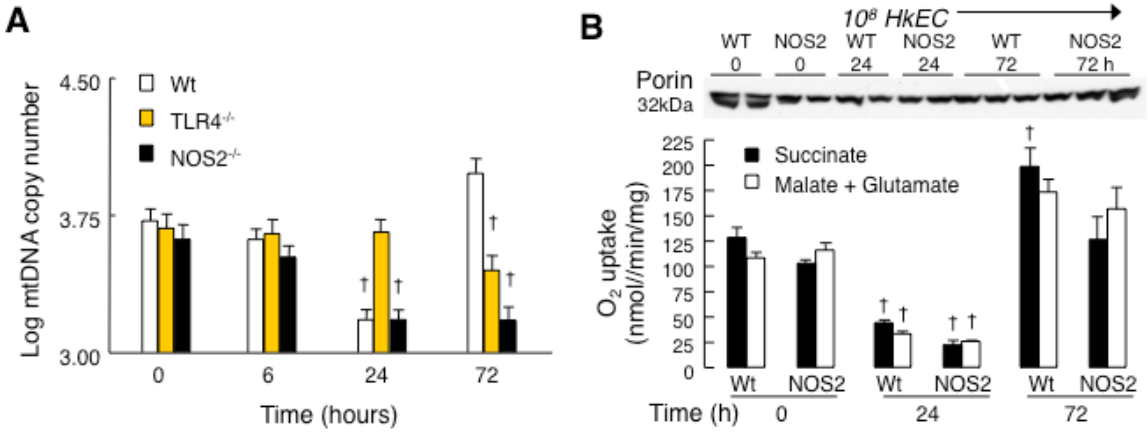

Figure 7: Analysis of mtDNA and mitochondrial function after *HkEC*. Hearts from Wt, TLR4$^{-/-}$, and NOS2$^{-/-}$ mice after 10^8 *HkEC*. ***A:*** MtDNA copy number, as determined by qRT-PCR of cytochrome *b*, plotted logarithmically. ***B:*** State 3 respiration in isolated mitochondria of Wt and NOS2-deficient mice. Outer mitochondrial membrane protein, porin, shown as a loading control. While Wt and NOS2$^{-/-}$ mice both recovered respiratory function after peritonitis, only Wt were able to repair mtDNA damage. †p<0.05 vs 0 h Wt or NOS2$^{-/-}$, respectively. (n=2-5 mice per point)

2.3. *Mitochondrial biogenesis in Wt, NOS2$^{-/-}$, and TLR4$^{-/-}$ mice*

In response to mtDNA damage, cells must increase the production of transcriptosomal proteins that work within mitochondria. Two of the key regulatory

proteins involved in mitochondrial biogenesis, Tfam and pol-γ, were therefore measured in mitochondrial preparations by Western blot. *HkEC* induced the accumulation of both Tfam and Pol-γ by 24 hours in Wt mice but not in TLR4 and NOS2 KO mice (***Figure 8***). The expression of these transcriptosomal proteins preceded the recovery of mtDNA copy number in Wt mice; subsequently, the reduced accumulation of these mitochondrial factors provides an explanation for why NOS2$^{-/-}$ mice are unable to repair their damaged mtDNA.

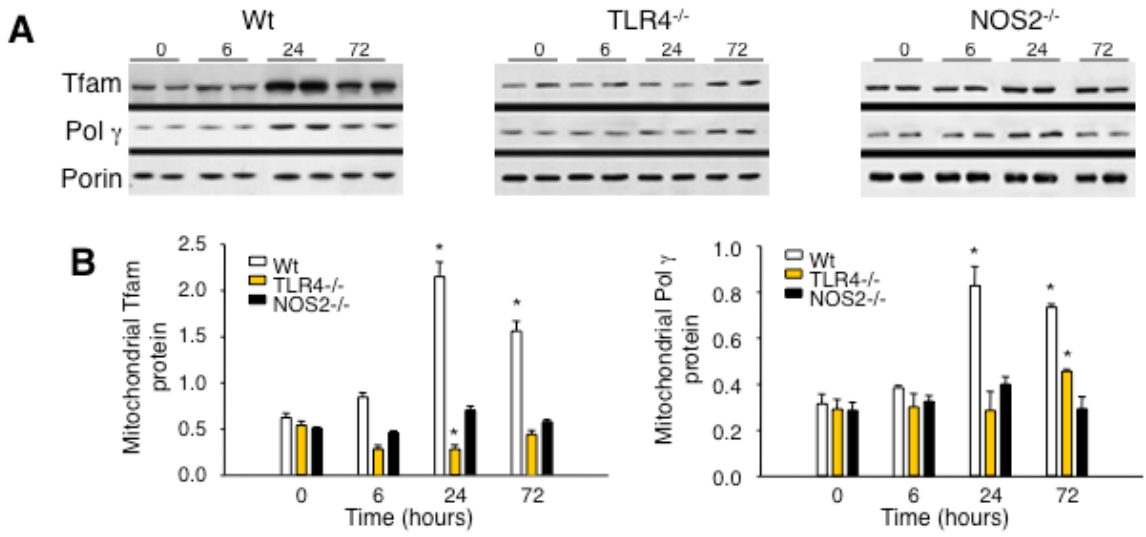

Figure 8: Expression of mitochondrial proteins involved in biogenesis. ***A:*** Western blot of mitochondrial Tfam and Pol-γ in cardiac tissue from *HkEC*-treated Wt, TLR4-, and NOS2-deficient mice. Porin shown as a loading control. ***B:*** Densitometry of westerns represented graphically. Mitochondrial accumulation of these proteins is impaired in KO mice. *p<0.05 vs time 0 and the other two strains. (n=2 per group)

NRF-1 transcription factor and the PGC-1α co-activator coordinate the bi-genomic transcription that occurs in mitochondrial biogenesis by facilitating expression of mitochondrial factors like Tfam and Pol-γ. Evaluation of these upstream regulators

showed that NRF-1 and PGC-1α increased 24 hours after *HkEC* and declined by 72 hours in Wt mice (***Figure 9***). Conversely, the accumulation of these factors is reduced in both knockout mouse strains. Although data is not shown here, activity of Akt and AMP kinase that normally increases six hours after *HkEC* in Wt mice is blunted in KO mice. These pro-survival kinases are known to activate NRF-1 and PGC-1α [68, 138]. Therefore, this data suggests that in the heart, NOS2 is required for the repair of mtDNA through mitochondrial biogenesis by enabling pro-survival kinase activation and subsequent protein expression.

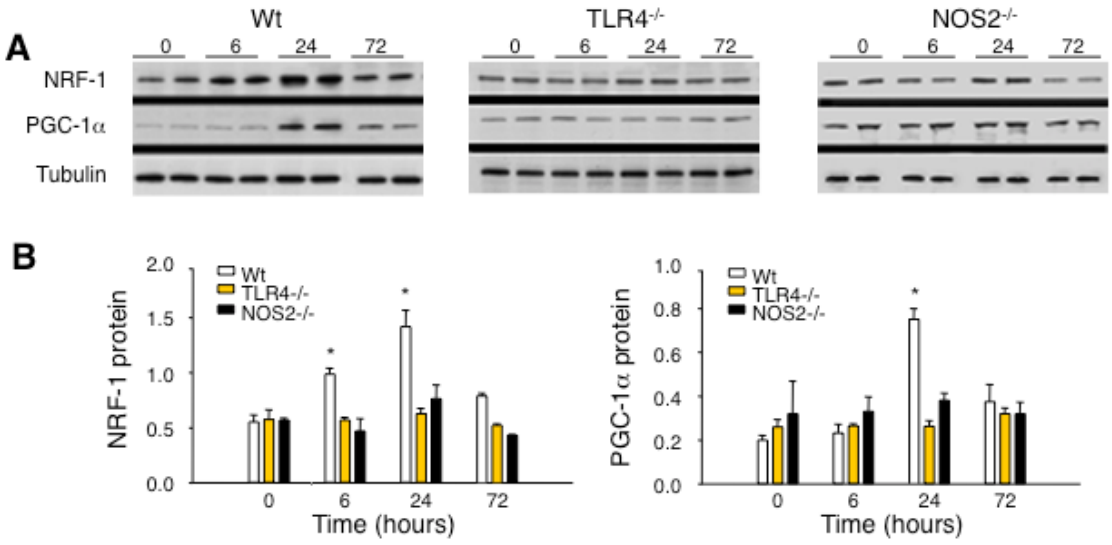

Figure 9: Expression of nuclear proteins involved in mitochondrial biogenesis. ***A:*** Western blot of NRF-1 and PGC-1α in cardiac tissue from Wt, TLR4-, and NOS2-deficient mice after *HkEC* administration. Tubulin shown as a loading control. ***B:*** Densitometry of westerns represented graphically. Nuclear accumulation of these proteins is impaired in KO mice. **p*<0.05 vs time 0 and the other two strains..

2.4. Localization of NOS2 and TLR4 expression following HkEC exposure

NOS2 is expressed in immune cells such as macrophages but also localizes to other cell types including cardiac myocytes and hepatocytes [139-141]. To localize both TLR4 and NOS2 expression in cardiac tissue and evaluate its association with loss of mitochondrial mass, transgenic mice containing a COX8 mitochondrial-tagged green fluorescent protein (GFP) reporter were injected intraperitoneally with *HkEC*. Cardiac sections from these animals were stained using antibodies against TLR4 or NOS2 (red fluorescence). Mitochondrial mass was tracked with green fluorescence. Fluorescence microscopy demonstrated that *HkEC* promoted a loss of cardiomyocyte mitochondrial mass at six and 24 hours, which recovered by 72 hours (***Figure 10A and 10B***, ***a-e***). Since the COX8 mitochondrial leader sequence (MLS) attached to the GFP protein localizes GFP to the mitochondria, the loss of GFP in six-24 hours reflects mitochondrial damage and clearance (mitophagy).

In control hearts, TLR4 expression is seen at low intensity in vascular endothelium but not within the myocardium. However, six hours after *HkEC*, TLR4 expression increases, localizing primarily to the plasma membranes of mononuclear and endothelial cells, and progressively emerging near the sarcolemma and in contiguous cardiomyocytes (concluded from higher magnification photos) (***Figure 10A, f-j)***. The presence of TLR4, therefore, associates first with the onset of mitochondrial damage and then recovery through mitochondrial biogenesis, both of which have been identified as TLR4-dependent processes.

NOS2 protein was also not visualized in control hearts but evident six hours after *HkEC* challenge, primarily in the vascular wall and less prominently in the sarcoplasm at six, 24, and 24 hours (***Figure 10B***, ***f-j***). Accordingly, the induction of NOS2 appears to coincide with mitochondrial damage and persist through the initiation of mitochondrial recovery, supporting both damaging and protective roles of NOS2 *in vivo*.

The findings presented in this first Aim demonstrate that NOS2 is necessary for protection in Gram-negative challenge because it optimizes the mitochondrial biogenic response to mtDNA damage in the heart. Even in the absence of NOS2, *HkEC* damages mitochondria likely by other TLR4-mediated inflammatory mediators such as TNF-α, but $NOS2^{-/-}$ mice show a clear deficiency in their ability to recover from this mtDNA damage. Furthermore, NOS2 appears to participate in the early activation of mitochondrial biogenesis. In the liver, NOS2 is involved in the phosphorylation of kinases, Akt and AMPK, quote possibly through activation of the NO/cGMP pathway [142]. In cardiac tissue following *HkEC* peritonitis, NOS2 is required for S-nitrosylation of Hsp60, a chaperone protein that aids in mitochondrial importation [143], and subsequent association with Tfam [135]. Therefore, NOS2 supports mitochondrial biogenesis in the heart and liver of *E. coli* challenged mice by at least two mechanisms: optimal expression of mitochondrial biogenic proteins and translocation of proteins into the mitochondria.

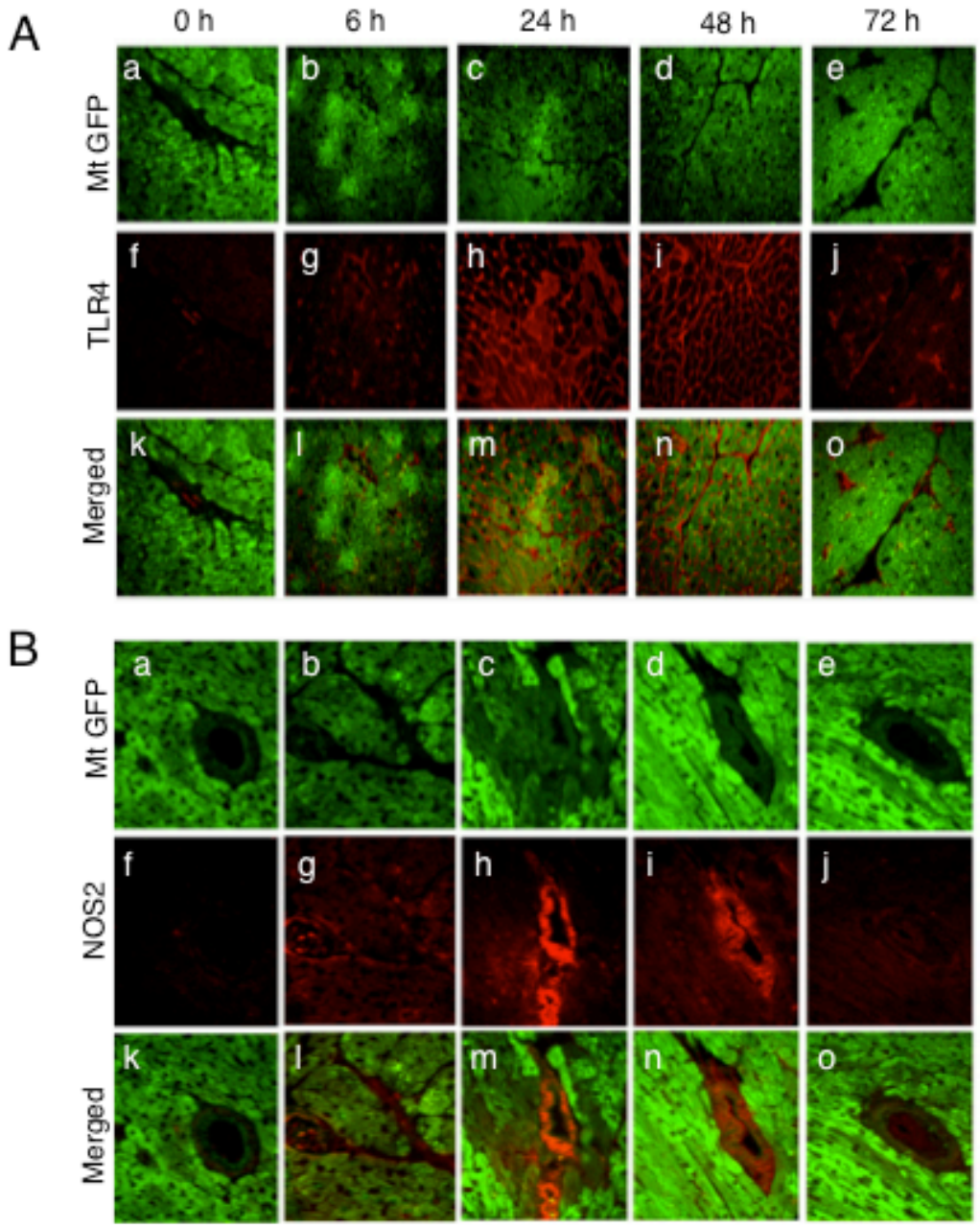

Figure 10: Immunofluorescence for COX8, TLR4, and NOS2 in mitochondrial reporter mice following *HkEC* exposure. ***A:*** Formalin-fixed, paraffin-embedded cardiac tissue visualized for ***a-e:*** COX8 (green fluorescence), ***f-j:*** TLR4 (red fluorescence), and superimposed in panels ***k-o*****.** *B:* Formalin-fixed, paraffin-embedded cardiac tissue visualized for *a-e*: COX8 (green fluorescence), ***f-j*****:** NOS2 (red fluorescence), and superimposed in panels ***k-o*****.** TLR4 and NOS2 were induced with mitochondrial damage and sustained through initiation of mitochondrial recovery**.**

3. The Role of HO-1 in *Nos2* Transcriptional Regulation during *HkEC* Peritonitis

The second Aim of this research project was to evaluate NOS2 expression in a model of Gram-negative peritonitis when HO-1 enzyme activity is enhanced. This objective was based on the hypothesis that HO-1 dampens the immune response through endogenous CO generation from heme metabolism, in part by specifically repressing *Nos2* expression. To test this hypothesis, C56BL/6 wild type (Wt) mice were challenged with a sub-lethal dose of 10^8 CFU *HkEC* and the effect of HO-1 activation was evaluated in the liver. The endpoints being measured included mRNA expression of *Hmox1*, *Nos2*, and acute phase cytokines; protein expression of NOS2 and HO-1; and availability of IκBα and NF-κB. A visual representation of the experimental setup is shown in ***Figure 11***.

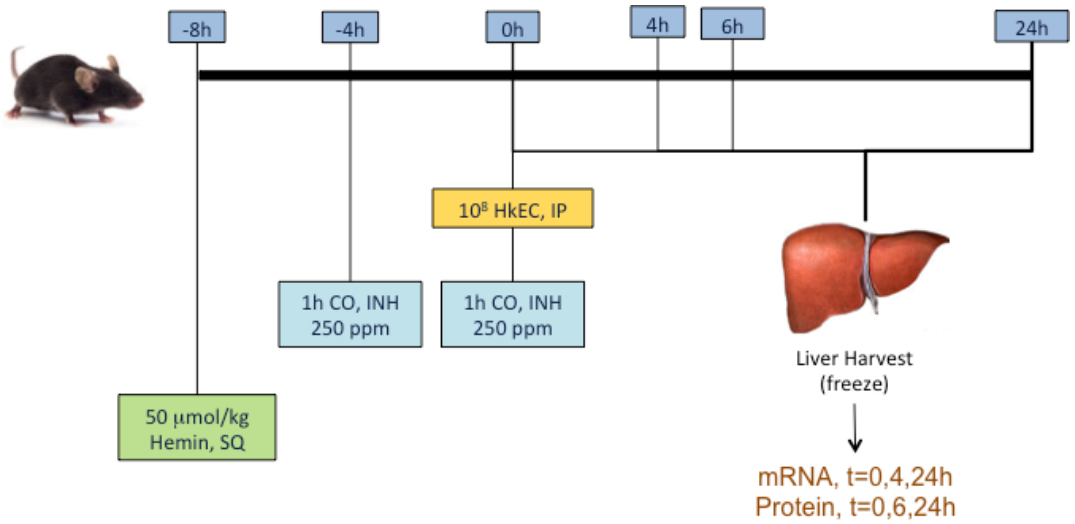

Figure 11: Experimental design for *in vivo* mouse *HkEC* peritonitis studies. Mice were administered subcutaneous (SQ) hemin 8 hours before *HkEC* or inhaled (INH) CO 4h before and at the time of 10^8 *HkEC* injection. Liver was harvested at indicated times.

3.1. HO-1 control on NOS2 expression

In order to evaluate the effect of HO-1 on NOS2 expression, the gene expression profiles of both *Nos2* and *Hmox1* were analyzed after injection of a single dose of 10^8 CFU *HkEC* in Wt mice (***Figure 12***). As expected for Gram-negative challenge, expression of *Nos2* in the liver increased quickly, with an approximate 300x induction evident at 4 hours that quickly declined through 24 hours (***Figure 12A***). *Hmox1* mRNA levels rose more gradually, steadily increasing through 24 hours (***Figure 12B***). For the duration of the *in vivo* work, changes in *Nos2* expression were evaluated four hours after *HkEC* exposure. This time was selected because it corresponded to peak *Nos2* mRNA expression. Furthermore, it is feasible that transcriptional control mechanisms that could suppress the most acute and robust *Nos2* response would also be effective at later, less intense stages of transcriptional activation. Unfortunately, the high variability in peak mRNA levels in animals harvested at this early time point was not initially considered but became problematic in later analysis.

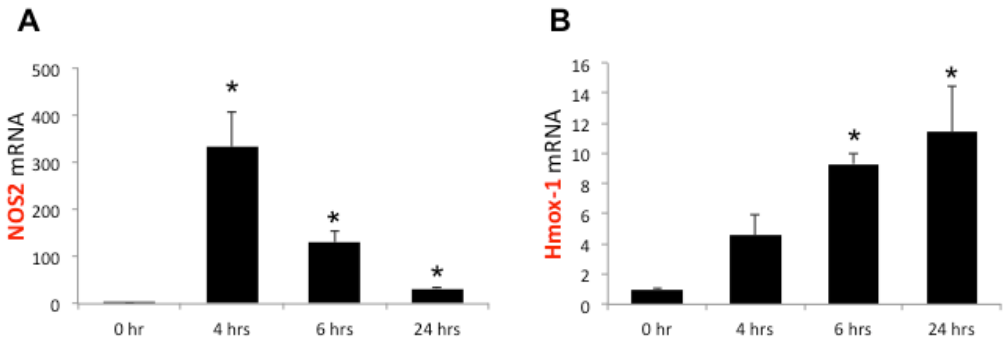

Figure 12: Induction of *Nos2* and *Hmox1* mRNA following *HkEC* peritonitis in mice. Wt mice were injected with 10^8 *HkEC* IP. ***A:*** *Nos2* and ***B:*** *Hmox1* mRNA expression in the liver using qRT-PCR. Values plotted as fold change vs 0 hr controls. *p<0.05 vs 0 hr controls. (n=3-7 mice per time point)

In this mouse model of *HkEC* peritonitis, HO-1 activity was enhanced by pretreating the mice with hemin or CO. Hemin is a substrate for the HO-1 enzyme and a potent inducer of the gene, thus stimulating enzyme activity and the endogenous production of CO, biliverdin, and iron. Exogenous CO acts downstream of the HO-1 enzyme but also exerts positive feedback on protein expression. The increase in HO-1 activity over *HkEC* alone in the liver was confirmed when animals were pretreated with subcutaneous (SQ) hemin (50 μmol/kg) (***Figure 13)***. Although a single 4h pretreatment of inhaled (INH) CO (250 ppm x 1 hour) before *HkEC* did not significantly increase HO-1 activity, two doses of CO (2xCO) did enhance 4h enzyme activity over *HkEC* alone. Therefore, subsequent animal experiments used hemin and 2xCO pretreatments for HO-1 activation. In an attempt to suppress HO-1 activity, zinc protoporphyrin (ZnPP, 3 mg/kg) was given four hours before *HkEC* exposure but these mice demonstrated no change in enzyme activity over *HkEC* alone (data not shown) and were not analyzed in any experiments described in this dissertation.

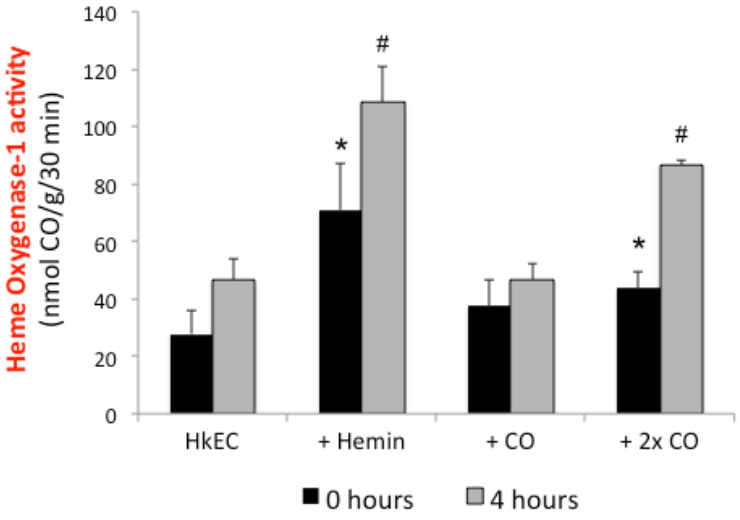

Figure 13: HO-1 activity was induced in *HkEC*-treated Wt liver by pretreatment with hemin or 2xCO. Wt mice given hemin or CO prior to 10^8 *HkEC*. Mice sacrificed at the time of *HkEC* injection (black bars) or four hours later (grey bars). HO-1 activity approximated using CO detection by gas chromatography. *p<0.05 vs 0h *HkEC*, $^{\#}p$<0.05 vs 0h matched treatment. (n=3-4 per group)

After establishing that hemin and CO activated HO-1 enzyme activity, mRNA expression was then evaluated in control animals. Wt mice were given hemin or 2xCO alone before quantifying hepatic *Nos2* and *Hmox1* mRNA expression. Hemin-treated mice were evaluated at 8 hours and 2xCO-treated mice at four hours to assess mRNA levels at the time when *HkEC* would be administered (0 hours, relative to *HkEC* injection). Hemin treatment induced *Nos2* and *Hmox1* expression at 8 hours with *Nos2* expression continuing to increase through 24 hours (***Figure 14, A-B***). CO treatment had minimal effects on mRNA levels for either gene (***Figure 14, C-D***). This was in contrast to previous data from my lab and from other labs that have verified the ability of CO to enhance *Hmox1* mRNA expression. This discrepancy is unexplained, but could

potentially indicate baseline *Hmox1* gene activation in some healthy control animals that disguised fold change differences at low levels of mRNA induction.

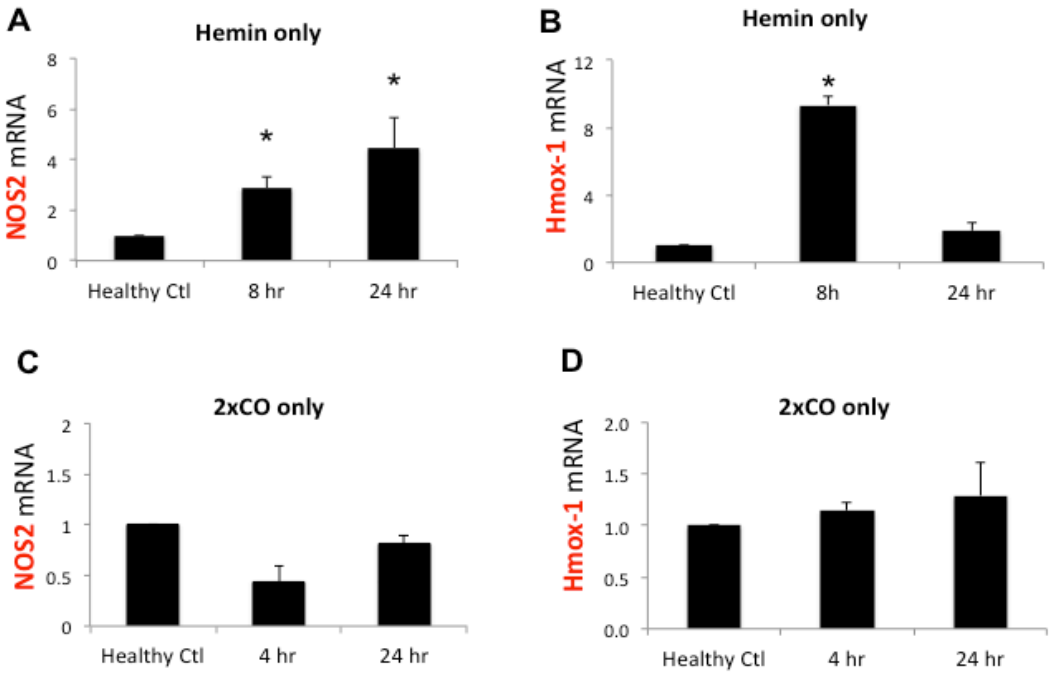

Figure 14: Hepatic *Nos2* and *Hmox1* mRNA expression induced in hemin but not 2xCO control-treated mice. Mice were given ***A-B:*** hemin or ***C-D:*** 2xCO and *Nos2* and *Hmox1* mRNA quantified using qRT-PCR. Results plotted as fold change vs healthy control. **p*<0.05 vs healthy control. (n=3 mice per group)

Mice were then pretreated with hemin or 2xCO prior to *HkEC* challenge. Four hours later, *Nos2* expression was reduced and *Hmox1* enhanced by hemin and 2xCO relative to *HkEC* alone; this was not statistically significant due to the wide range of values obtained (***Figure 15, A-B***). Fold change values were much higher than those seen in Figure 12 because samples were analyzed on the StepOne Plus Real-Time PCR system, which exhibited higher sensitivity than the 7700 Sequence Detector System used for earlier gene quantification (*Figures 6-7, 12, 14*). Protein expression correlated with

mRNA levels. Six hours after *HkEC,* NOS2 protein expression was inhibited by hemin and 2xCO while HO-1 protein levels increased with both treatments (***Figure 16***).

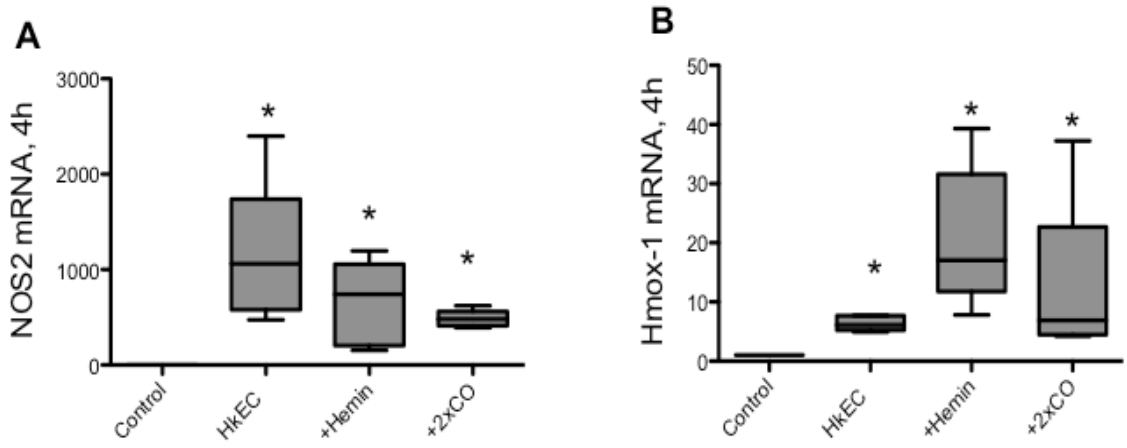

Figure 15: HO-1 activation suppressed hepatic *Nos2* and increased *Hmox1* mRNA expression during *HkEC* challenge. Wt mice pretreated with hemin or 2xCO before *HkEC*. Hepatic ***A:*** *Nos2* and ***B:*** *Hmox1* mRNA expression quantified by qRT-PCR. Results plotted as fold change vs control. **p*<0.05 vs healthy controls. (n=5 per group)

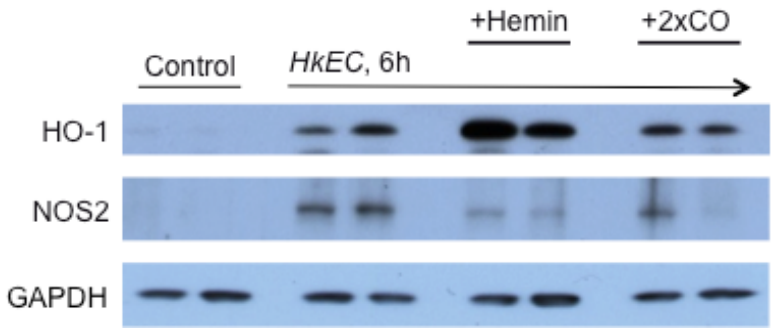

Figure 16: HO-1 activation inhibited NOS2 and induced HO-1 protein expression in mouse liver relative to *HkEC* alone. Wt mice treated with hemin or 2xCO before *HkEC* challenge. Western blot of HO-1 and NOS2 protein expression 6 hours after *HkEC*. GAPDH used as a loading control. Blot is representative of duplicate experiments. (n=2 per group)

3.2. HO-1 and NF-κB activation

Initiation of TLR4 signaling by Gram-negative PAMPs leads to the activation of NF-κB, the most important transcription factor involved in the expression of NOS2 and pro-inflammatory cytokines. To determine whether hemin and CO may be causing global cytokine suppression in *HkEC*-challenged liver, the gene expression profiles of other acute phase cytokines were examined. Pro-inflammatory cytokines TNF-α, IL-6 and IFN-γ were analyzed because they represent the most common early inflammatory mediators produced during infection and all were attenuated by hemin pretreatment (***Figure 17, A-C***). Hemin slightly, but not significantly, increased the expression of the anti-inflammatory cytokine, IL-10, over *HkEC* alone at four hours, although significant attenuation was observed at 24 hours (***Figure 17D***).

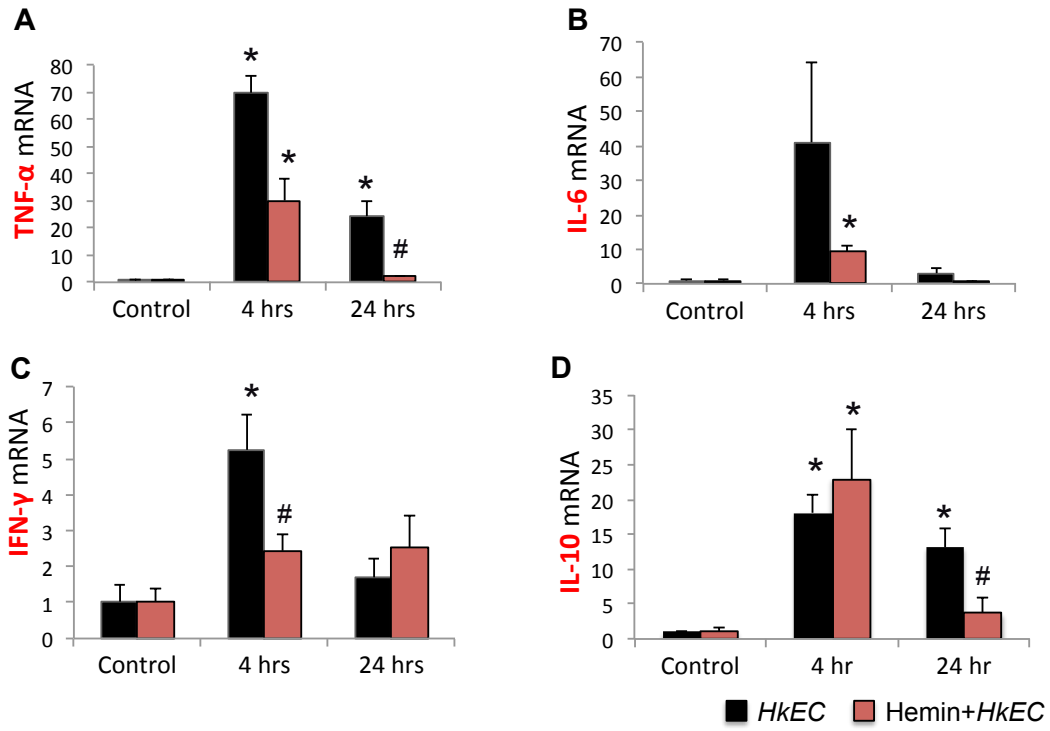

Figure 17: Hemin suppressed hepatic pro-inflammatory cytokine expression in *HkEC* peritonitis. Wt mice treated with *HkEC* only or hemin+*HkEC*. Liver ***A:*** *TNF-α*, ***B:*** *IL-6*, ***C:*** *IFN-γ*, and ***D:*** *IL-10* mRNA quantified by qRT-PCR. Results plotted as fold change vs untreated control. **p*<0.05 vs control, #*p*<0.05 vs time-matched *HkEC*. (n=5-8 per point)

Pretreatment with 2xCO showed a more complex cytokine profile. CO slightly augmented IL-6, IFN-γ, and IL-10 expression four hours after *HkEC* while TNF-α was the only cytokine to be mildly suppressed by CO (***Figure 17, A-D***). One explanation for this early cytokine enhancement may be the initial cellular stress caused by CO exposure. CO is known to bind to cytochrome c oxidase and increase ROS production in mitochondria, which may initially exacerbate early inflammatory responses. However, ROS ultimately contribute to cytoprotection through mechanisms such as increased nuclear factor (erythroid-derived 2)-like 2 (Nrf2) expression, induction of antioxidant

genes containing anti-oxidant response element (ARE) motifs in their promoter regions, and activation of mitochondrial biogenesis [144-146].

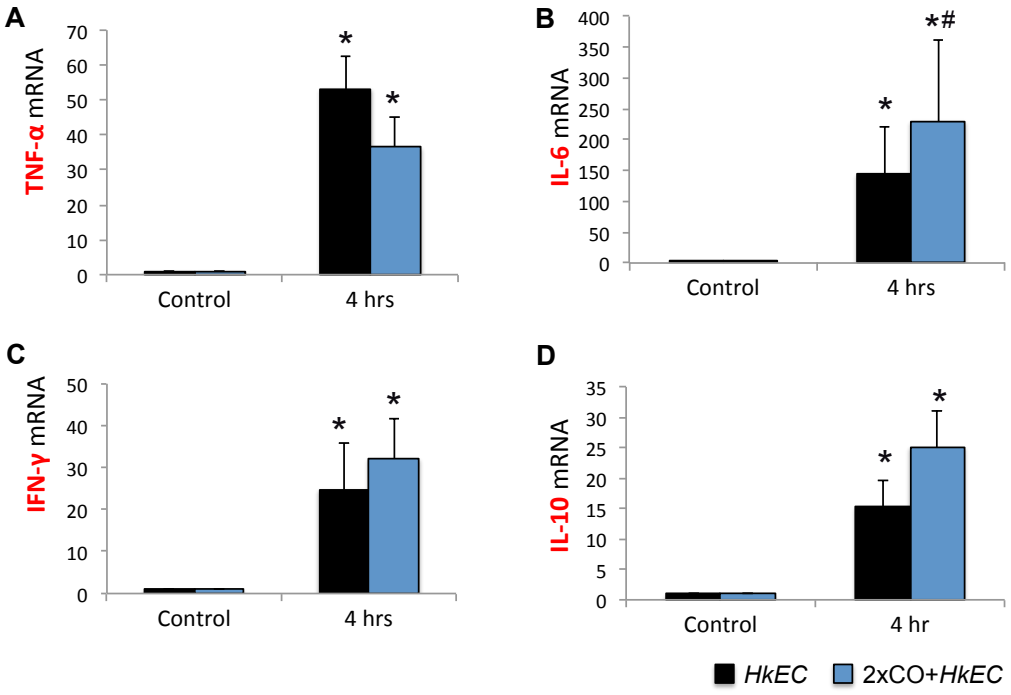

Figure 18: CO suppressed hepatic cytokine expression when given prior to *HkEC* peritonitis. Wt mice treated with *HkEC* only or 2xCO+*HkEC*. Liver ***A:*** *TNF-α*, ***B:*** *IL-6*, ***C:*** *IFN-γ*, and ***D:*** *IL-10* mRNA quantified by qRT-PCR. Results plotted as fold change vs untreated control. **p*<0.05 vs control, $^{\#}p$<0.05 vs time-matched *HkEC*. (n=5-8 per point)

Activation of NF-κB was then evaluated by comparing expression of nuclear p65 to total p65. Although peak NF-κB activation is detected 2–4 hours after challenge [147], hepatic nuclear p65 remained well elevated in *HkEC*-treated mice at 6 hours. Hemin and 2xCO both reduced p65 nuclear accumulation, as seen by Western blot (***Figure 19A***) and densitometry (***Figure 19, B-C***). This data supports previous work showing that hemin

reduces NF-κB in murine macrophages [148] and HO-1 silencing promotes NF-κB activation in human monocytes [149].

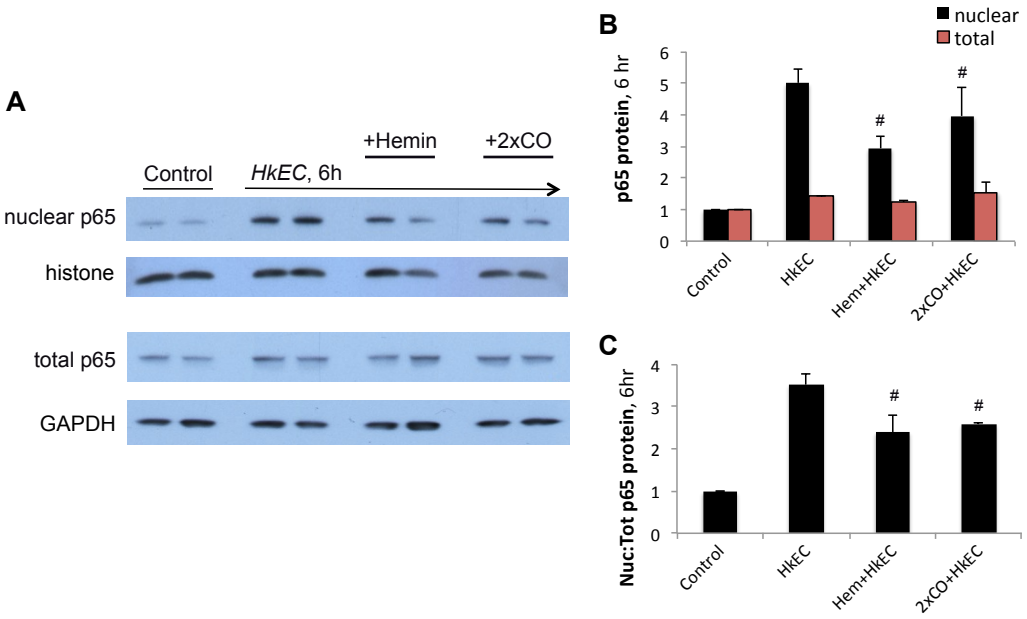

Figure 19: Hemin and CO suppression of *HkEC*-induced p65 nuclear accumulation in mouse liver. Wt mice treated with hemin or 2xCO before *HkEC* challenge. ***A:*** Western blot of 6-hour nuclear p65 with histone control and total p65 with GAPDH control. Densitometry used to plot ***B:*** total plus nuclear p65 and ***C:*** nuclear:total p65 ratio as fold change vs control. Blot is representative of duplicate experiments. $^{\#}p<0.05$ vs *HkEC.* (n=2 per group)

During the innate response to inflammation, nuclear translocation of NF-κB occurs when the nuclear scaffold protein, IκB is degraded, releasing NF-κB from its cytoplasmic sequestration. To evaluate the effect of HO-1 activation on IκB, total expression of the subunit, IκBα, was measured by Western blot analysis. Total IκBα was slightly increased in hemin-pretreated mice (***Figure 20, A-B)***, suggesting that the activation of NF-κB may be facilitated, in part, by a reduction in phosphorylation and degradation of IκB. Conversely, it is possible that early NF-κB activation by hemin

results in the nuclear depletion of IκB at 6 hours, allowing IκB levels to recover by the time of my observation. To test these theories, quantification of nuclear p65 and total IκBα at an earlier time point (i.e. two hours) would have provided more information regarding temporal activation of this pathway. Alternatively, evaluating IκB/NF-κB status in hemin or 2xCO control treated mice would have assessed HO-1-dependent NF-κB activation, although this was not performed in the current work.

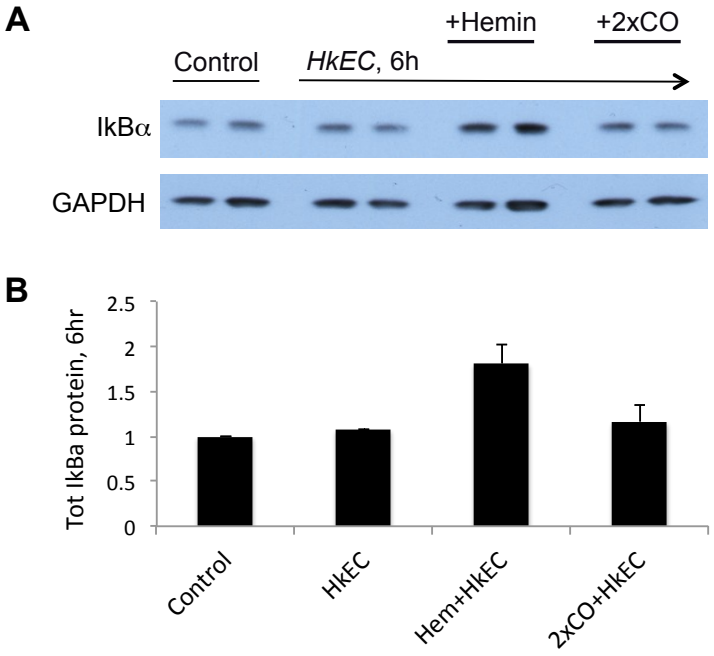

Figure 20: Effects of hemin and CO on *HkEC*-induced IκBα expression in mouse liver. Wt mice treated with hemin or 2xCO before *HkEC* challenge. *A:* Western blot of 6 hour total IκBα with GAPDH control. *B:* Blots densitized and plotted as fold change vs control. Blot is representative of duplicate experiments. Results do not achieve statistical significance. (n=2 per group)

The data shown in the *in vivo* mouse model of *HkEC* peritonitis demonstrates that hemin and CO can reduce the expression of *Nos2* mRNA and protein. This occurs in

conjunction with the inhibition of NF-κB activation, suggesting that HO-1-mediated immunosuppression occurs, at least in part, by reducing the extent of downstream TLR signal transduction in response to LPS challenge.

4. The role of HO-1 in NOS2 transcriptional regulation during *in vitro* LPS challenge of hepatocytes

After demonstrating that HO-1 activation can suppress early transcription of the hepatic *NOS2* gene in a mouse *HkEC* peritonitis model, the final Aim was to explore the molecular mechanism for this relationship using an *in vitro* approach in hepatic cells. To accomplish this objective, murine AML-12 and Hepa 1-6 cell lines were exposed to LPS with or without TNF-α. Murine liver cell lines were selected for these experiments to correlate with the *in vivo* studies in mouse liver. HO-1 activity was enhanced using hemin, a proprietary CO-releasing molecule (CORM), and bilirubin; inhibition of HO-1 was accomplished by gene silencing. While the initial intent was to evaluate the effect of HO-1 on the recruitment of several known transcription factors to the *Nos2* promoter, early *Nos2* transcriptional control *in vitro* was not affected by HO-1 modifiers as seen *in vivo*. Subsequently, the work presented here highlights the pattern of *Nos2* gene expression in hepatocyte cell lines and some limitations of the chosen *in vitro* model for evaluating HO-1 effects on early *Nos2* induction. A visual representation of the experimental setup is shown in ***Figure 21***. Of note, CORMs have been used as effective CO delivery systems and the proprietary CORM used in this experiment is notable for its increased solubility, stability in aqueous media, and non-toxic metal complex that remains after CO is released [150]. Additionally, although biliverdin is the direct metabolite of HO-1, bilirubin was used because of its increased stability in culture conditions.

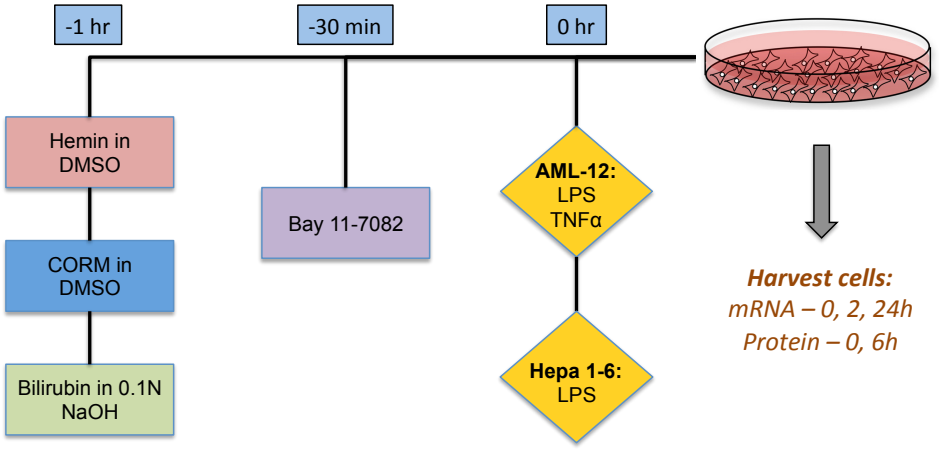

Figure 21: Experimental design for *in vitro studies*. AML-12 or Hepa 1-6 cells were exposed to hemin, CORM, or bilirubin 1 hr before LPS (10ug/mL) with or without TNF-α (10ng/mL). To inhibit NF-κB, Bay 11-7082 was given 30 minutes prior to LPS challenge. Cells were harvested for mRNA at indicated times.

4.1. AML-12 cell line

To evaluate regulation of *Nos2* gene expression by HO-1 in cell culture, experiments were first performed in AML-12 cells grown in complete DMEM/F-12 medium to 70-80% confluence before being treated with LPS+TNF-α. AML-12 cells are non-transformed mouse hepatocytes that express high levels of human transforming growth factor (TGF)-α, demonstrate normal hepatocyte histology, and do not form tumors *in vivo* [151]. Cells were exposed to a range of LPS + TNF-α (hereafter abbreviated as LT) concentrations and a working dose of 10 μg/mL LPS + 10 ng/mL TNF-α was selected for its ability to adequately induce both *Nos2* and *Hmox1*. A time course study demonstrated that *Nos2* and *Hmox1* were both maximally expressed two hours after LT (***Figure 22***). This time point was selected for additional AML-12 studies in

an effort to best simulate mouse *in vivo* experiments where maximal *Nos2* expression was observed four hours after *HkEC*.

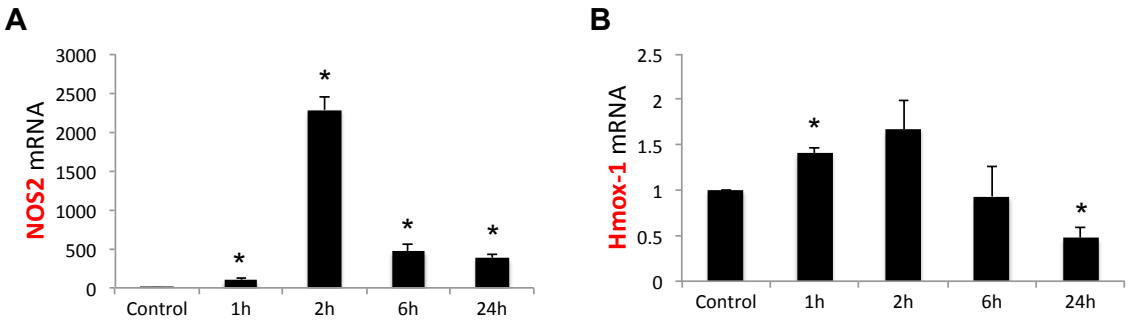

Figure 22: *Nos2* and *Hmox1* mRNA induction peaks 2 hours after LT challenge in AML-12 cells. Cells were treated with LPS (10 μg/mL) + TNF-a (10 ng/mL). ***A:*** *Nos2* and ***B:*** *Hmox1* mRNA quantified by qRT-PCR. Values plotted as fold change vs control. **p*<0.05 vs control. (n=3-4 per time point)

Cells were pretreated with hemin, CORM, or bilirubin one hour before LT exposure and *Nos2* mRNA levels were quantified two hours later using qRT-PCR. In contrast to the effects of HO-1 activation *in vivo*, induction of *Nos2* mRNA was not attenuated by any of the HO-1 activators (***Figure 23***). Specifically, hemin and CORM had no effect while 40 μM bilirubin further exacerbated *Nos2* expression. Doses of unconjugated bilirubin greater than 25 μM have been associated with apoptosis in murine hepatoma Hepa 1c1c7 cells [152], which may have accounted for the *Nos2* effects seen here.

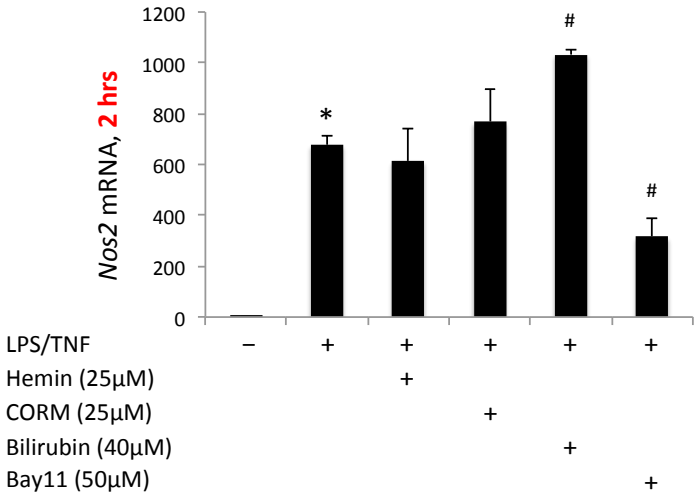

Figure 23: HO-1 modifiers do not suppress *Nos2* gene expression following LT challenge in AML-12 cells. Cells pretreated with hemin, CORM, bilirubin, or Bay 11-7082 prior to LT. *Nos2* mRNA quantified two hours later using qRT-PCR. Values are plotted as fold change vs untreated control and representative of duplicate experiments. $^{*}p<0.05$ vs control, $^{\#}p<0.05$ vs LT. (n=3 per group)

To verify that NF-κB mediated the induction of *Nos2* expression in these cells, the NF-κB inhibitor, Bay 11-7082, was given 30 minutes prior to endotoxin challenge. Bay11 significantly blunted LT-induced *Nos2* transcription, but the values were still greatly elevated above controls (*Figure 23*). AML-12 cell lines are transformed by human TGF-α and a previous report determined that these cells have constitutively active NF-κB [153]. Therefore, it is possible that *Nos2* transcriptional induction is exaggerated in AML-12 cells, counteracting some of the potential effects of HO-1 activation by hemin, CORM, or bilirubin. Therefore, murine hepatoma cell lines without known NF-κB aberrancy were considered and the Hepa 1-6 cell line selected for use in further *in vitro* studies.

4.2. Hepa 1-6 cell line

4.2.1. Response of early NOS2 transcription to HO-1 activation

Hepa 1-6 cells used for additional *in vitro* studies were cultured in complete DMEM medium to 70-80% confluence before endotoxin challenge. The LPS-dependent transcriptional response in Hepa 1-6 cells was first characterized using the dose of LT administered to AML-12 cells. Under these conditions, peak *Nos2* expression was delayed relative to that seen in AML-12 cells with peak *Nos2* mRNA levels observed at six hours (***Figure 24***). Alternatively, Hepa 1-6 cells were given LPS or TNF-α alone and analyzed after two hours. LPS alone activated *Nos2* and *Hmox1* transcription more than the combined LT challenge, suggesting that TNF-α attenuated LPS-mediated expression. Time course analysis of LPS alone in this cell line revealed maximal induction of *Nos2* and *Hmox1* genes at two hours and HO-1 protein at six hours (***Figure 25***). Therefore, subsequent experiments used LPS only, rather than LT, and focused on gene expression changes two hours after LPS exposure.

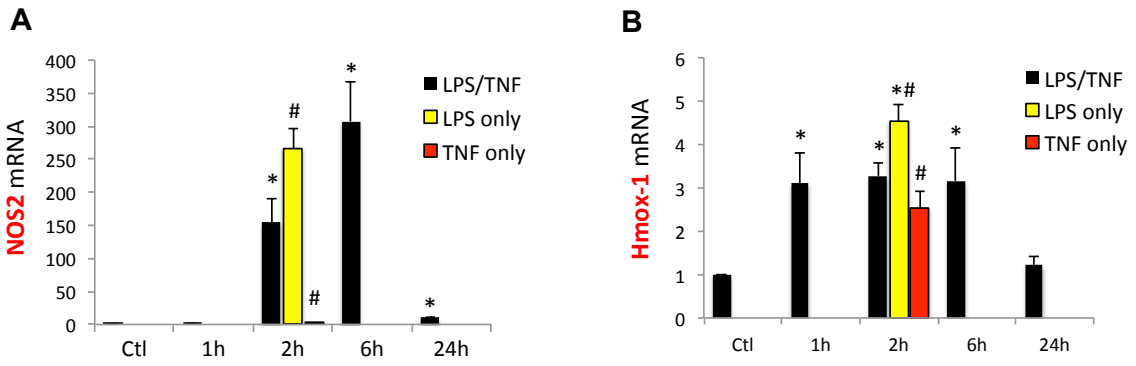

Figure 24: Induction of *Nos2* and *Hmox1* mRNA by LPS+TNFα in Hepa 1-6 cells. Cells were treated with LPS (10 μg/mL) + TNF-a (10 ng/mL), LPS alone at two hours, or TNF alone at two hours. ***A:*** *Nos2* and ***B:*** *Hmox1* mRNA quantified by qRT-PCR. Values plotted as fold change vs control. LPS-mediated induction was suppressed by TNF-α. **p*<0.05 vs control, #*p*<0.05 vs LPS. (n=3-4 per time point)

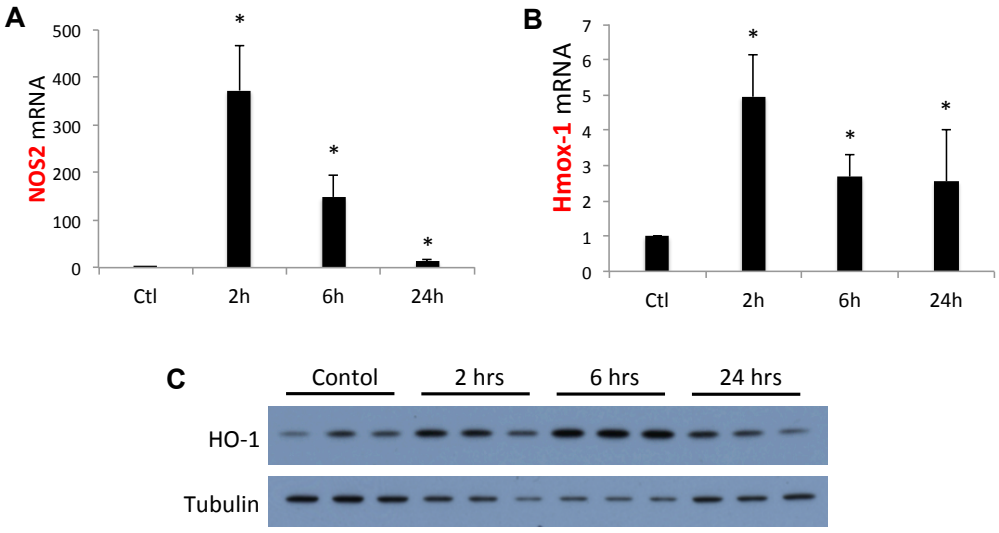

Figure 25: Induction of *Nos2* and *Hmox1* by LPS alone in Hepa 1-6 cells. Cells were treated with LPS (10 μg/mL). ***A:*** *Nos2* and ***B:*** *Hmox1* mRNA quantified by qRT-PCR. Values plotted as fold change vs control. **p*<0.05 vs control, #*p*<0.05 vs LPS. (n=3-4 per time point) ***C:*** HO-1 protein expression by Western with tubulin loading control. (n=3 per time point)

Induction of HO-1 was achieved by pretreating cells with the enzyme substrate, hemin, and downstream mediators, CORM and bilirubin, one hour prior to LPS challenge. All HO-1 activators caused a 2-4-fold enhancement of two-hour *Nos2* expression over LPS alone, despite these doses being reported in other cell studies without toxicity (***Figure 26***). Surprisingly, CORM caused the greatest increase in *Nos2* transcription. This induction by CORM may reflect early oxidative stress that precedes the recruitment of protective compensatory pathways.

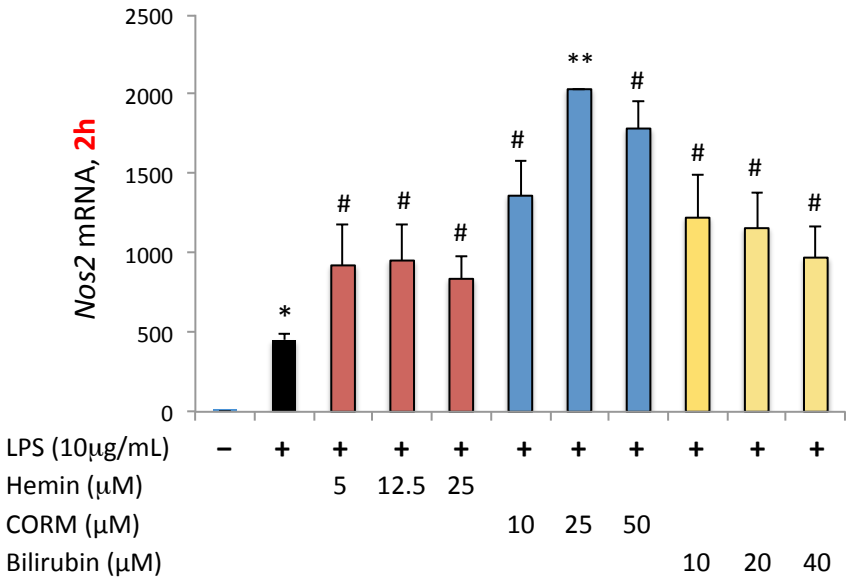

Figure 26: HO-1 activation exacerbates acute *Nos2* transcription in LPS-treated Hepa 1-6 cells. Cells exposed to LPS alone or with 1-hour pretreatment of hemin, CORM, or bilirubin at indicated doses. Values plotted as fold change vs control. **p*<0.05 vs control, ***p*<0.05 vs LPS, #*p*<0.05 vs control and LPS. (n=3 per group)

Dose-dependent *Nos2* expression was also semi-quantified using conventional RT-PCR with primers designed to amplify exon 7 of the mouse *Nos2* transcript. Results

from this conventional assay showed trends that differed from the qRT-PCR data. Lower doses of all drugs reduced *Nos2* mRNA expression, intermediate doses elicited little change, and higher doses impaired *Nos2* transcription except for CORM (50 μM), which further induced *Nos2* mRNA levels (***Figure 27)***. One potential reason for the discrepancies in PCR results could be the decreased sensitivity of the conventional assay. *Nos2* gene expression was increased by ~300 hundred fold when analyzed by qRT-PCR while conventional RT-PCR showed differences of only 25-30 fold. Therefore, conventional amplification of *Nos2* mRNA in Figure 27 may inadequately reflect true quantities of this highly induced message.

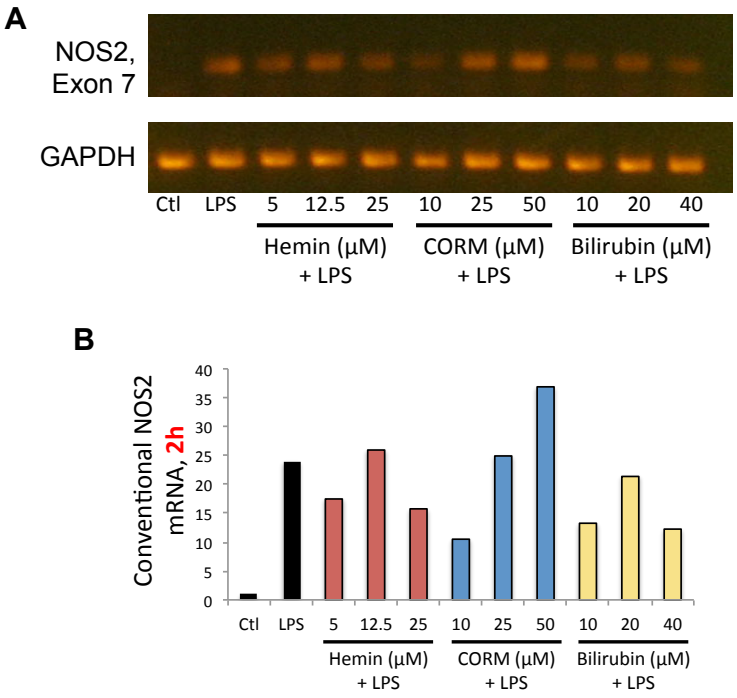

Figure 27: Conventional RT-PCR quantification of *Nos2* mRNA in LPS-treated Hepa 1-6 cells. Cells were exposed to LPS alone or with one-hour pretreatment of hemin, CORM, or bilirubin at indicated doses. ***A:*** Agarose gel visualization of PCR product**. *B:*** Densitometry plotted as fold change vs control after being normalized to *GAPDH* control. (n=1 per group)

Since the range of doses for hemin, CORM, and bilirubin pretreatment in the prior experiment had similar effects on *Nos2* expression, the intermediate doses (12.5μM hemin, 25μM CORM, and 20μM bilirubin) were selected for subsequent studies. Repeat analysis of *Nos2* gene expression in response to HO-1 activators showed that CORM was the only compound to significantly enhance *Nos2* transcription (***Figure 28A***). Pretreatment of Hepa 1-6 cells with Bay 11-7082 confirmed that the LPS-mediated *Nos2* transcriptional response was entirely NF-κB dependent. However, CORM was able to induce *Nos2* transcription in the presence of Bay-11, suggesting that it does so by a NF-κB-independent mechanism (***Figure 28B***). Inactive CORM had no effect on LPS-mediated *Nos2* transcription. Furthermore, the potent antioxidant drug, N-acetyl L-cysteine, also blocked the effects of CORM on *Nos2* induction (***Figure 29***). Collectively, it appears that CO initially causes mild oxidative stress within these hepatocytes, further exacerbating early *Nos2* transcription independent of NF-κB. An alternative explanation may be the activation of protein kinase A (PKA)/cAMP by CO, thereby recruiting transcription factors such as C/EBP and CREB to the NOS2 promoter [154].

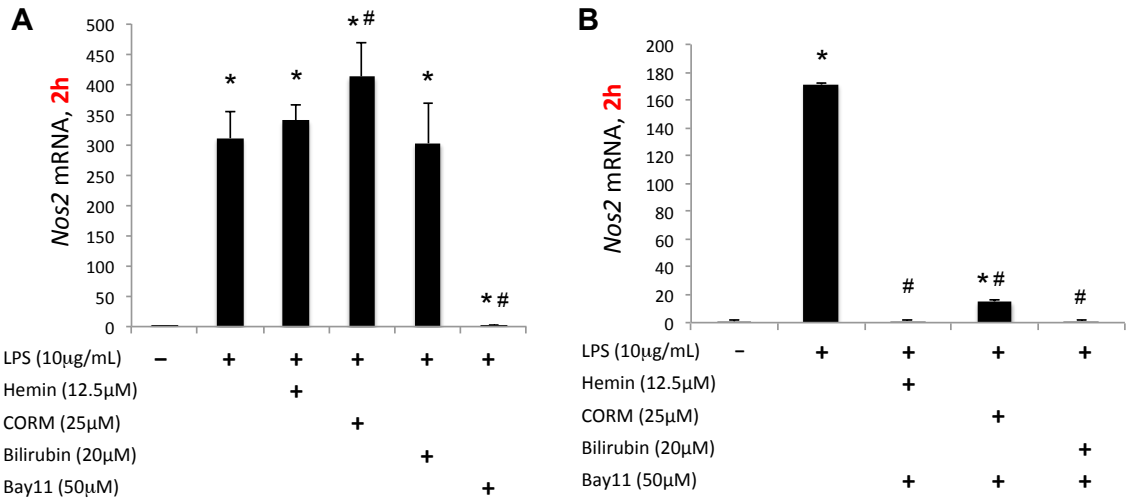

Figure 28: Effect of NF-κB inhibition on acute *Nos2* expression in LPS-treated Hepa 1-6 cells. ***A:*** *Nos2* mRNA in cells pretreated with hemin, CORM, bilirubin or Bay-11. ***B:*** *Nos2* mRNA response to HO-1 activators plus Bay-11. Values plotted as fold change vs control. Enhanced *Nos2* transcription by CORM is NF-κB-independent. **p*<0.05 vs control, $^{\#}p$<0.05 vs LPS. (n=3 per group)

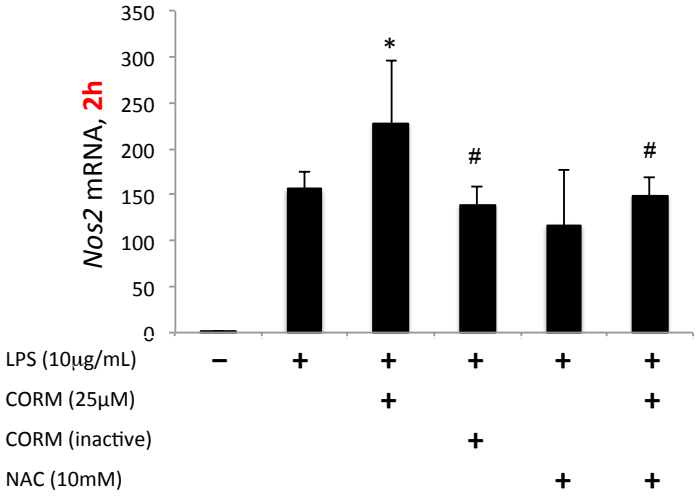

Figure 29: Characterization of enhanced *Nos2* expression by CORM in LPS-treated Hepa 1-6 cells. Levels of *Nos2* mRNA in cells pretreated with CORM, inactivated CORM, or N-acetyl L-cysteine (NAC) prior to two-hour LPS challenge. Values plotted as fold change vs control. Enhanced *Nos2* transcription by CORM occurs via oxidative stress induced by CO release. **p*<0.05 vs control, $^{\#}p$<0.05 vs LPS. (n=3 per group)

To examine the impact of HO-1 inhibition on *Nos2* expression, murine *Hmox1* or scrambled (control) shRNA plasmids were transfected into Hepa 1-6 cells. After resting for 24 hours, transfected cells were then challenged with LPS for two and six hours to detect mRNA and protein, respectively. Western analysis confirmed that HO-1 was absent in *Hmox1*-silenced cells and induced in control-transfected cells six hours after LPS (***Figure 30***). Additionally, NOS2 protein expression was slightly higher in LPS-treated *Hmox1* silenced cells than LPS-treated scrambled shRNA controls. Transcriptional analysis of transfected cells two hours after LPS also demonstrated a modest increase in *Nos2* mRNA levels in *Hmox1* silenced cells (***Figure 31***). In the absence of HO-1; hemin, CORM, and bilirubin all increased *Nos2* expression over LPS alone. The greatest increase in *Nos2* transcription was seen in the presence of hemin, perhaps due to the toxicity of this substrate that is not effectively metabolized in cells lacking a functional HO-1 enzyme. Overall, these findings suggest that HO-1 may, in fact, exert some inhibitory control on *Nos2* gene expression. However, the use of hemin, CORM, and bilirubin in the current *in vitro* model is not enough to overcome early *Nos2* induction by LPS.

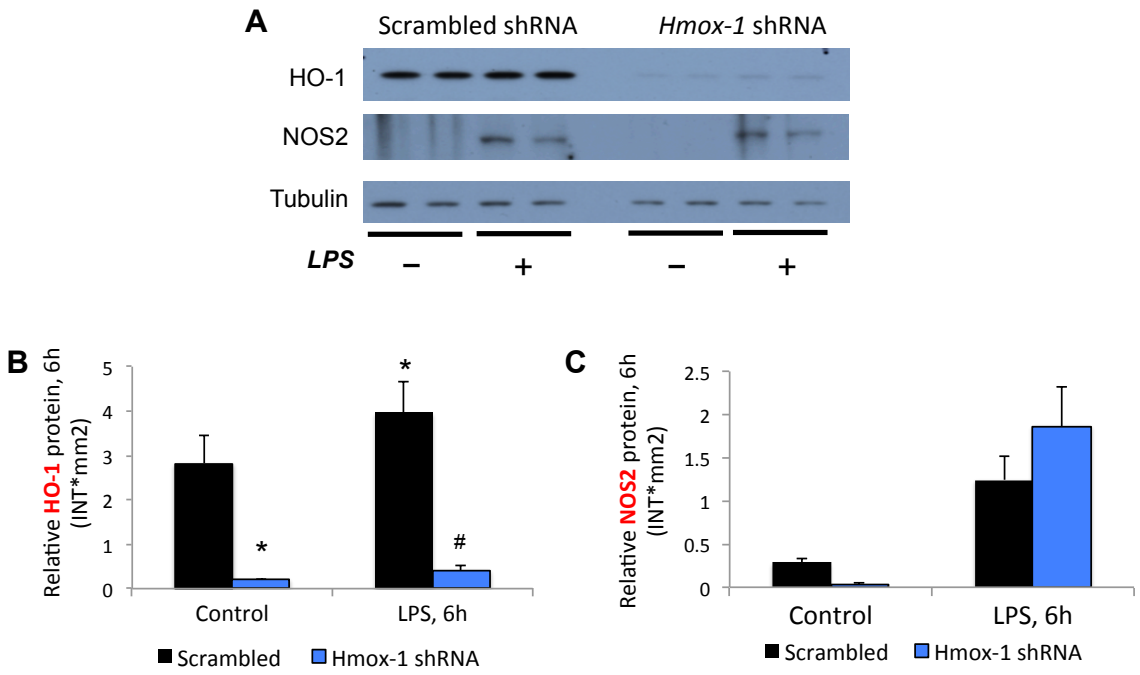

Figure 30: Verification of *Hmox1* silencing in Hepa 1-6 cells. Cells were transfected with murine *Hmox1* or scrambled shRNA and evaluated for protein expression six hours after LPS. ***A:*** Western blot of HO-1 and NOS2 protein with tubulin loading control. Densitometry values were plotted for ***B:*** HO-1 and ***C:*** NOS2 proteins. Data is representative of duplicate experiments. *$p<0.05$ vs scrambled control, $^{\#}p<0.05$ vs scrambled+LPS. (n=2 per group)

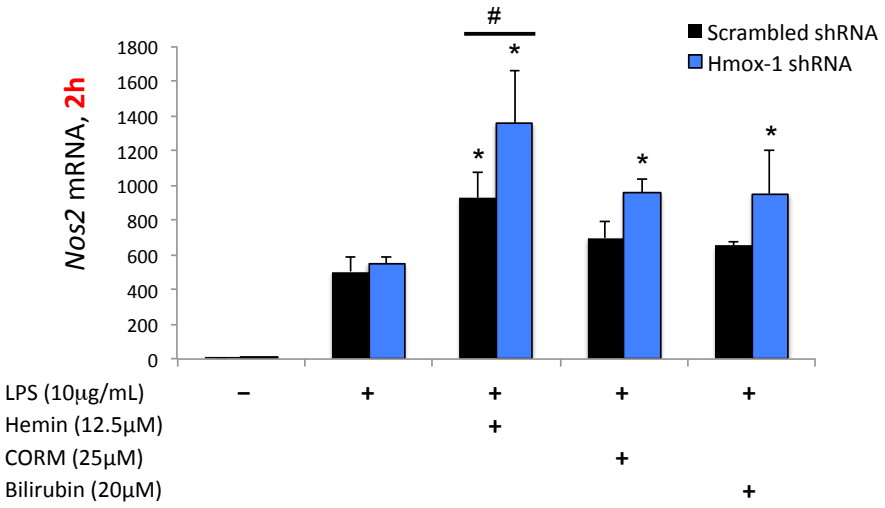

Figure 31: *Nos2* expression in HO-1 silenced Hepa 1-6 cells. Cells were transfected with murine *Hmox1* or scrambled shRNA and evaluated for *Nos2* expression after two hours LPS. Hemin, CORM, or bilirubin was administered one hour before LPS as indicated. Values are plotted as fold change vs control and representative of duplicate experiments. $p<0.05$ for all groups vs control, $*p<0.05$ vs matched shRNA+LPS, # $p<0.05$ vs matched treatment. (n=3 per group)

The findings described in Hepa 1-6 cells thus far show that HO-1 activation by one hour pretreatment with hemin, exogenous CO, or bilirubin before LPS challenge is unable to suppress early *Nos2* mRNA expression. Instead, CO creates oxidative pressure on hepatocytes, which exacerbates two-hour LPS-mediated *Nos2* expression. Silencing of HO-1 does lead to an increase in *Nos2* mRNA expression, suggesting that HO-1 may exert some inhibition on *Nos2*. However, the specific model used in this aim was unable to exaggerate this potential relationship during the acute immune phase and would not be useful for mechanistic evaluation of HO-1 repression on two-hour *Nos2* transcription. Suggestions for improving the model are provided in Future Directions.

4.2.2. Response of late phase NOS2 transcription to HO-1 activation

To determine if the regulatory potential of HO-1 was time-dependent, *Nos2* expression 24 hours after LPS challenge was evaluated under the conditions described above. As expected, LPS generated a much less intense *Nos2* response, increasing only about 15 times greater than control (***Figure 32***). Hemin pretreatment reduced this expression by approximately 50% while the modest inhibition by bilirubin did not reach statistical significance. Furthermore, CORM attenuated *Nos2* expression by approximately 30% but without reaching significance (***Figure 33***). The use of inactive CORM or CORM with NAC both reversed this suppression.

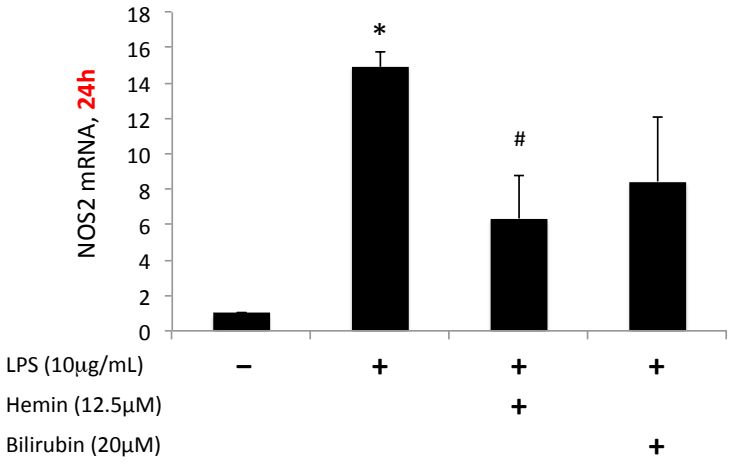

Figure 32: HO-1 activation attenuates *Nos2* transcription 24 hours after LPS challenge in Hepa 1-6 cells. Cells were pretreated with hemin or bilirubin prior LPS exposure. Values are plotted as fold change vs control and representative of duplicate experiments. *$p<0.05$ vs control, $^{\#}p<0.05$ vs LPS. (n=3 per group)

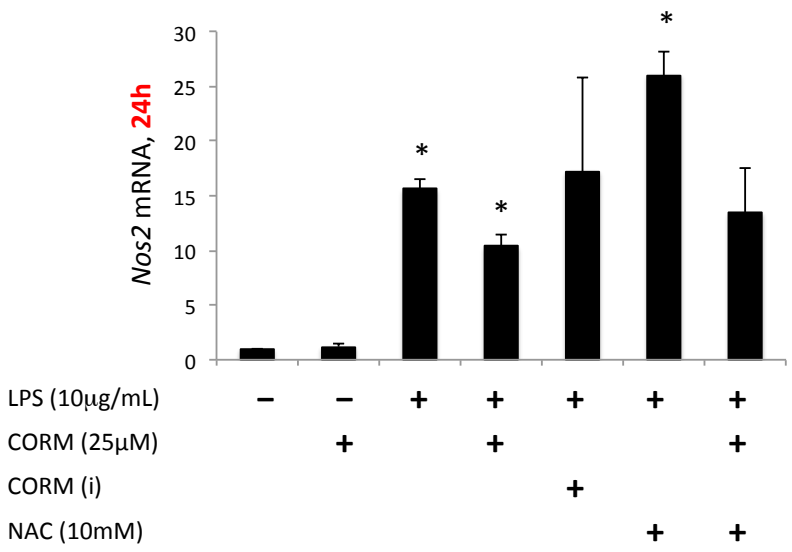

Figure 33: Effect of CORM pretreatment on 24 hour *Nos2* expression in LPS-treated Hepa 1-4 cells. *Nos2* mRNA quantified in cells pretreated with CORM, inactivated CORM, or N-acetyl L-cysteine (NAC) prior to 24 hour LPS challenge. Values plotted as fold change vs control. Moderate reduction of 24 hour *Nos2* transcription by CORM depends on CO release and is reversed by NAC. *$p<0.05$ vs control. (n=3 per group)

Once differences in HO-1 regulation on two versus 24-hour *Nos2* expression were identified, a MTT cell growth assay was used to determine whether this was secondary to cell cytotoxicity. The treatment regimens used for Hepa 1-6 cells were not associated with any significant cell death at two or 24 hours (***Figure 34***). Increased conversion of tetrazolium dye was observed at two hours with the treatment of CORM+LPS and at 24 hours with LPS only. Since the MTT assay ultimately reflects mitochondrial metabolic activity, these findings corroborate the documented ability CORM and LPS to stimulate mitochondrial biogenesis.

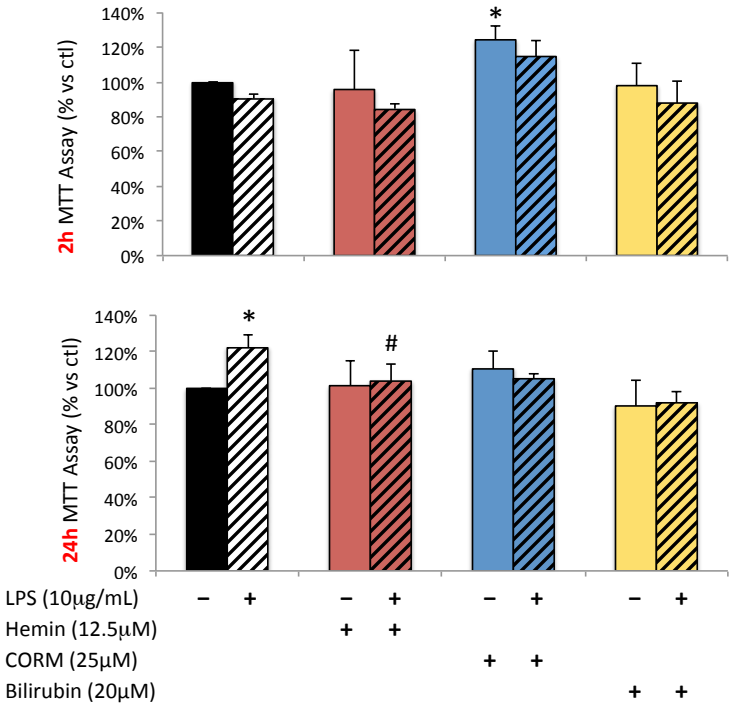

Figure 34: MTT assay evaluating metabolic activity and toxicity in Hepa 1-6 cells 2 and 24 hours after LPS. Cells cultured in 96-well plates were pretreated with hemin, CORM, and bilirubin with or without LPS. MTT reagent was added at two or 24 hours and color development terminated four hours later. Absorbance values were obtained at 570 nm and plotted as percentage of untreated cells. Graph is representative of duplicate experiments. *p<0.05 vs control, #p<0.05 vs LPS only.

From the work presented in this Aim, it is evident that HO-1 regulation of *Nos2* transcription is more complex than originally hypothesized, showing variability in acute versus late stage *in vivo* inflammation. HO-1 activators were unable to inhibit early, two-hour induction of *Nos2* although transcription was enhanced in cells deficient in HO-1. In contrast, *Nos2* expression was reduced with hemin, CORM, and bilirubin pretreatment when evaluated 24 hours after LPS exposure. These temporal differences could be due to variable transcriptional complexes regulating two- versus 24-hour *Nos2*

expression. Alternatively, a specific degree of HO-1 activation could be required for this pathway to have any transcriptional influence; perhaps this threshold was reached 24 hours after endotoxin challenge but not at two hours. Suggestions for modifications of the model and potential experiments that would further explore these theories will be described in the next chapter.

5. Conclusions

5.1. Interpretation of the main findings and their limitations

The work presented in this dissertation brings attention to two poorly defined areas within the literature: 1) the supportive role of NOS2 in mitochondrial biogenesis and 2) the mechanism by which the heme oxygenase-1/CO system, another key regulator of mitochondrial biogenesis, may counter *Nos2* transcription activation in the liver. The work presented here demonstrated that NOS2 participates not only in cellular damage during sepsis, but is also necessary for prompt recovery following that injury. NOS2 is required for optimal activation of the mitochondrial biogenesis pathway. In the absence of *Nos2*, damage to mtDNA cannot be repaired because the expression of both nuclear and mitochondrial proteins needed for this process is diminished. Additionally, impaired nuclear and mitochondrial protein accumulation in NOS2-deficient mice is associated with decreased activation of the pro-survival kinases, Akt and AMP kinase. The association of NOS2 with these kinases connects NOS2 to mitochondrial biogenesis but also offers a potential avenue by which NOS2 may interact with a number of other pro-survival pathways such as glucose metabolism, angiogenesis, and cell cycle progression [155-158]. Nevertheless, my lab has also demonstrated that NOS2 is necessary for activation of mitochondrial biogenesis in the liver, in part by facilitating protein importation across the mitochondrial membranes. S-nitrosylation of Hsp60 was shown to be necessary for the importation of Tfam into the mitochondria following *HkEC* peritonitis [135]. Fundamentally then, NOS2 is indispensible for mitochondrial

repair after acute inflammation, so ways to regulate NO production and optimize NOS2-specific cytoprotective pathways should continue to be explored in the future.

The second Aim of this dissertation was to explore the potential regulatory relationship between the HO-1/CO system and NOS2. This approach to *Nos2* transcriptional control is favorable because HO-1 provides a link that could combine immunomodulation with mitochondrial biogenesis, simultaneously subverting cellular damage and allowing compromised mitochondria to be repaired or replaced. In a murine model of *HkEC*-peritonitis, current data shows that HO-1/CO disrupts acute, high–level *Nos2* expression, in part by antagonizing NF-κB activity. It is a valid argument that the *HkEC* mouse model used here is not the ideal surrogate for clinical sepsis for reasons stated previously. However, one must consider that if HO-1 can attenuate an intense NOS2 induction like that elicited by *HkEC,* it would likely be effective in actual live sepsis, which is characterized by a more gradual increase in cytokine and NOS2 expression. Moreover, it has been shown in our laboratory that a close relationship exists between HO-1 and counter-inflammation in murine *E. coli* fibrin clot sepsis, a more accepted correlate for the human response to sepsis [120]. Therefore, confirmation of the HO-1/CO-mediated regulatory control on mitochondrial biogenesis and immunomodulation in a fibrin clot model of murine sepsis provides plausibility for application of this system to human disease.

When attempting to recapitulate the mouse *in vivo* findings in a hepatocyte cell culture system, critical design flaws limited the conclusions that could be made about

the possible counter-regulation of the two systems of interest. In stark contrast to several studies reporting HO-1 attenuation of NOS2, the strategy used here to enhance HO-1 activity in LPS-treated AML-12 and Hepa 1-6 hepatocytes was unable to suppress early peak *Nos2* mRNA expression. Conversely, 24-hour *Nos2* transcription was more responsive to HO-1 control. The majority of *in vitro* studies addressing this HO-1/NOS2 counter-regulation have analyzed NOS2 expression at later time points, i.e. 18 or 24 hours. Three theories may explain why these temporal differences may exist. First, HO-1 may not have been induced early enough to influence transcriptional networks directed at the *Nos2* promoter immediately following LPS exposure. In response to LPS alone, HO-1 protein expression is highest at six hours (*Figure 25*), whereas peak *Nos2* mRNA expression occurs at two hours (*Figure 22*). NF-κB nuclear translocation occurs 30-60 minutes after LPS exposure in cell culture [159], simultaneously targeting both *Nos2* and *Hmox1* promoters. Therefore, pretreatment with hemin, CORM, and bilirubin just one hour prior to LPS administration may not enhance HO-1 early enough to block NF-κB or other transcription factors that facilitate initial acute *Nos2* promoter activation. Second, it is also probable that *Nos2*-specific transcriptional complexes employed at 24 hours differ significantly from that at two hours. It is well understood that several transcription factors are required for optimal expression of *Nos2* but whether certain combinations have activating versus inhibitory roles is unclear. Finally, the dose of LPS used for this study may overwhelm any HO-1 dependent repression that may have occurred early in the time course. It is unclear how the dose used in cell culture systems correlates to

clinical endotoxin exposure, but with such high *Nos2* induction seen in this model, it is possible that more significant HO-1 regulation would be evident at lower LPS doses. Suggestions for *in vitro* model adjustments and ideas for potential experiments to explore some of these theories are presented in the Future Directions section below.

The work presented here does provide additional information about the role and regulation of NOS2 during Gram-negative challenge. It demonstrated that NOS2 protects against mitochondrial and cellular dysfunction through mitochondrial biogenesis. Furthermore, it suggests that a pathway known to promote mitochondrial biogenesis can also offer negative feedback regulation on *Nos2* transcription. HO-1 appears to exert negative regulatory control on *Nos2* in mouse liver, but additional confirmatory studies should be paired with more advanced studies of the molecular mechanism in cell culture models.

5.2. Future Direction

After summarizing the conclusions from this dissertation project, several questions regarding the liver-specific HO-1/NOS2 relationship were not answered due to limitations of the *in vitro* and *in vivo* models. In the mouse model, HO-1 activators were administered prior to *HkEC* but no model suppressing HO-1 activity was generated for comparison. This could be accomplished in several ways. Classically, chemical inhibition of HO-1 was accomplished through the use of metalloporphyrins, such as zinc protoporphyrin IX (ZnPP) and tin protoporphyrin IX (SnPP). These compounds are potent inhibitors of heme oxygenase but also interfere with NOS activity

[160, 161], making them a poor choice for use in studies evaluating both HO and NOS enzymes. Another option is the use of genetically engineered mice. Mice with homozygous deletion of *Hmox1* have low postnatal survival and display anemia, iron accumulation in kidney and liver, and chronic inflammation [162]. However, *Hmox1* conditional knockout mice have been described for studies in myeloid cells [163] and could be explored for liver specific deletion of HO-1. Mice with liver-specific ablation of *Hmox1* could then be challenged with live or *HkEC* to determine effects on *Nos2* transcription. HO-1 can also be transiently silenced in Wt mice using *in vivo* siRNA. Use of RNA interference has been limited to cell culture because of rapid degradation, impeded cellular uptake, and heightened immune responses when long RNA segments have been administered *in vivo* [164]. However, Merck & Co., Inc. have successfully improved this technique by creating a lipid nanoparticle (LNP) delivery system that effectively delivers siRNA via tail vein injection with minimal immune reactivity [165, 166]. If performing this experiment, *Hmox1* siRNA would be designed and assembled into LNPs administered to C57BL/6 mice by tail vein injection. These mice could then be used to evaluate the impact of HO-1 deficiency on *Nos2* expression and upstream regulatory pathways.

The *in vitro* data presented in Chapter 4 could also be enhanced by a few additional experiments. The temporal expression of HO-1 protein was not evaluated following hemin, CORM, and bilirubin but this might address whether these reagents stimulate HO-1 function earlier than LPS alone – before *Nos2* transcription is initiated.

Therefore, the pretreatments could be given more than an hour before LPS to ensure that HO-1 is activated before *Nos2* is expressed. Alternatively, the gold standard for evaluating potential therapeutic HO-1 activation would be to use an overexpression vector to ensure HO-1 protein is expressed prior to endotoxin challenge. In addition to the shRNA constructs used in this project, Origene provides an *Hmox1* cDNA ORF clone in a pCMV6-AC-GFP cloning vector that could be transfected into Hepa 1-6 cells. In contrast, additional evaluation of the effect of HO-1 inhibition would be useful. *Hmox1* silenced cells were used to evaluate *Nos2* expression two hours post LPS challenge but the degree of transcriptional response was not quantified at 24 hours. Comparison of *Nos2* expression at two and 24 hours in this system may have revealed whether inherent transcriptional control was significantly different during early vs late inflammation.

One of the significant limitations of prior studies relating the HO-1/CO and NOS2 pathways is the characterization of specific changes in transcriptional complexes at the *Nos2* promoter. Reports have suggested that NF-κB and STAT-1 are affected by HO-1 activity but studies have inadequately established that this directly impacts *Nos2* transcription during inflammation. Future evaluation should therefore evaluate changes in direct transcription factor binding, i.e. by NF-κB, Stat-1, CREB and IRF-1 by chromatin immunoprecipitation (ChIP). Luciferase reporter systems are also useful for defining promoter regions and could be used in this case. Perrella, et al. has designed murine Wt and mutated NOS2 luciferase reporters that would be ideal for application in this cell culture model [167, 168]. These constructs were used in macrophages challenged with

LPS to show that the distamycin A, an antibody that binds the DNA minor groove and interferes with IRF-1 binding, reduces *Nos2* expression and protects from LPS endotoxemia [169]. This suggests that additional evaluation of individual and collaborative binding of transcription factors on the *Nos2* promoter would provide more definitive information on a major regulatory target for treatment of inflammatory diseases such as sepsis.

Ultimately, the information gained from studies in mouse models would need to be translated to a human system for clinical relevance. While human HepG2 or primary hepatocytes could be utilized for *in vitro* studies, caution must be taken since the human and mouse *Nos2* promoters vary greatly and share little homology. For instance, two additional AP-1 sites and one NF-κB site are important for human *Nos2* promoter activity but are not present in the mouse promoter [170]. Therefore, evaluation of the specific transcriptional complexes involved in *Nos2* expression will need to accommodate these differences.

Appendix: Materials and Methods

Reagents

LPS (from E. coli 0111:B4, Sigma, St. Louis, MO) was dissolved in sterile water and used at a final concentration of 10μg/mL. TNF-α was obtained from Prospec Bio (Israel), reconstituted in water, and used at 10 ng/mL. Hemin in 0.1% DMSO (Sigma), was used at 50 μmol/kg in animal studies and 5, 12.5, or 25 μM in cell culture. The proprietary CORM-2 compound (CORM) was a gift from Fabio Zobi at the University of Zurich and was used at a final concentration of 25 μM in 0.1% DMSO [150]. The half-life of CO release from CORM is 20 minutes, so fresh CORM solution was prepared immediately prior to each experiment. To inactivate CORM, CO was released by incubation of the compound in media for 30 minutes before applying to cells. Bilirubin (USB Corp) was dissolved in 0.1N NaOH to a working concentration of 15 mM and administered to cells at a final concentration of 10, 20, or 40μM. N-acetyl L-cysteine (Sigma) was dissolved in water for final concentration of 10 mM. Bay 11-7082 was resuspended in water and used at a final concentration of 50 μM. Lipofectamine 2000 (Invitrogen) was used for shRNA transfections.

Antibodies used for Western blots included NRF-1, PGC-1α, Tfam, Pol-γ, histone H3, NF-κB p65, IκBα (Santa Cruz), NOS2 (Millipore), TLR4 and HO-1 (StressGen), GAPDH (GeneTex), and tubulin (Sigma). Taqman real-time RT-PCR (qRT-PCR) primers were all obtained from Applied Biosystems and included mouse *Nos2*, *Hmox1*, cytochrome *b*, *TNF-α*, *IL-6*, *ICAM-1*, *IL-1β*, *IFN-γ*, and *IL-10*.

Mouse Studies.

C57BL/6J and NOS2$^{-/-}$ mice used in animal experiments were obtained from Jackson Laboratories (Bar Harbor, ME) and the NOS2 mice bred at our institution. TLR4$^{-/-}$ mice were generously provided by Dr. S. Akira of Osaka University [10, 34] and then speed congenically backcrossed onto a C57BL/6J background. For immunofluorescence studies, transgenic reporter mice expressing green fluorescent protein (GFP) exclusively in mitochondria (mtGFP-tg) were a gift from Hiroshi Shitara and Hiromichi Yonekawa of Tokyo Metropolitan Institute of Medical Science [171]. Mice were kept in pathogen-free housing on dry bedding and studies were conducted with 20–25 g males on approved protocols that conform to the NIH Guide for the Care and Use of Laboratory Animals.

Surgical implantation of a fibrin clot containing 10^8 CFU *E. coli* was performed on mice anesthetized with intraperitoneal ketamine and xylazine. The abdomen was shaved and cleaned with povidone-iodine. A midline laparotomy was performed and the infected clot inserted into the peritoneum. The peritoneum and abdomen were closed with proline sutures and mice were resuscitated with 1 mL of subcutaneous 0.9% NaCl. Mice included in the survival study were monitored for seven days with free access to food and water. Mice used for quantification of bacterial burden were sacrificed 24 hours following surgery by overexposure to isoflurane and blood was collected from the heart using syringe aspiration.

Mice treated with 1 x 10^8 *HkEC* were injected intraperitoneally with 0.5 mL bacteria in sterile saline. Animals were harvested at 4, 6, or 24 hours following this injection by overexposure to isoflurane and liver or heart were snap-frozen and stored at -80°C. Healthy controls were also sacrificed in this same manner. Pretreatment studies involved subcutaneous injection of hemin 8 hours before *HkEC* exposure. CO was inhaled for one hour at 250 ppm four hours before and again immediately following *HkEC* injection. This dose of CO has been associated with 10% carboxyhemoglobin levels, <1% methemoglobin, and induction of mitochondrial biogenesis [172].

Mice injected with *HkEC* were killed under anesthesia at 0, 4, 6, 24, and 72 h and the hearts or livers collected immediately. The organs were flash-frozen in liquid nitrogen for all mRNA and protein analysis and stored at −80 °C until processed. Hearts for immunofluorescence studies were fresh-fixed in 10% formalin for 24 h and then stored in 70% ethanol and phosphate-buffered saline until processed as described below.

Bacterial Preparation

Live bacteria were grown from lyophilized *E. coli* stored at -80°C (serotype 086a:K61; American Type Tissue Culture Collection, Rockville, MD, USA) by inoculating them on sterile agar slants and incubating at 37°for 18 hours. Bacteria were resuspended to a concentration of 10^9 CFU/mL the morning of the surgery using previously described methods [173]. Fibrin clots were prepared by suspending 10^8 CFU *E. coli* in 500 μL fibrin (500 μL of 10 mg/mL bovine fibrinogen plus 10 μL of 1.2 U/μL bovine plasma thrombin, Sigma).

To prepare heat-killed *E. coli* (*HkEC*), a solution with an approximate concentration of 1 x 10^{10} CFU/mL was heat-inactivated at 65°C for 1 hour and stored at -80°C until use. Final quantification of the bacterial solution was achieved by counting pour plate colonies of a sample removed prior to heating. Efficacy of heat-inactivation was > 99.9% as verified by pour plates. *HkEC* were thawed once and diluted with sterile 0.9% NaCl to a concentration of 2×10^{8} CFU/mL and 0.5 ml was administered by single intraperitoneal injection to groups of three to six mice per time point. Preliminary studies showed that this sublethal dose of bacteria was subnecrotic in heart and liver and lacked mortality in the mice used for this study.

To determine bacterial burden, blood from cardiac aspiration was mixed with heparin to prevent clotting, serially diluted using sterile water, and plated on LB agar plates. Inoculated plates were incubated at 37°C for 18 hours and observed for colony growth.

Cell Culture

Mouse AML-12 cells were obtained from ATCC (Manassas, VA) and cultured in 5% CO in DMEM/F-12 medium (GIBCO) supplemented with 10% FBS, 5 μg/mL insulin, 5 μg/mL transferrin, 5 ng/mL selenium, 40 ng/mL dexamethasone, and 1x antimycotic antibiotic (GIBCO). Cells were treated with LPS (10 μg/mL) + TNF-α (10 ng/mL) upon reaching 70-80% confluence. Hepa 1-6 cells were obtained from ATCC (Manassas, VA) and cultured in 5% CO in DMEM medium (GIBCO) supplemented with 10% FBS and 1x antimycotic antibiotic. Transfection studies were conducted at 50% confluence while

other studies were initiated at 70-80% confluence. Following treatment, cells were frozen at -80°C until processed for mRNA or protein.

Hemin, CORM, and bilirubin were administered one hour before adding LPS to the media. Bay 11-7082 was given 30 minutes before LPS.

Cell Transfection

Hmox1 and scrambled shRNA plasmids were obtained from Origene (Rockville, MD) and amplified by first transforming the plasmids into NEB 5α supercompetent *E. coli* cells according to the manufacturer's protocol (Biolabs, Ipswich, MA). In brief, transformed bacteria were plated on LB agar with 25 μg/mL kanamycin overnight after which a single colony was selected for expansion. Bacteria were grown overnight in LB medium with 25 μg/mL kanamycin and pelleted by centrifugation at 6,000g for 15 minutes. Plasmids were purified using the Endofree Plasmid Maxi Kit according to the manufacturer's protocol (Qiagen). In brief, bacteria were lysed and passed through a syringe filter to remove cellular debris. Filtered lysate was applied to a DNA binding column, washed, and eluted with isopropanol. DNA was centrifuged and the pellet washed in 70% ethanol before being resuspended in endotoxin-free buffer. Plasmid concentration was determined by spectrophotometry at 260 nm and quality was checked using agarose gel electrophoresis. Plasmids were diluted to a concentration of 1 μg/μL for transfections.

Hepa 1-6 cells were cultured to 50% confluence and then transfected using Lipofectamine 2000 in 2:1 ratio with *Hmox1* or scrambled shRNA plasmids, achieving

efficiency of >90%. After 24 hours, transfection media was removed and cells were allowed to rest in fresh complete medium for 24 hours. Cells were then pretreated with hemin, CORM, or bilirubin one hour before LPS was added and cells harvested at two hours for mRNA analysis and six hours for protein verification.

Nuclear and total protein isolation

While isolating nuclei from frozen liver, samples were kept on ice at all times. Approximately 0.5 g frozen liver tissue was first homogenized in Buffer A (250 mM sucrose, 5 mM $MgCl_2$, 10 mM Tris/HCl, pH 7.4) with 1x protease and phosphatase inhibitors. Homogenate was centrifuged at 600g for 15 minutes, pellet washed once in Buffer A, and resuspended in Buffer B (2 M sucrose, 1 mM $MgCL_2$, and 10 mM Tris/HCl, pH 7.4) with inhibitors. Nuclei were centrifuged at 16,000g for 30 minutes and supernatant and fatty debris removed to leave just a clean nuclear pellet. Nuclei were resuspended in RIPA buffer with inhibitors, sonicated, and centrifuged at max speed for 15 minutes to obtain nuclear protein. Protein concentration was quantified using the Bicinchoninic acid (BCA) protein assay.

To prepare tissue for Western blotting, hearts were divided longitudinally so that atrial and ventricular tissues were represented in each sample. Approximately 0.2 g frozen liver tissue was used to prepare liver homogenate. Total protein was obtained by mechanically homogenizing liver or cardiac tissue in complete RIPA buffer with protease and phosphatase inhibitors. Homogenate was solicited and centrifuged at max

speed for 15 minutes at 4°C. Supernatant was decanted and quantified using the BCA protein assay.

HO-1 activity

HO enzyme activity was measured in liver homogenates using the reduction gas method for the analysis of CO byproduct [174]. Frozen mouse liver tissue was weighed, mechanically homogenized, and briefly sonicated in 4 volumes of 0.1 M potassium phosphate, pH 7.4. After centrifuging at 13,000g for 2 minutes at 4°C, supernatant was collected for enzyme activity and protein assay. Sample homogenate was mixed with hemin/albumin substrate and NADPH before placing vials in 37°C water bath for 30 minutes. The reaction was stopped with 60% 5'-sulfosalicylic acid (SSA). CO generation was detected using RGA5 Process Gas Analyzer (Trace Analytical, Menlo Park, CA) and normalized to sample protein concentration to obtain values of nmol CO/g/30 min.

Western blot analysis

Total and nuclear protein samples were prepared in 2x Laemmli buffer + DTT. After heating at 95°C for 10 minutes, protein samples were separated by SDS-PAGE and transferred to PVDF membranes for Western analysis. Membranes were blocked in 5% milk in TBST and then incubated with validated polyclonal or monoclonal antibodies against PGC-1α, NRF1, Tfam, Pol-γ, Akt, pAkt, AMPK, p-AMPK, NOS2, HO-1, p65, or IκBα. Anti-tubulin, GAPDH, histone or porin was used as a loading control. After three washes in TBST, membranes were incubated in HRP-conjugated goat anti-rabbit or anti-mouse IgG (Santa Cruz) at 1:2000 or 1:5000 dilutions, respectively. Blots were developed

with ECL and proteins quantified by densitometry of digitized images from the mid-dynamic range using the QuantityOne program (and expressed relative to GAPDH or tubulin.

Real-time PCR and gene expression

Total cardiac RNA was isolated from tissue using Trizol Reagent (Invitrogen, Carlsbad, CA). Mouse liver RNA was additionally treated with turbo DNA-free kit (Ambion) using the protocol for rigorous treatment. Synthesis of cDNA was performed with the ImProm-II Reverse Transcriptase system (Promega) according to product instructions. Reactions to quantify per sample levels of *TNF-α, IL-6, IL-1β, ICAM-1*, and cytochrome *b* in mouse liver and heart were carried out on a 7700 Sequence Detector System (Applied Biosystems) using Taqman Master Mix as described [60]. TLR-4 mRNA expression was determined as described [175] using gene-specific primer pairs [136]. Expression of *Hmox1, Nos2, TNF-α, IL-6, IFN-γ, and IL-10* genes in mouse liver (*Figures 14 and 15*) and liver cell lines was quantified using the StepOne Plus Real-Time PCR system (Applied Biosystems). Each sample was assayed in duplicate and mean values were reported. The RNA data were normalized to 18S rRNA expression levels.

Mitochondrial isolation, respiration, and DNA copy number

Intact mitochondria were isolated from fresh hearts using sucrose density centrifugation [59]. Respiration was measured at 35 °C in water-jacketed cuvettes with calibrated polarographic oxygen electrodes (Diamond General, Ann Arbor, MI) using 0.5 mM ADP and either succinate (5 mM) or malate+ glutamate (2.5 mM each) as

substrates. MtDNA was isolated from intact mitochondria [56, 175] and the copy number quantified using real-time PCR for cytochrome b (cyt b) as described [60]. Samples were analyzed in triplicate and the mtDNA copy number per nanogram total cellular DNA was reported by logarithmic expression relative to known DNA standards.

Immunofluorescence microscopy

Four-micrometer, formalin-fixed, paraffin-embedded cardiac sections were processed for immunostaining as described [68]. Anti-TLR4 (StressGen) and anti-NOS2 (Upstate) primary antisera were used at a working dilution of 1:100. Conventional fluorescence images were obtained using a Nikon Microphot-FXA fluorescence microscope. MtGFP-tg was visualized in green fluorescence and all other proteins in red fluorescence.

MTT Assay

Cell viability and metabolic activity were evaluated using the colorimetric (MTT) kit from Millipore (Billerica, MA). Cells were grown in 96-well plates to 70-80% confluence. Treatments were given as described for cell culture experiments above. Two or 24 hours after LPS, 0.01 mL MTT reagent (3-(4,5-dimethylthiazol-2-yl)-2,5-diphenyl tetrasodium bromide) was added to each well, mixed gently, and incubated at 37°C for four hours. To facilitate color development, 0.1 mL isopropanol with 0.04 N HCl was added to each well and plates were read within one hour. The BioTek Synergy 2 microplate reader (BioTek, Winooski, VT), courtesy of Dr. Herman Staats, was used to obtain absorbance values at 570 nm with reference of 630 nm.

Statistics

Group values were expressed as means ± SD. The n values refer to independent samples. Data analyses were performed using Excel to calculate Student's unpaired t test and GraphPad Prism 5 to calculate 2-way ANOVA followed by Bonferroni post-tests. Regression analyses were performed using Statview (SAS, Version 5.0.1). A $p<0.05$ was considered significant.

References

[1] Kung, H. C.; Hoyert, D. L.; Xu, J.; Murphy, S. L. Deaths: final data for 2005. *Natl Vital Stat Rep* **56:**1-120; 2008.

[2] Angus, D. C.; Linde-Zwirble, W. T.; Lidicker, J.; Clermont, G.; Carcillo, J.; Pinsky, M. R. Epidemiology of severe sepsis in the United States: analysis of incidence, outcome, and associated costs of care. *Crit Care Med* **29:**1303-1310; 2001.

[3] Bone, R. C.; Balk, R. A.; Cerra, F. B.; Dellinger, R. P.; Fein, A. M.; Knaus, W. A.; Schein, R. M.; Sibbald, W. J. Definitions for sepsis and organ failure and guidelines for the use of innovative therapies in sepsis. The ACCP/SCCM Consensus Conference Committee. American College of Chest Physicians/Society of Critical Care Medicine. *Chest* **101:**1644-1655; 1992.

[4] Remick, D. G. Pathophysiology of sepsis. *Am J Pathol* **170:**1435-1444; 2007.

[5] Merx, M. W.; Weber, C. Sepsis and the heart. *Circulation* **116:**793-802; 2007.

[6] Dellinger, R. P.; Levy, M. M.; Rhodes, A.; Annane, D.; Gerlach, H.; Opal, S. M.; Sevransky, J. E.; Sprung, C. L.; Douglas, I. S.; Jaeschke, R.; Osborn, T. M.; Nunnally, M. E.; Townsend, S. R.; Reinhart, K.; Kleinpell, R. M.; Angus, D. C.; Deutschman, C. S.; Machado, F. R.; Rubenfeld, G. D.; Webb, S. A.; Beale, R. J.; Vincent, J. L.; Moreno, R.; Surviving Sepsis Campaign, G. Surviving Sepsis Campaign: International Guidelines for Management of Severe Sepsis and Septic Shock: 2012. *Critical Care Medicine* **41:**580-637; 2013.

[7] Hotchkiss, R. S.; Swanson, P. E.; Freeman, B. D.; Tinsley, K. W.; Cobb, J. P.; Matuschak, G. M.; Buchman, T. G.; Karl, I. E. Apoptotic cell death in patients with sepsis, shock, and multiple organ dysfunction. *Critical Care Medicine* **27:**1230-1251; 1999.

[8] Kawai, T.; Akira, S. The role of pattern-recognition receptors in innate immunity: update on Toll-like receptors. *Nature Immunology* **11:**373-384; 2010.

[9] Akira, S.; Uematsu, S.; Takeuchi, O. Pathogen recognition and innate immunity. *Cell* **124:**783-801; 2006.

[10] Takeuchi, O.; Hoshino, K.; Kawai, T.; Sanjo, H.; Takada, H.; Ogawa, T.; Takeda, K.; Akira, S. Differential roles of TLR2 and TLR4 in recognition of gram-negative and gram-positive bacterial cell wall components. *Immunity* **11:**443-451; 1999.

[11] Lien, E.; Means, T. K.; Heine, H.; Yoshimura, A.; Kusumoto, S.; Fukase, K.; Fenton, M. J.; Oikawa, M.; Qureshi, N.; Monks, B.; Finberg, R. W.; Ingalls, R. R.; Golenbock, D. T. Toll-like receptor 4 imparts ligand-specific recognition of bacterial lipopolysaccharide. *Journal of Clinical Investigation* **105:**497-504; 2000.

[12] Cohen, J. The immunopathogenesis of sepsis. *Nature* **420:**885-891; 2002.

[13] Erridge, C.; Bennett-Guerrero, E.; Poxton, I. R. Structure and function of lipopolysaccharides. *Microbes and Infection* **4:**837-851; 2002.

[14] Park, B. S.; Song, D. H.; Kim, H. M.; Choi, B. S.; Lee, H.; Lee, J. O. The structural basis of lipopolysaccharide recognition by the TLR4-MD-2 complex. *Nature* **458:**1191-U1130; 2009.

[15] Palsson-McDermott, E. M.; O'Neill, L. A. J. Signal transduction by the lipopolysaccharide receptor, Toll-like receptor-4. *Immunology* **113:**153-162; 2004.

[16] Akira, S.; Takeda, K. Toll-like receptor signalling. *Nature Reviews Immunology* **4:**499-511; 2004.

[17] Kawai, T.; Akira, S. Toll-like receptor downstream signaling. *Arthritis Res Ther* **7:**12-19; 2005.

[18] Chow, J. C.; Young, D. W.; Golenbock, D. T.; Christ, W. J.; Gusovsky, F. Toll-like receptor-4 mediates lipopolysaccharide-induced signal transduction. *Journal of Biological Chemistry* **274:**10689-10692; 1999.

[19] O'Neill, L. A. J.; Bowie, A. G. The family of five: TIR-domain-containing adaptors in Toll-like receptor signalling. *Nature Reviews Immunology* **7:**353-364; 2007.

[20] Baeuerle, P. A.; Henkel, T. Function and activation of NF-kappa-B in the immune system. *Annual Review of Immunology* **12:**141-179; 1994.

[21] Vallabhapurapu, S.; Karin, M. Regulation and Function of NF-kappa B Transcription Factors in the Immune System. *Annual Review of Immunology*. Palo Alto: Annual Reviews; 2009: 693-733.

[22] Gilmore, T. D. Introduction to NF-kappa B: players, pathways, perspectives. *Oncogene* **25:**6680-6684; 2006.

[23] Karin, M.; Ben-Neriah, Y. Phosphorylation meets ubiquitination: The control of NF-kappa B activity. *Annual Review of Immunology* **18:**621-+; 2000.

[24] Aderem, A.; Ulevitch, R. J. Toll-like receptors in the induction of the innate immune response. *Nature* **406:**782-787; 2000.

[25] Xie, Q. W.; Kashiwabara, Y.; Nathan, C. Role of transcription factor NF-kappa B/Rel in induction of nitric oxide synthase. *J Biol Chem* **269:**4705-4708; 1994.

[26] Alderton, W. K.; Cooper, C. E.; Knowles, R. G. Nitric oxide synthases: structure, function and inhibition. *Biochemical Journal* **357:**593-615; 2001.

[27] Thannickal, V. J.; Fanburg, B. L. Reactive oxygen species in cell signaling. *American Journal of Physiology-Lung Cellular and Molecular Physiology* **279:**L1005-L1028; 2000.

[28] Parrish, W. R.; Gallowitsch-Puerta, M.; Czura, C. J.; Tracey, K. J. Experimental Therapeutic Strategies for Severe Sepsis Mediators and Mechanisms. *Neural Signaling: Opportunities for Novel Diagnostic Approaches and Therapies* **1144:**210-236; 2008.

[29] Vincent, J. L.; Zhang, H.; Szabo, C.; Preiser, J. C. Effects of nitric oxide in septic shock. *American Journal of Respiratory and Critical Care Medicine* **161:**1781-1785; 2000.

[30] Beutler, B.; Milsark, I. W.; Cerami, A. C. Passive-immunization against cachectin tumor necrosis factor protects mice from lethal effect of endotoxin. *Science* **229:**869-871; 1985.

[31] Ohlsson, K.; Bjork, P.; Bergenfeldt, M.; Hageman, R.; Thompson, R. C. Interleukin-1 receptor antagonist reduces mortality from endotoxin-shock. *Nature* **348:**550-552; 1990.

[32] Latifi, S. Q.; O'Riordan, M. A.; Levine, A. D. Interleukin-10 controls the onset of irreversible septic shock. *Infection and Immunity* **70:**4441-4446; 2002.

[33] Song, G. Y.; Chung, C. S.; Chaudry, I. H.; Ayala, A. What is the role of interleukin 10 in polymicrobial sepsis: Anti-inflammatory agent or immunosuppressant? *Surgery* **126:**378-383; 1999.

[34] Hoshino, K.; Takeuchi, O.; Kawai, T.; Sanjo, H.; Ogawa, T.; Takeda, Y.; Takeda, K.; Akira, S. Cutting edge: Toll-like receptor 4 (TLR4)-deficient mice are hyporesponsive to lipopolysaccharide: evidence for TLR4 as the Lps gene product. *J Immunol* **162:**3749-3752; 1999.

[35] Tavener, S. A.; Long, E. M.; Robbins, S. M.; McRae, K. M.; Van Remmen, H.; Kubes, P. Immune cell Toll-like receptor 4 is required for cardiac myocyte impairment during endotoxemia. *Circ Res* **95:**700-707; 2004.

[36] Poltorak, A.; He, X.; Smirnova, I.; Liu, M. Y.; Van Huffel, C.; Du, X.; Birdwell, D.; Alejos, E.; Silva, M.; Galanos, C.; Freudenberg, M.; Ricciardi-Castagnoli, P.; Layton, B.; Beutler, B. Defective LPS signaling in C3H/HeJ and C57BL/10ScCr mice: mutations in Tlr4 gene. *Science* **282:**2085-2088; 1998.

[37] Weiss, D. S.; Raupach, B.; Takeda, K.; Akira, S.; Zychlinsky, A. Toll-like receptors are temporally involved in host defense. *J Immunol* **172:**4463-4469; 2004.

[38] Hotchkiss, R. S.; Coopersmith, C. M.; McDunn, J. E.; Ferguson, T. A. Tilting toward immunosuppression. *Nature Medicine* **15:**496-497; 2009.

[39] Hotchkiss, R. S.; Opal, S. Immunotherapy for Sepsis - A New Approach against an Ancient Foe. *New England Journal of Medicine* **363:**87-89; 2010.

[40] Ziegler, E. J.; Fisher, C. J.; Sprung, C. L.; Straube, R. C.; Sadoff, J. C.; Foulke, G. E.; Wortel, C. H.; Fink, M. P.; Dellinger, R. P.; Teng, N. N. Treatment of gram-negative

bacteremia and septic shock with HA-1A human monoclonal antibody against endotoxin. A randomized, double-blind, placebo-controlled trial. The HA-1A Sepsis Study Group. *N Engl J Med* **324:**429-436; 1991.

[41] Fisher, C. J.; Agosti, J. M.; Opal, S. M.; Lowry, S. F.; Balk, R. A.; Sadoff, J. C.; Abraham, E.; Schein, R. M.; Benjamin, E. Treatment of septic shock with the tumor necrosis factor receptor:Fc fusion protein. The Soluble TNF Receptor Sepsis Study Group. *N Engl J Med* **334:**1697-1702; 1996.

[42] Abraham, E.; Anzueto, A.; Gutierrez, G.; Tessler, S.; San Pedro, G.; Wunderink, R.; Dal Nogare, A.; Nasraway, S.; Berman, S.; Cooney, R.; Levy, H.; Baughman, R.; Rumbak, M.; Light, R. B.; Poole, L.; Allred, R.; Constant, J.; Pennington, J.; Porter, S. Double-blind randomised controlled trial of monoclonal antibody to human tumour necrosis factor in treatment of septic shock. NORASEPT II Study Group. *Lancet* **351:**929-933; 1998.

[43] Fisher, C. J.; Dhainaut, J. F.; Opal, S. M.; Pribble, J. P.; Balk, R. A.; Slotman, G. J.; Iberti, T. J.; Rackow, E. C.; Shapiro, M. J.; Greenman, R. L. Recombinant human interleukin 1 receptor antagonist in the treatment of patients with sepsis syndrome. Results from a randomized, double-blind, placebo-controlled trial. Phase III rhIL-1ra Sepsis Syndrome Study Group. *JAMA* **271:**1836-1843; 1994.

[44] Root, R. K.; Lodato, R. F.; Patrick, W.; Cade, J. F.; Fotheringham, N.; Milwee, S.; Vincent, J. L.; Torres, A.; Rello, J.; Nelson, S.; Pneumonia Sepsis Study, G. Multicenter, double-blind, placebo-controlled study of the use of filgrastim in patients hospitalized with pneumonia and severe sepsis. *Critical Care Medicine* **31:**367-373; 2003.

[45] Orozco, H.; Arch, J.; Medina-Franco, H.; Pantoja, J. P.; Gonzalez, Q. H.; Vilatoba, M.; Hinojosa, C.; Vargas-Vorackova, F.; Sifuentes-Osornio, J. Molgramostim (GM-CSF) associated with antibiotic treatment in nontraumatic abdominal sepsis - A randomized, double-blind, placebo-controlled clinical trial. *Archives of Surgery* **141:**150-153; 2006.

[46] Döcke, W. D.; Randow, F.; Syrbe, U.; Krausch, D.; Asadullah, K.; Reinke, P.; Volk, H. D.; Kox, W. Monocyte deactivation in septic patients: restoration by IFN-gamma treatment. *Nat Med* **3:**678-681; 1997.

[47] Polk, H. C.; Cheadle, W. G.; Livingston, D. H.; Rodriguez, J. L.; Starko, K. M.; Izu, A. E.; Jaffe, H. S.; Sonnenfeld, G. A randomized prospective clinical trial to determine

the efficacy of interferon-gamma in severely injured patients. *Am J Surg* **163:**191-196; 1992.

[48] Wasserman, D.; Ioannovich, J. D.; Hinzmann, R. D.; Deichsel, G.; Steinmann, G. G. Interferon-gamma in the prevention of severe burn-related infections: a European phase III multicenter trial. The Severe Burns Study Group. *Crit Care Med* **26:**434-439; 1998.

[49] Wheeler, D. S.; Zingarelli, B.; Wheeler, W. J.; Wong, H. R. Novel pharmacologic approaches to the management of sepsis: targeting the host inflammatory response. *Recent Pat Inflamm Allergy Drug Discov* **3:**96-112; 2009.

[50] Osuchowski, M. F.; Welch, K.; Siddiqui, J.; Remick, D. G. Circulating cytokine/inhibitor profiles reshape the understanding of the SIRS/CARS continuum in sepsis and predict mortality. *Journal of Immunology* **177:**1967-1974; 2006.

[51] Mela, L.; Bacalzo, L. V.; Miller, L. D. Defective oxidative metabolism of rat liver mitochondria in hemorrhagic and endotoxin shock. *Am J Physiol* **220:**571-577; 1971.

[52] Kantrow, S. P.; Taylor, D. E.; Carraway, M. S.; Piantadosi, C. A. Oxidative metabolism in rat hepatocytes and mitochondria during sepsis. *Arch Biochem Biophys* **345:**278-288; 1997.

[53] Lush, C. W.; Kvietys, P. R. Microvascular dysfunction in sepsis. *Microcirculation* **7:**83-101; 2000.

[54] Fink, M. Cytopathic hypoxia in sepsis: a true problem? *Minerva Anestesiol* **67:**290-291; 2001.

[55] Crouser, E. Mitochondrial dysfunction in septic shock and multiple organ dysfunction syndrome. *Mitochondrion* **4:**729-741; 2004.

[56] Suliman, H. B.; Carraway, M. S.; Piantadosi, C. A. Postlipopolysaccharide oxidative damage of mitochondrial DNA. *Am J Respir Crit Care Med* **167:**570-579; 2003.

[57] Nisoli, E.; Carruba, M. O. Nitric oxide and mitochondrial biogenesis. *J Cell Sci* **119:**2855-2862; 2006.

[58] Suliman, H. B.; Carraway, M. S.; Welty-Wolf, K. E.; Whorton, A. R.; Piantadosi, C. A. Lipopolysaccharide stimulates mitochondrial biogenesis via activation of nuclear respiratory factor-1. *J Biol Chem* **278:**41510-41518; 2003.

[59] Suliman, H. B.; Welty-Wolf, K. E.; Carraway, M.; Tatro, L.; Piantadosi, C. A. Lipopolysaccharide induces oxidative cardiac mitochondrial damage and biogenesis. *Cardiovasc Res* **64:**279-288; 2004.

[60] Suliman, H. B.; Welty-Wolf, K. E.; Carraway, M. S.; Schwartz, D. A.; Hollingsworth, J. W.; Piantadosi, C. A. Toll-like receptor 4 mediates mitochondrial DNA damage and biogenic responses after heat-inactivated E. coli. *FASEB J* **19:**1531-1533; 2005.

[61] Finck, B. N.; Kelly, D. P. Peroxisome proliferator-activated receptor gamma coactivator-1 (PGC-1) regulatory cascade in cardiac physiology and disease. *Circulation* **115:**2540-2548; 2007.

[62] Puigserver, P.; Adelmant, G.; Wu, Z.; Fan, M.; Xu, J.; O'Malley, B.; Spiegelman, B. M. Activation of PPARgamma coactivator-1 through transcription factor docking. *Science (New York, N.Y* **286:**1368-1371; 1999.

[63] Lin, J.; Puigserver, P.; Donovan, J.; Tarr, P.; Spiegelman, B. M. Peroxisome proliferator-activated receptor gamma coactivator 1beta (PGC-1beta), a novel PGC-1-related transcription coactivator associated with host cell factor. *Journal of Biological Chemistry* **277:**1645-1648; 2002.

[64] Andersson, U.; Scarpulla, R. C. Pgc-1-related coactivator, a novel, serum-inducible coactivator of nuclear respiratory factor 1-dependent transcription in mammalian cells. *Mol Cell Biol* **21:**3738-3749; 2001.

[65] Scarpulla, R. C. Transcriptional paradigms in mammalian mitochondrial biogenesis and function. *Physiol Rev* **88:**611-638; 2008.

[66] Virbasius, J. V.; Scarpulla, R. C. Activation of the human mitochondrial transcription factor A gene by nuclear respiratory factors: a potential regulatory link between nuclear and mitochondrial gene expression in organelle biogenesis. *Proc Natl Acad Sci U S A* **91:**1309-1313; 1994.

[67] Bonawitz, N. D.; Clayton, D. A.; Shadel, G. S. Initiation and beyond: multiple functions of the human mitochondrial transcription machinery. *Molecular cell* **24:**813-825; 2006.

[68] Suliman, H. B.; Carraway, M. S.; Ali, A. S.; Reynolds, C. M.; Welty-Wolf, K. E.; Piantadosi, C. A. The CO/HO system reverses inhibition of mitochondrial biogenesis and prevents murine doxorubicin cardiomyopathy. *J Clin Invest* **117:**3730-3741; 2007.

[69] Haden, D. W.; Suliman, H. B.; Carraway, M. S.; Welty-Wolf, K. E.; Ali, A. S.; Shitara, H.; Yonekawa, H.; Piantadosi, C. A. Mitochondrial biogenesis restores oxidative metabolism during Staphylococcus aureus sepsis. *Am J Respir Crit Care Med* **176:**768-777; 2007.

[70] Larsson, N. G.; Wang, J.; Wilhelmsson, H.; Oldfors, A.; Rustin, P.; Lewandoski, M.; Barsh, G. S.; Clayton, D. A. Mitochondrial transcription factor A is necessary for mtDNA maintenance and embryogenesis in mice. *Nat Genet* **18:**231-236; 1998.

[71] Tran, M.; Tam, D.; Bardia, A.; Bhasin, M.; Rowe, G. C.; Kher, A.; Zsengeller, Z. K.; Akhavan-Sharif, M. R.; Khankin, E. V.; Saintgeniez, M.; David, S.; Burstein, D.; Karumanchi, S. A.; Stillman, I. E.; Arany, Z.; Parikh, S. M. PGC-1 alpha promotes recovery after acute kidney injury during systemic inflammation in mice. *Journal of Clinical Investigation* **121:**4003-4014; 2011.

[72] MacGarvey, N. C.; Suliman, H. B.; Bartz, R. R.; Fu, P.; Withers, C. M.; Welty-Wolf, K. E.; Piantadosi, C. A. Activation of Mitochondrial Biogenesis by Heme Oxygenase-1-mediated NF-E2-related Factor-2 Induction Rescues Mice from Lethal Staphylococcus aureus Sepsis. *American Journal of Respiratory and Critical Care Medicine* **185:**851-861; 2012.

[73] Athale, J.; Ulrich, A.; MacGarvey, N. C.; Bartz, R. R.; Welty-Wolf, K. E.; Suliman, H. B.; Piantadosi, C. A. Nrf2 promotes alveolar mitochondrial biogenesis and resolution of lung injury in Staphylococcus aureus pneumonia in mice. *Free Radical Biology and Medicine* **53:**1584-1594; 2012.

[74] Suliman, H. B.; Sweeney, T. E.; Withers, C. M.; Piantadosi, C. A. Co-regulation of nuclear respiratory factor-1 by NFkappaB and CREB links LPS-induced inflammation to mitochondrial biogenesis. *J Cell Sci* **123:**2565-2575; 2010.

[75] Ryter, S. W.; Alam, J.; Choi, A. M. Heme oxygenase-1/carbon monoxide: from basic science to therapeutic applications. *Physiol Rev* **86:**583-650; 2006.

[76] Lancel, S.; Hassoun, S. M.; Favory, R.; Decoster, B.; Motterlini, R.; Neviere, R. Carbon Monoxide Rescues Mice from Lethal Sepsis by Supporting Mitochondrial Energetic Metabolism and Activating Mitochondrial Biogenesis. *Journal of Pharmacology and Experimental Therapeutics* **329:**641-648; 2009.

[77] Suliman, H. B.; Carraway, M. S.; Tatro, L. G.; Piantadosi, C. A. A new activating role for CO in cardiac mitochondrial biogenesis. *J Cell Sci* **120:**299-308; 2007.

[78] Rhodes, M. A.; Carraway, M. S.; Piantadosi, C. A.; Reynolds, C. M.; Cherry, A. D.; Wester, T. E.; Natoli, M. J.; Massey, E. W.; Moon, R. E.; Suliman, H. B. Carbon monoxide, skeletal muscle oxidative stress, and mitochondrial biogenesis in humans. *Am J Physiol Heart Circ Physiol* **297:**H392-399; 2009.

[79] Brealey, D.; Brand, M.; Hargreaves, I.; Heales, S.; Land, J.; Smolenski, R.; Davies, N. A.; Cooper, C. E.; Singer, M. Association between mitochondrial dysfunction and severity and outcome of septic shock. *Lancet* **360:**219-223; 2002.

[80] Feng, Q.; Lu, X.; Jones, D. L.; Shen, J.; Arnold, J. M. Increased inducible nitric oxide synthase expression contributes to myocardial dysfunction and higher mortality after myocardial infarction in mice. *Circulation* **104:**700-704; 2001.

[81] Ullrich, R.; Scherrer-Crosbie, M.; Bloch, K. D.; Ichinose, F.; Nakajima, H.; Picard, M. H.; Zapol, W. M.; Quezado, Z. M. N. Congenital deficiency of nitric oxide synthase 2 protects against endotoxin-induced myocardial dysfunction in mice. *Circulation* **102:**1440-1446; 2000.

[82] Poderoso, J. J.; Carreras, M. C.; Lisdero, C.; Riobo, N.; Schopfer, F.; Boveris, A. Nitric oxide inhibits electron transfer and increases superoxide radical production in rat heart mitochondria and submitochondrial particles. *Archives of Biochemistry and Biophysics* **328:**85-92; 1996.

[83] Bogenhagen, D. F.; Rousseau, D.; Burke, S. The layered structure of human mitochondrial DNA nucleoids. *Journal of Biological Chemistry* **283:**3665-3675; 2008.

[84] Grover, R.; Zaccardelli, D.; Colice, G.; Guntupalli, K.; Watson, D.; Vincent, J. L. An open-label dose escalation study of the nitric oxide synthase inhibitor, N(G)-methyl-L-arginine hydrochloride (546C88), in patients with septic shock. Glaxo Wellcome International Septic Shock Study Group. *Crit Care Med* **27:**913-922; 1999.

[85] López, A.; Lorente, J. A.; Steingrub, J.; Bakker, J.; McLuckie, A.; Willatts, S.; Brockway, M.; Anzueto, A.; Holzapfel, L.; Breen, D.; Silverman, M. S.; Takala, J.; Donaldson, J.; Arneson, C.; Grove, G.; Grossman, S.; Grover, R. Multiple-center, randomized, placebo-controlled, double-blind study of the nitric oxide synthase inhibitor 546C88: effect on survival in patients with septic shock. *Crit Care Med* **32:**21-30; 2004.

[86] Bakker, J.; Grover, R.; McLuckie, A.; Holzapfel, L.; Andersson, J.; Lodato, R.; Watson, D.; Grossman, S.; Donaldson, J.; Takala, J.; Group, G. W. I. S. S. S. Administration of the nitric oxide synthase inhibitor NG-methyl-L-arginine hydrochloride (546C88) by intravenous infusion for up to 72 hours can promote the resolution of shock in patients with severe sepsis: results of a randomized, double-blind, placebo-controlled multicenter study (study no. 144-002). *Crit Care Med* **32:**1-12; 2004.

[87] Kim, Y. M.; Kim, T. H.; Chung, H. T.; Talanian, R. V.; Yin, X. M.; Billiar, T. R. Nitric oxide prevents tumor necrosis factor alpha-induced rat hepatocyte apoptosis by the interruption of mitochondrial apoptotic signaling through S-nitrosylation of caspase-8. *Hepatology* **32:**770-778; 2000.

[88] Zhu, X.; Zhao, H.; Graveline, A. R.; Buys, E. S.; Schmidt, U.; Bloch, K. D.; Rosenzweig, A.; Chao, W. MyD88 and NOS2 are essential for toll-like receptor 4-mediated survival effect in cardiomyocytes. *Am J Physiol Heart Circ Physiol* **291:**H1900-1909; 2006.

[89] Hatano, E.; Bennett, B.; Manning, A.; Qian, T.; Lemasters, J.; Brenner, D. NF-kappaB stimulates inducible nitric oxide synthase to protect mouse hepatocytes from TNF-alpha- and Fas-mediated apoptosis. *Gastroenterology* **120:**1251-1262; 2001.

[90] Nisoli, E.; Falcone, S.; Tonello, C.; Cozzi, V.; Palomba, L.; Fiorani, M.; Pisconti, A.; Brunelli, S.; Cardile, A.; Francolini, M.; Cantoni, O.; Carruba, M. O.; Moncada, S.;

Clementi, E. Mitochondrial biogenesis by NO yields functionally active mitochondria in mammals. *Proc Natl Acad Sci U S A* **101:**16507-16512; 2004.

[91] Beltran, B.; Mathur, A.; Duchen, M. R.; Erusalimsky, J. D.; Moncada, S. The effect of nitric oxide on cell respiration: A key to understanding its role in cell survival or death. *Proceedings of the National Academy of Sciences of the United States of America* **97:**14602-14607; 2000.

[92] Gutsaeva, D. R.; Carraway, M. S.; Suliman, H. B.; Demchenko, I. T.; Shitara, H.; Yonekawa, H.; Piantadosi, C. A. Transient hypoxia stimulates mitochondrial biogenesis in brain subcortex by a neuronal nitric oxide synthase-dependent mechanism. *J Neurosci* **28:**2015-2024; 2008.

[93] Han, Y. X.; Lin, Y. T.; Xu, J. J.; Cao, L. L.; Liu, X. W.; Jiang, H.; Chi, Z. F. Status epilepticus stimulates peroxisome proliferator-activated receptor gamma coactivator 1-alpha/mitochondrial antioxidant system pathway by a nitric oxide-dependent mechanism. *Neuroscience* **186:**128-134; 2011.

[94] Nisoli, E.; Clementi, E.; Paolucci, C.; Cozzi, V.; Tonello, C.; Sciorati, C.; Bracale, R.; Valerio, A.; Francolini, M.; Moncada, S.; Carruba, M. Mitochondrial biogenesis in mammals: the role of endogenous nitric oxide. *Science* **299:**896-899; 2003.

[95] Duval, D. L.; Miller, D. R.; Collier, J.; Billings, R. E. Characterization of hepatic nitric oxide synthase: Identification as the cytokine-inducible form primarily regulated by oxidants. *Molecular Pharmacology* **50:**277-284; 1996.

[96] Ding, A. H.; Nathan, C. F.; Stuehr, D. J. Release of reactive nitrogen intermediates and reactive oxygen intermediates from mouse peritoneal-macrophages - comparison of activating cytokines and evidence for independent production. *Journal of Immunology* **141:**2407-2412; 1988.

[97] Flodstrom, M.; Eizirik, D. L. Interferon-gamma-induced interferon regulatory factor-1 (IRF-1) expression in rodent and human islet cells precedes nitric oxide production. *Endocrinology* **138:**2747-2753; 1997.

[98] Kamijo, R.; Harada, H.; Matsuyama, T.; Bosland, M.; Gerecitano, J.; Shapiro, D.; Le, J.; Koh, S. I.; Kimura, T.; Green, S. J.; Mak, T. W.; Taniguchi, T.; Vilcek, J. Requirement

for transcription factor IRF-1 in NO synthase induction in macrophages. *Science* **263:**1612-1615; 1994.

[99] Jacobs, A. T.; Ignarro, L. J. Lipopolysaccharide-induced expression of interferon-beta mediates the timing of inducible nitric-oxide synthase induction in RAW 264.7 macrophages. *J Biol Chem* **276:**47950-47957; 2001.

[100] Pautz, A.; Art, J.; Hahn, S.; Nowag, S.; Voss, C.; Kleinert, H. Regulation of the expression of inducible nitric oxide synthase. *Nitric Oxide* **23:**75-93; 2010.

[101] Kleinert, H.; Euchenhofer, C.; IhrigBiedert, I.; Forstermann, U. Glucocorticoids inhibit the induction of nitric oxide synthase II by down-regulating cytokine-induced activity of transcription factor nuclear factor-kappa B. *Molecular Pharmacology* **49:**15-21; 1996.

[102] De Vera, M. E.; Taylor, B. S.; Wang, Q.; Shapiro, R. A.; Billiar, T. R.; Geller, D. A. Dexamethasone suppresses iNOS gene expression by upregulating I-kappa B alpha and inhibiting NF-kappa B. *American Journal of Physiology-Gastrointestinal and Liver Physiology* **273:**G1290-G1296; 1997.

[103] Sawle, P.; Foresti, R.; Mann, B. E.; Johnson, T. R.; Green, C. J.; Motterlini, R. Carbon monoxide-releasing molecules (CO-RMs) attenuate the inflammatory response elicited by lipopolysaccharide in RAW264.7 murine macrophages. *British Journal of Pharmacology* **145:**800-810; 2005.

[104] Sheng, W. S.; Hu, S. X.; Nettles, A. R.; Lokensgard, J. R.; Vercellotti, G. M.; Rock, R. B. Hemin inhibits NO production by IL-1 beta-stimulated human astrocytes through induction of heme oxygenase-1 and reduction of p38 MAPK activation. *Journal of Neuroinflammation* **7**; 2010.

[105] Wang, R. Two's company, three's a crowd: can H2S be the third endogenous gaseous transmitter? *Faseb Journal* **16:**1792-1798; 2002.

[106] Pun, P. B. L.; Lu, J.; Kan, E. M.; Moochhala, S. Gases in the mitochondria. *Mitochondrion* **10:**83-93; 2010.

[107] Brown, G. C.; Cooper, C. E. Nanomolar concentrations of nitric-oxide reversibly inhibit synaptosomal respiration by competing with oxygen at cytochrome-oxidase. *Febs Letters* **356:**295-298; 1994.

[108] Zuckerbraun, B. S.; Chin, B. Y.; Bilban, M.; d'Avila, J. C.; Rao, J.; Billiar, T. R.; Otterbein, L. E. Carbon monoxide signals via inhibition of cytochrome c oxidase and generation of mitochondrial reactive oxygen species. *Faseb Journal* **21:**1099-1106; 2007.

[109] Li, Q.; Guo, Y.; Ou, Q.; Cui, C.; Wu, W.; Tan, W.; Zhu, X.; Lanceta, L.; Sanganalmath, S.; Dawn, B.; Shinmura, K.; Rokosh, G.; Wang, S.; Bolli, R. Gene transfer of inducible nitric oxide synthase affords cardioprotection by upregulating heme oxygenase-1 via a nuclear factor-{kappa}B-dependent pathway. *Circulation* **120:**1222-1230; 2009.

[110] Grion, N.; Repetto, E. M.; Pomeraniec, Y.; Calejman, C. M.; Astort, F.; Sanchez, R.; Pignataro, O. P.; Arias, P.; Cymerying, C. B. Induction of nitric oxide synthase and heme oxygenase activities by endotoxin in the rat adrenal cortex: involvement of both signaling systems in the modulation of ACTH-dependent steroid production. *Journal of Endocrinology* **194:**11-20; 2007.

[111] Liu, X. M.; Peyton, K. J.; Ensenat, D.; Wang, H.; Hannink, M.; Alam, J.; Durante, W. Nitric oxide stimulates heme oxygenase-1 gene transcription via the Nrf2/ARE complex to promote vascular smooth muscle cell survival. *Cardiovascular Research* **75:**381-389; 2007.

[112] Choi, B. M.; Pae, H. O.; Kim, Y. M.; Chung, H. T. Nitric oxide-mediated cytoprotection of hepatocytes from glucose deprivation-induced cytotoxicity: Involvement of heme oxygenase-1. *Hepatology* **37:**810-823; 2003.

[113] Immenschuh, S.; Tan, M.; Ramadori, G. Nitric oxide mediates the lipopolysaccharide dependent upregulation of the heme oxygenase-1 gene expression in cultured rat Kupffer cells. *Journal of Hepatology* **30:**61-69; 1999.

[114] Kaizu, T.; Ikeda, A.; Nakao, A.; Tsung, A.; Toyokawa, H.; Ueki, S.; Geller, D. A.; Murase, N. Protection of transplant-induced hepatic ischemia/reperfusion injury with carbon monoxide via MEK/ERK1/2 pathway downregulation. *American Journal of Physiology-Gastrointestinal and Liver Physiology* **294:**G236-G244; 2008.

[115] Suliburk, J. W.; Ward, J. L.; Helmer, K. S.; Adams, S. D.; Zuckerbraun, B. S.; Mercer, D. W. Ketamine-induced hepatoprotection: the role of heme oxygenase-1. *American Journal of Physiology-Gastrointestinal and Liver Physiology* **296:**G1360-G1369; 2009.

[116] Ashino, T.; Yamanaka, R.; Yamamoto, M.; Shimokawa, H.; Sekikawa, K.; Iwakura, Y.; Shioda, S.; Numazawa, S.; Yoshida, T. Negative feedback regulation of lipopolysaccharide-induced inducible nitric oxide synthase gene expression by heme oxygenase-1 induction in macrophages. *Molecular Immunology* **45:**2106-2115; 2008.

[117] Srisook, K.; Han, S. S.; Choi, H. S.; Li, M. H.; Ueda, H.; Kim, C.; Cha, Y. N. CO from enhanced HO activity or from CORM-2 inhibits both O-2(-) and NO production and downregulates HO-1 expression in LPS-stimulated macrophages. *Biochemical Pharmacology* **71:**307-318; 2006.

[118] Albakri, Q. A.; Stuehr, D. J. Intracellular assembly of inducible NO synthase is limited by nitric oxide-mediated changes in heme insertion and availability. *J Biol Chem* **271:**5414-5421; 1996.

[119] Otterbein, L. E.; Bach, F. H.; Alam, J.; Soares, M.; Tao Lu, H.; Wysk, M.; Davis, R. J.; Flavell, R. A.; Choi, A. M. Carbon monoxide has anti-inflammatory effects involving the mitogen-activated protein kinase pathway. *Nat Med* **6:**422-428; 2000.

[120] Piantadosi, C. A.; Withers, C. M.; Bartz, R. R.; MacGarvey, N. C.; Fu, P.; Sweeney, T. E.; Welty-Wolf, K. E.; Suliman, H. B. Heme oxygenase-1 couples activation of mitochondrial biogenesis to anti-inflammatory cytokine expression. *J Biol Chem* **286:**16374-16385; 2011.

[121] Lee, T. S.; Chau, L. Y. Heme oxygenase-1 mediates the anti-inflammatory effect of interleukin-10 in mice. *Nat Med* **8:**240-246; 2002.

[122] Matsuoka, Y.; Masuda, H.; Yokoyama, M.; Kihara, K. Protective effects of bilirubin against cyclophosphamide induced hemorrhagic cystitis in rats. *J Urol* **179:**1160-1166; 2008.

[123] Lanone, S.; Bloc, S.; Foresti, R.; Almolki, A.; Taillé, C.; Callebert, J.; Conti, M.; Goven, D.; Aubier, M.; Dureuil, B.; El-Benna, J.; Motterlini, R.; Boczkowski, J. Bilirubin

decreases nos2 expression via inhibition of NAD(P)H oxidase: implications for protection against endotoxic shock in rats. *FASEB J* **19:**1890-1892; 2005.

[124] Wang, W.; Smith, D.; Zucker, S. Bilirubin inhibits iNOS expression and NO production in response to endotoxin in rats. *Hepatology* **40:**424-433; 2004.

[125] Seok, J.; Warren, H. S.; Cuenca, A. G.; Mindrinos, M. N.; Baker, H. V.; Xu, W. H.; Richards, D. R.; McDonald-Smith, G. P.; Gao, H.; Hennessy, L.; Finnerty, C. C.; Lopez, C. M.; Honari, S.; Moore, E. E.; Minei, J. P.; Cuschieri, J.; Bankey, P. E.; Johnson, J. L.; Sperry, J.; Nathens, A. B.; Billiar, T. R.; West, M. A.; Jeschke, M. G.; Klein, M. B.; Gamelli, R. L.; Gibran, N. S.; Brownstein, B. H.; Miller-Graziano, C.; Calvano, S. E.; Mason, P. H.; Cobb, J. P.; Rahme, L. G.; Lowry, S. F.; Maier, R. V.; Moldawer, L. L.; Herndon, D. N.; Davis, R. W.; Xiao, W. Z.; Tompkins, R. G.; Inflammation Host Response, I. Genomic responses in mouse models poorly mimic human inflammatory diseases. *Proceedings of the National Academy of Sciences of the United States of America* **110:**3507-3512; 2013.

[126] Esmon, C. T. Why do animal models (sometimes) fail to mimic human sepsis? *Critical Care Medicine* **32:**S219-S222; 2004.

[127] Riedemann, N. C.; Guo, R. F.; Ward, P. A. The enigma of sepsis. *Journal of Clinical Investigation* **112:**460-467; 2003.

[128] Copeland, S.; Warren, H. S.; Lowry, S. F.; Calvano, S. E.; Remick, D.; Inflammation Host, R. Acute inflammatory response to endotoxin in mice and humans. *Clinical and Diagnostic Laboratory Immunology* **12:**60-67; 2005.

[129] Remick, D. G.; Newcomb, D. E.; Bolgos, G. L.; Call, D. R. Comparison of the mortality and inflammatory response of two models of sepsis: Lipopolysaccharide vs. cecal ligation find puncture. *Shock* **13:**110-116; 2000.

[130] Buras, J. A.; Holzmann, B.; Sitkovsky, M. Animal models of sepsis: setting the stage. *Nat Rev Drug Discov* **4:**854-865; 2005.

[131] Kinasewitz, G. T.; Chang, A. C. K.; Peer, G. T.; Hinshaw, L. B.; Taylor, F. B. Peritonitis in the baboon: A primate model which simulates human sepsis. *Shock* **13:**100-109; 2000.

[132] Natanson, C.; Fink, M. P.; Ballantyne, H. K.; Macvittie, T. J.; Conklin, J. J.; Parrillo, J. E. Gram-negative bacteremia produces both severe systolic and diastolic cardiac dysfunction in a canine model that simulates human septic shock. *Journal of Clinical Investigation* **78:**259-270; 1986.

[133] Baker, C. C.; Chaudry, I. H.; Gaines, H. O.; Baue, A. E. Evaluation of factors affecting mortality-rate after sepsis in a murine cecal ligation and puncture model. *Surgery* **94:**331-335; 1983.

[134] Nemzek, J. A.; Hugunin, K. M.; Opp, M. R. Modeling sepsis in the laboratory: Merging sound science with animal well-being. *Comparative Medicine* **58:**120-128; 2008.

[135] Suliman, H. B.; Babiker, A.; Withers, C. M.; Sweeney, T. E.; Carraway, M. S.; Tatro, L. G.; Bartz, R. R.; Welty-Wolf, K. E.; Piantadosi, C. A. Nitric oxide synthase-2 regulates mitochondrial Hsp60 chaperone function during bacterial peritonitis in mice. *Free Radic Biol Med* **48:**736-746; 2010.

[136] Reynolds, C.; Suliman, H.; Hollingsworth, J.; Welty-Wolf, K.; Carraway, M.; Piantadosi, C. Nitric oxide synthase-2 induction optimizes cardiac mitochondrial biogenesis after endotoxemia. *Free Radic Biol Med* **46:**564-572; 2009.

[137] Wei, X. Q.; Charles, I. G.; Smith, A.; Ure, J.; Feng, C. J.; Huang, F. P.; Xu, D. M.; Muller, W.; Moncada, S.; Liew, F. Y. Altered immune-responses in mice lacking inducible nitric-oxide synthase. *Nature* **375:**408-411; 1995.

[138] Chaturvedi, R. K.; Calingasan, N. Y.; Yang, L. C.; Hennessey, T.; Johri, A.; Beal, M. F. Impairment of PGC-1alpha expression, neuropathology and hepatic steatosis in a transgenic mouse model of Huntington's disease following chronic energy deprivation. *Human Molecular Genetics* **19:**3190-3205; 2010.

[139] Xie, Q. W.; Cho, H. J.; Calaycay, J.; Mumford, R. A.; Swiderek, K. M.; Lee, T. D.; Ding, A.; Troso, T.; Nathan, C. Cloning and characterization of inducible nitric oxide synthase from mouse macrophages. *Science* **256:**225-228; 1992.

[140] Geller, D. A.; Lowenstein, C. J.; Shapiro, R. A.; Nussler, A. K.; Disilvio, M.; Wang, S. C.; Nakayama, D. K.; Simmons, R. L.; Snyder, S. H.; Billiar, T. R. Molecular-cloning

and expression of inducible nitric-oxide synthase from human hepatocytes. *Proceedings of the National Academy of Sciences of the United States of America* **90:**3491-3495; 1993.

[141] Balligand, J. L.; Ungureanulongrois, D.; Simmons, W. W.; Pimental, D.; Malinski, T. A.; Kapturczak, M.; Taha, Z.; Lowenstein, C. J.; Davidoff, A. J.; Kelly, R. A.; Smith, T. W.; Michel, T. Cytokine-inducible nitric-oxide synthase (iNOS) expression in cardiac myocytes - characterization and regulation of iNOS expression and detection of iNOS activity in single cardiac myocytes in-vitro. *Journal of Biological Chemistry* **269:**27580-27588; 1994.

[142] Ha, K. S.; Kim, K. M.; Kwon, Y. G.; Bai, S. K.; Nam, W. D.; Yoo, Y. M.; Kim, P. K. M.; Chung, H. T.; Billiar, T. R.; Kim, Y. M. Nitric oxide prevents 6-hydroxydopamine-induced apoptosis in PC12 cells through cGMP-dependent PI3 kinase/Akt activation. *Faseb Journal* **17:**1036-1047; 2003.

[143] Koll, H.; Guiard, B.; Rassow, J.; Ostermann, J.; Horwich, A. L.; Neupert, W.; Hartl, F. U. Antifolding activity of HSP60 couples protein import into the mitochondrial matrix with export to the intermembrane space. *Cell* **68:**1163-1175; 1992.

[144] Piantadosi, C. A.; Carraway, M. S.; Babiker, A.; Suliman, H. B. Heme oxygenase-1 regulates cardiac mitochondrial biogenesis via Nrf2-mediated transcriptional control of nuclear respiratory factor-1. *Circ Res* **103:**1232-1240; 2008.

[145] Chen, X. L.; Kunsch, C. Induction of cytoprotective genes through Nrf2/antioxidant response element pathway: A new therapeutic approach for the treatment of inflammatory diseases. *Current Pharmaceutical Design* **10:**879-891; 2004.

[146] Ma, Q. Role of Nrf2 in oxidative stress and toxicity. *Annu Rev Pharmacol Toxicol* **53:**401-426; 2013.

[147] Blackwell, T. S.; Yull, F. E.; Chen, C. L.; Venkatakrishnan, A.; Blackwell, T. R.; Hicks, D. J.; Lancaster, L. H.; Christman, J. W.; Kerr, L. D. Multiorgan nuclear factor kappa B activation in a transgenic mouse model of systemic inflammation. *American Journal of Respiratory and Critical Care Medicine* **162:**1095-1101; 2000.

[148] Tsai, P. S.; Chen, C. C.; Yang, L. C.; Huang, W. Y.; Huang, C. J. Heme oxygenase 1, nuclear factor E2-related factor 2, and nuclear factor kappa B are involved in hemin

inhibition of type 2 cationic amino acid transporter expression and L-arginine transport in stimulated macrophages. *Anesthesiology* **105:**1201-1210; 2006.

[149] Rushworth, S. A.; MacEwan, D. J.; O'Connell, M. A. Lipopolysaccharide-Induced Expression of NAD(P)H:Quinone Oxidoreductase 1 and Heme Oxygenase-1 Protects against Excessive Inflammatory Responses in Human Monocytes. *Journal of Immunology* **181:**6730-6737; 2008.

[150] Zobi, F.; Blacque, O.; Jacobs, R. A.; Schaub, M. C.; Bogdanova, A. Y. 17 e-rhenium dicarbonyl CO-releasing molecules on a cobalamin scaffold for biological application. *Dalton Trans* **41:**370-378; 2012.

[151] Wu, J. C.; Merlino, G.; Fausto, N. Establishment and characterization of differentiated, nontransformed hepatocyte cell lines derived from mice transgenic for transforming growth factor alpha. *Proc Natl Acad Sci U S A* **91:**674-678; 1994.

[152] Seubert, J. M.; Darmon, A. J.; El-Kadi, A. O. S.; D'Souza, S. J. A.; Bend, J. R. Apoptosis in murine hepatoma Hepa 1c1c7 wild-type, C12, and C4 cells mediated by bilirubin. *Molecular Pharmacology* **62:**257-264; 2002.

[153] Fitzgerald, M. J.; Webber, E. M.; Donovan, J. R.; Fausto, N. Rapid DNA-binding by nuclear factor kappa B in hepatocytes at the start of liver-regeneration. *Cell Growth & Differentiation* **6:**417-427; 1995.

[154] Galea, E.; Feinstein, D. L. Regulation of the expression of the inflammatory nitric oxide synthase (NOS2) by cyclic AMP. *Faseb Journal* **13:**2125-2137; 1999.

[155] Chen, J. H.; Somanath, P. R.; Razorenova, O.; Chen, W. S.; Hay, N.; Bornstein, P.; Byzova, T. V. Akt1 regulates pathological angiogenesis, vascular maturation and permeability in vivo. *Nature Medicine* **11:**1188-1196; 2005.

[156] Cho, H.; Mu, J.; Kim, J. K.; Thorvaldsen, J. L.; Chu, Q. W.; Crenshaw, E. B.; Kaestner, K. H.; Bartolomei, M. S.; Shulman, G. I.; Birnbaum, M. J. Insulin resistance and a diabetes mellitus-like syndrome in mice lacking the protein kinase Akt2 (PKB beta). *Science* **292:**1728-1731; 2001.

[157] Chang, F.; Lee, J. T.; Navolanic, P. M.; Steelman, L. S.; Shelton, J. G.; Blalock, W. L.; Franklin, R. A.; McCubrey, J. A. Involvement of PI3K/Akt pathway in cell cycle progression, apoptosis, and neoplastic transformation: a target for cancer chemotherapy. *Leukemia* **17:**590-603; 2003.

[158] Hardie, D. G. Minireview: The AMP-activated protein kinase cascade: The key sensor of cellular energy status. *Endocrinology* **144:**5179-5183; 2003.

[159] Noursadeghi, M.; Tsang, J.; Haustein, T.; Miller, R. F.; Chain, B. M.; Katz, D. R. Quantitative imaging assay for NF-kappa B nuclear translocation in primary human macrophages. *Journal of Immunological Methods* **329:**194-200; 2008.

[160] Luo, D. S.; Vincent, S. R. Metalloporphyrins inhibit nitric oxide-dependent cGMP formation in vivo. *European Journal of Pharmacology-Molecular Pharmacology Section* **267:**263-267; 1994.

[161] Trakshel, G. M.; Sluss, P. M.; Maines, M. D. Comparative effects of tin-protoporphyrin and zinc-protoporphyrin on steroidogenesis: tin-protoporphyrin is a potent inhibitor of cytochrome p-450-dependent activities in the rat adrenals. *Pediatric Research* **31:**196-201; 1992.

[162] Poss, K. D.; Tonegawa, S. Heme oxygenase 1 is required for mammalian iron reutilization. *Proceedings of the National Academy of Sciences of the United States of America* **94:**10919-10924; 1997.

[163] Tzima, S.; Victoratos, P.; Kranidioti, K.; Alexiou, M.; Kollias, G. Myeloid heme oxygenase-1 regulates innate immunity and autoimmunity by modulating IFN-beta production. *Journal of Experimental Medicine* **206:**1167-1179; 2009.

[164] Sioud, M. Promises and challenges in developing RNAi as a research tool and therapy. *Methods Mol Biol* **703:**173-187; 2011.

[165] Abrams, M. T.; Koser, M. L.; Seitzer, J.; Williams, S. C.; DiPietro, M. A.; Wang, W.; Shaw, A. W.; Mao, X.; Jadhav, V.; Davide, J. P.; Burke, P. A.; Sachs, A. B.; Stirdivant, S. M.; Sepp-Lorenzino, L. Evaluation of efficacy, biodistribution, and inflammation for a potent siRNA nanoparticle: effect of dexamethasone co-treatment. *Mol Ther* **18:**171-180; 2010.

[166] Li, C. X.; Parker, A.; Menocal, E.; Xiang, S.; Borodyansky, L.; Fruehauf, J. H. Delivery of RNA interference. *Cell Cycle* **5:**2103-2109; 2006.

[167] Perrella, M. A.; Patterson, C.; Tan, L.; Yet, S. F.; Hsieh, C. M.; Yoshizumi, M.; Lee, M. E. Suppression of interleukin-1 beta-induced nitric-oxide synthase promoter/enhancer activity by transforming growth factor-beta 1 in vascular smooth muscle cells - Evidence for mechanisms other than NF-kappa B. *Journal of Biological Chemistry* **271:**13776-13780; 1996.

[168] Chen, Y. H.; Layne, M. D.; Chung, S. W.; Ejima, K.; Baron, R. M.; Yet, S. F.; Perrella, M. A. Elk-3 is a transcriptional repressor of nitric-oxide synthase 2. *Journal of Biological Chemistry* **278:**39572-39577; 2003.

[169] Baron, R. M.; Carvajal, I. M.; Liu, X. L.; Okabe, R. O.; Fredenburgh, L. E.; Macias, A. A.; Chen, Y. H.; Ejima, K.; Layne, M. D.; Perrella, M. A. Reduction of nitric oxide synthase 2 expression by distamycin A improves survival from endotoxemia. *Journal of Immunology* **173:**4147-4153; 2004.

[170] Chu, S. C.; Marks-Konczalik, J.; Wu, H. P.; Banks, T. C.; Moss, J. Analysis of the cytokine-stimulated human inducible nitric oxide synthase (iNOS) gene: characterization of differences between human and mouse iNOS promoters. *Biochem Biophys Res Commun* **248:**871-878; 1998.

[171] Shitara, H.; Kaneda, H.; Sato, A.; Iwasaki, K.; Hayashi, J.; Taya, C.; Yonekawa, H. Non-invasive visualization of sperm mitochondria behavior in transgenic mice with introduced green fluorescent protein (GFP). *FEBS Lett* **500:**7-11; 2001.

[172] Suliman, H. B.; Carraway, M. S.; Ali, A. S.; Reynolds, C. M.; Welty-Wolf, K. E.; Piantadosi, C. A. The CO/HO system reverses inhibition of mitochondrial biogenesis and prevents murine doxorubicin cardiomyopathy. *J Clin Invest* **117:**3730-3741; 2007.

[173] Welty-Wolf, K. E.; Carraway, M. S.; Huang, Y. C.; Simonson, S. G.; Kantrow, S. P.; Piantadosi, C. A. Bacterial priming increases lung injury in gram-negative sepsis. *Am J Respir Crit Care Med* **158:**610-619; 1998.

[174] Vreman, H. J.; Stevenson, D. K. Heme oxygenase activity as measured by carbon-monoxide production. *Analytical Biochemistry* **168:**31-38; 1988.

[175] Suliman, H. B.; Carraway, M. S.; Velsor, L. W.; Day, B. J.; Ghio, A. J.; Piantadosi, C. A. Rapid mtDNA deletion by oxidants in rat liver mitochondria after hemin exposure. *Free Radic Biol Med* **32:**246-256; 2002.

Biography

Crystal Michele Withers was born on June 18, 1981 in Clinton, MD as the 4th of 8 children of Arthur Sr. and Margaret Reynolds. She grew up in Halifax County, VA where her parents still reside. After graduating from Halifax County High School as #7 in her class, she matriculated to Norfolk State University (NSU) in 1999 with a full scholarship through the Dozoretz National Institute for Minorities in Applied Sciences (DNIMAS) program. She graduated summa cum laude from NSU with a B.S. in Chemistry Pre-Medicine in May 2003. After participating in the Post-Baccalaureate Research Education Program (PREP) at Duke University, she started medical school at Duke in 2004. She then entered the Pathology Graduate program in August 2008. She returned to the School of Medicine in May 2013 to complete her final year of medical school and graduate in May 2014. Since being at Duke, she received the Medical School Faculty Wives Scholarship (2005-2006), Dean's Tuition Scholarship for Medical School (2004-2008), Duke Endowment Fellowship and James B. Duke Fellowship for Grad School (2008-2011), and the UNCF/Merck Graduate Dissertation Fellowship (2012-2013) as well as Member of the Year and Duke Chapter of the Year for the Student National Medical Association (2007). She has one first author publication, "Nitric oxide synthase-2 induction optimizes cardiac mitochondrial biogenesis after endotoxemia" [136] and is a co-author on 8 other papers featured in *Am J Respir Crit Care Med, J Biol Chem, J Cell Sci, Free Radic Biol Med, J Mol Cell Cardiol, Am J Physiol Heart Circ Physio,* and *J. Clin. Invest.*